

AIRGAP-WOUND ALTERNATORS FOR LARGE-SCALE
POWER GENERATION.

A thesis submitted for the degree of
DOCTOR OF PHILOSOPHY.

EDWARD SPOONER
THE UNIVERSITY OF ASTON IN BIRMINGHAM.

THESIS
621-3133 SPo
-6DEC72 156821

November 1972.

Summary.

The airgap-wound or slotless alternator is similar to the conventional type of alternator used for central power generation, but the windings of both the fixed and rotating components are situated in the gap normally separating the two, rather than in slots milled into the steel surfaces. It is shown that this seemingly trivial modification can result in large reductions in the length, weight, losses and cost of generators if properly designed. In addition output capacities about four times that of the largest possible conventional machine could be obtained.

In chapters 1, 2 and 3 the constraints applying to the new layout are explained, methods of obtaining optimum dimensions and specific loadings are set out and several designs are compiled to demonstrate the possibilities of the slotless design. In chapter 5, comparison is made between slotless and conventional machines and it is seen that the slotless type offers several advantages. In particular, a 660 MW slotless machine would be about 4 m shorter, 150 tonne lighter, would have about 2 MW lower losses and would give a total cost saving of about £400,000.

The design of certain critical components is examined in chapter 4 and some specific problem areas are considered in the appendices.

CONTENTS.

Summary

<u>Chapter</u>	<u>Title</u>	<u>Page</u>
1	Introduction .	3
2	Fundamental Concepts .	15
3	Outline Design Studies .	54
4	Detailed Design .	78
5	Discussion .	112
6	Conclusions .	133
	Acknowledgements .	136

Appendix

1	Generator Transformer Connections for Twelve-Phase Windings.	138
2	Forces and Stress in Stator Winding Structure.	142
3	Rotor Surface Eddy Current Loss .	152
4	Calculation of Reactances .	156
	Bibliography	163

Chapter 1.

Introduction.

- 1.1 The need for large turbogenerators.
- 1.2 Airgap windings as a means of achieving high outputs.
- 1.3 Design constraints.
- 1.4 Purpose of the study.
- 1.5 Development of the study.
 - 1.5.1 Slotless stator work.
 - 1.5.2 Fully slotless machines.
- 1.6 Overall plan of the thesis.

1. Introduction.

1.1 The Need for Large Turbogenerators.

As the demand for electric power has grown in the past so have the ratings of the power generating units. Demand is expected to continue increasing and, for reasons of economy and amenity, the capacity of generating plant will probably increase to match this growth. Over the past few decades, higher generator ratings have been achieved by increasing physical sizes and by larger increases in specific electric loadings; that is by using deeper conductors and higher current densities. The basic layout of these large two-pole synchronous generators (fig. 1a) has not changed and it is widely felt that the present form cannot be developed beyond about 2 GVA.

1.2 Airgap Windings as a means of achieving high outputs.

The slotless or airgap-wound machine (fig. 1b) offers an attractive method of generating up to 5 or 6 GVA at 50 Hz from a single-shaft, two-pole machine. The rotor consists of a smooth steel cylinder which carries the field winding attached to the surface and held against centrifugal force by a set of hoops. The stator is a smooth cylindrical tube of laminated steel with the armature winding fixed to its inner surface. Neither winding is contained in slots but occupies part of the space between the rotor and stator steel surfaces, the airgap; otherwise the design is similar to that of a conventional machine. This arrangement is feasible in physical sizes larger than those of conventional machines and permits higher magnetic fields to be employed. The mechanical constraints governing the design are eased by the use of smooth

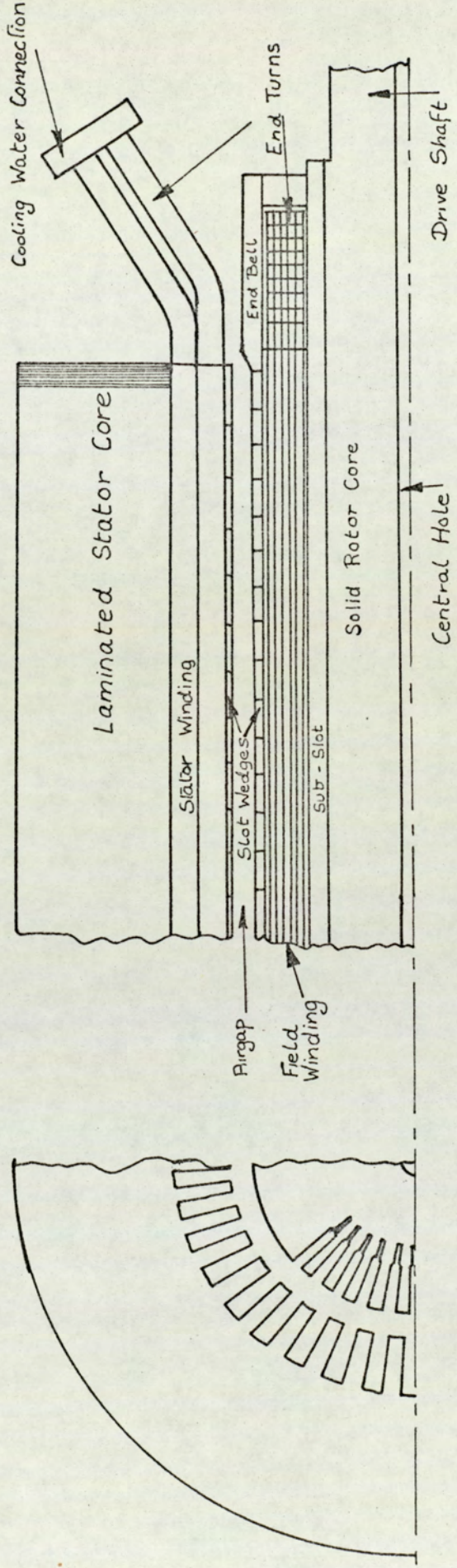


FIG 1a CONVENTIONAL ALTERNATOR

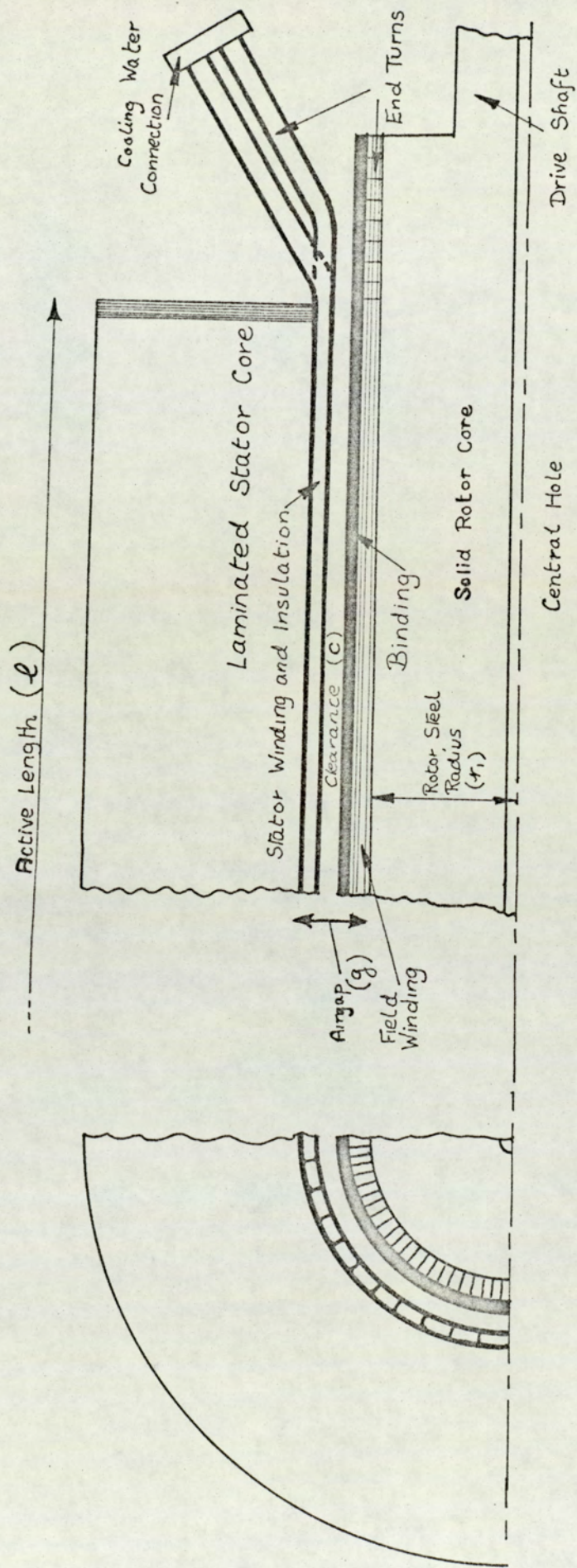


FIG 1b SLOTLESS ALTERNATOR

cylindrical components so that conventional materials and present day electric loadings can be used to greater effect.

The development needed to realise practical full size alternators is mainly confined to the rotor and stator winding support systems and the rotor cooling arrangements. The rest of the machine is essentially conventional.

1.3 Design Constraints.

The fully slotless layout eases the main constraints on the rotor design and in turn on the machine rating. In conventional machines the following restrictions apply:

- (i) The mechanical stresses in the steel due to centrifugal forces acting on the conductors, the wedges and the steel itself must nowhere exceed the maximum safe stress.
- (ii) The whirling or critical speeds of the rotor must not coincide with the normal running speed of the machine.
- (iii) The maximum flux density in the airgap is restricted by saturation of the rotor and stator teeth.
- (iv) The core of the rotor beneath the slots must be capable of carrying the whole of the flux.

Now the output of the machine is proportional to the square of the rotor radius, the active length, the airgap flux density and the stator electric loading. The first constraint imposes an upper limit to the radius of the rotor body. The maximum safe radius for slotted rotors made of currently available steels is about 0.64 m. The second constraint limits the ratio of length to diameter of the rotor. For rotors of the maximum safe radius the maximum practical active length is about 8 to 10 m. The third constraint sets an upper limit of 1.0 to 1.2 T to the sinusoidally distributed component of the flux density pattern at the rotor steel surface. The last constraint limits the depth of the rotor slots and this in turn limits the rotor electric loading. Because of this limit the

stator electric loading is restricted to 300 to 400 kA/m referred to the rotor surface. This limit coincides with that imposed by the need to restrict vibrational forces on the end connections.

The constraints are modified by the use of a slotless design in the following ways:

- (i) The functions of holding down the field winding and resisting rotational forces on the steel are divorced, therefore the steel may safely be of larger radius - up to 0.74 m with available steels.
- (ii) The whole section of the steel contributes to the axial stiffness of the rotor so that higher length to diameter ratios are possible. The maximum permissible length is thus increased by about 40%.
- (iii) The flux density in the airgap is restricted only by the saturation of the rotor steel as a whole and may take any value up to about 2 T providing the stator core can cope with such high fields.
- (iv) The depth available for the rotor winding depends upon the radial length of the airgap and the allocation of the gap between the two windings. Thus in principle the stator electric loading could be made very high by providing a large airgap, but in practice the end winding would vibrate excessively if the loading were significantly higher than in conventional machines.

Thus whereas a conventional machine of 1.95 GVA capacity (radius 0.64 m, length 10 m, flux density 1.2 T, electric

loading 400 kA/m) is the largest permitted by the constraints on its design (unless improved materials become available) and the dimensions and loadings are fully determined by those constraints, the modified constraints for the slotless machine permit ratings of up to 6.1 GVA. Furthermore the designer of a slotless 1.95 GVA machine has a wide choice of possible dimensions and loadings and may optimise them to produce a machine of low cost, weight and loss, of high reliability and with reactances compatible with stable operation.

1.4 Purpose of Study.

It is the aim of this study to examine the airgap-winding arrangement theoretically to discover its technical and economic merits and de-merits as a contender for the next generation of large turbogenerators. The procedure adopted has been to produce designs for slotless machines of several different ratings and to compare their features with those of conventional designs. In addition, a comparison has been made between slotless and superconducting designs because it has been suggested that these machines may become technically and economically feasible in the next decade or so.

A second objective is to assess certain important problems such as the containment of centrifugal forces and the transmission of torque and to suggest possible practical solutions.

1.5 Development of the Study.

1.5.1 Slotless Stator Work.

The work on fully slotless machines evolved from an earlier study of machines with stator windings in the airgap and with conventional slotted rotors. (Davies 1968, 1971.)

A number of patents have been filed relating to various aspects of such machines (see bibliography). The problems of eddy current loss in the stator windings, rotor surface loss, transmission of forces from the winding to the stator core and the choice of suitable winding types were studied. This work is relevant to the study of the fully slotless machine and most of it has been described briefly here.

It was realised at an early stage that the benefits to be gained by placing the stator windings in the gap were small compared with the possible benefits of a fully slotless design. A slotless stator machine would be lighter than its slotted counterpart because the core has a smaller mean radius; the iron loss would be less, and the quantity of insulation needed would be smaller. However, the output available from a machine is determined mainly by the rotor, therefore, it seems unlikely that the airgap-wound stator can offer any way of achieving significantly higher outputs unless the rotor were also made slotless.

1.5.2 Fully Slotless Machines.

The most obvious problem with slotless rotors is the restraint of the field winding against centrifugal force. This problem exists in conventional machines where the rotor conductors leave the ends of the slots and must be supported by the end bell. A similar solution could be used for the slotless machine by placing strong hoops over the full length of the rotor winding.

This imposes the constraint that the stress in the binding hoops due to centrifugal force on the winding and the hoops must be within the safe stress for the binding material. Bearing in mind this and the previous constraints, several outline designs were prepared to specifications which seemed reasonable. The results were disappointing and it became clear that a new approach was needed for the design of fully slotless machines and that preconceived ideas of the best "shape" for a generator do not necessarily apply to the new form.

An important part of the work has been in designing several airgap-wound machines from first principles to obtain the best possible shape in order that the advantages of the new layout may be fully realised. The relaxing of the constraints widens the range of feasible shapes for machines of moderate rating and considerable savings in loss, weight and cost can be achieved by careful choice of the dimensions and loadings.

1.6 Overall Plan of the Thesis.

The study may be divided into the following sections which correspond approximately with the succeeding chapters.

(a) Derivation of equations governing losses and reactances and choice of some dimensions (mainly winding depths) which can be optimised independently of the general shape of the machine. This is accounted in chapter 2.

(b) Use of the results from (a) to design machines of low loss, weight and cost. (Chapter 3).

(c) Consideration of the detailed aspects of the design: winding arrangements, cooling systems, attachment of the windings and design of the conductors. (Chapter 4).

(d) Comparison between airgap-wound, conventional and superconducting machines. (Chapter 5).

(e) Consideration of certain specific problem areas. These are dealt with briefly in appendices.

CHAPTER 2.

FUNDAMENTAL CONCEPTS.

- 2.1 Goodness Factor.
- 2.2 Constraints.
- 2.3 Ratings Obtainable.
 - 2.3.1 Output Equation.
 - 2.3.2 Calculation of maximum possible radius.
 - 2.3.3 Calculation of maximum possible length.
- 2.4 Feasibility.
 - 2.4.1 Calculation of cover thickness needed.
 - 2.4.2 Choice of Conductor and binding materials.
- 2.5 Calculation of losses.
 - 2.5.1 Copper Losses.
 - 2.5.1.1 I^2R losses.
 - 2.5.1.2 Eddy current losses.
 - 2.5.1.3 Removal of losses.
 - 2.5.1.4 Allocation of airgap space.
 - 2.5.1.5 Electric loadings.
 - 2.5.2 Iron loss.
 - 2.5.2.1 Calculation of magnetic fields in the iron.
 - 2.5.2.2 Assessment of non-linear effects.
 - 2.5.2.3 Total core loss.
 - 2.5.2.4 Optimisation of core depth.
 - 2.5.3 Bearing loss and rotor weight.
- 2.6 Choice of overall machine shape.
 - 2.6.1 Computer program for optimisation of Machine designs.

FUNDAMENTAL CONCEPTS.

2.1 Goodness Factor.

The goodness factor, G , (Laithwaite, 1965) is a fundamental figure of merit of electro-magnetic structures and is defined by:

$$G = \frac{w \mu_r \mu_0 \sigma A_m A_e}{l_m l_e} \quad (1)$$

In an airgap-wound alternator the effective lengths and areas of the electric and magnetic circuit vary approximately according to:

$$A_e \propto (g-c).r \quad (2a)$$

$$A_m \propto l.r \quad (2b)$$

$$l_e \propto l + \lambda \quad (2c)$$

$$l_m \propto g \quad (2d)$$

Where the dimensions are as shown in fig. 1b and λ is the length of conductor in the end turns, which is approximately proportional to the radius, r . Therefore the goodness factor of an airgap-wound machine, G_1 , is of the form:

$$G_1 \propto \frac{(g-c).r}{l + \lambda} \times \frac{l.r}{g} \quad (3)$$

The factor $(g-c)$ arises because the radial depth of the airgap space available for conductor is the airgap depth remaining after allocating space to insulation and mechanical clearance.

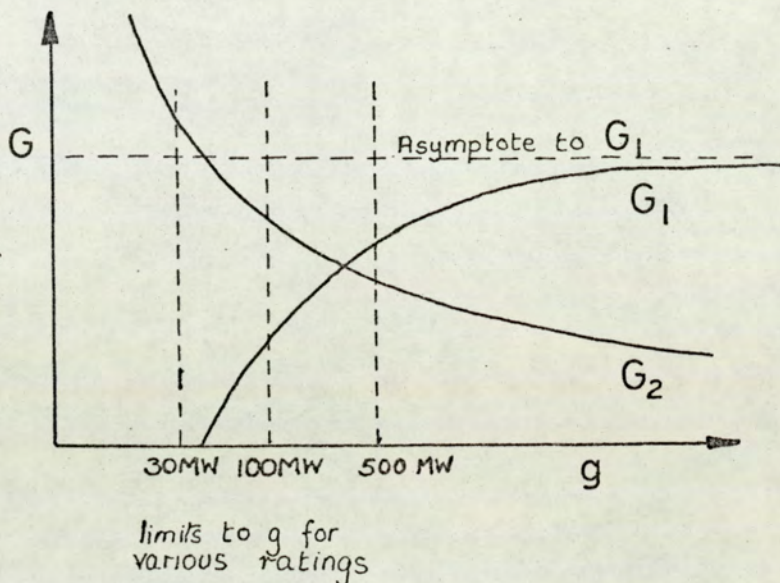
The term $(g-c)$ does not appear in the goodness factor of conventional machines, G_2 , because the conductor area is not significantly affected by the airgap when the windings are in slots. Otherwise the expression (3) remains unchanged. Thus G_2 is a function of the airgap of the form:

$$G_1 \propto 1-c/g \quad (4a)$$

$$\text{whereas } G_2 \propto 1/g \quad (4b)$$

G_1 and G_2 are plotted against g in fig. 2, the asymptote to G_1 results from the assumption that $l_m = g$. A more realistic calculation shows G_1 to be unlimited, but for practical ratios of $g : r$ the simple approach above is adequate.

FIG. 2. GOODNESS
FACTORS OF
SLOTLESS AND
CONVENTIONAL
MACHINES. G_1 & G_2
AS FUNCTIONS
OF AIRGAP, g



Clearly, good designs will have small airgaps in conventional machines and large ones in airgap-wound machines. In practice the airgap has to be larger than the minimum mechanical clearance required because electrical stability sets an upper limit to the synchronous reactance which varies approximately as $1/g$. Generally, the larger the machine rating the larger the necessary airgap. Fig. 2 shows lower limits to the airgap for different ratings. It can be seen that for low ratings (< 30 MW say) conventional designs using the smallest permitted airgap can be better than any airgap-wound design. For medium ratings (~ 500 MW say) airgap-wound machines with airgaps larger than the minimum can be better than conventional machines. For very high ratings (> 1000 MW say) airgap-wound machines can be better than the best conventional ones.

2.2 Constraints.

The foregoing consideration of the goodness factor illustrates the need to abandon preconceived ideas when dealing with the new arrangement. Experience drawn from the design of conventional machines must be used in the detailed design stage, but in determining the best overall shape and size of a slotless machine, such knowledge could be misleading. The features of interest in a basic outline design include:

- (a) Rating and terminal characteristics.
- (b) Main dimensions.
- (c) Specific electric and magnetic loadings.
- (d) Losses and capital cost.

Item (a) would be specified by the user as rated output power and power factor, terminal voltage and a range of acceptable synchronous and transient reactances. Items (b) and (c) constitute the design, and should be chosen to give the specified rating and acceptable reactances, together with the lowest possible losses and capital cost. The range from which the dimensions and loadings can be chosen is constrained by the properties of the materials used and the effectiveness of their use in the arrangement to be adopted. In the airgap-winding scheme the range of possible dimensions is wider than in the conventional type because the materials may be used more effectively in the following ways.

(i) The airgap flux density is no longer restricted by tooth saturation in either the rotor or the stator. Thus it may take any value up to the saturation value of the rotor steel, say 2 T. Typical conventional machines have airgap fields of 1.0 to 1.2 T.

(ii) For a given strength of rotor steel the maximum permitted radius is increased because the whole cross section can contribute to restraining the centrifugal force whereas in a slotted rotor only the central core beneath the slots performs this function.

(iii) For a given rotor diameter and range of permitted whirling speeds the length may be increased because the whole cross section contributes to the stiffness whereas only the central part of a slotted rotor resists bending.

(iv) The total depth of stator core needed for a given total flux is reduced due to the absence of teeth.

2.3 Ratings Obtainable.

2.3.1 Output Equation.

It can be shown (e.g. Say 1958) that the rated output, S , of a two-pole alternator is the product of the rated peak stator current loading, J_s , the peak airgap flux density, B , the volume of the rotor within the working region (the active volume) and the angular frequency, ω .

$$S = \omega \cdot \pi r_1^2 l \cdot J_s \cdot B \quad (5)$$

where J_s and B are both referred to the rotor radius r_1 .

The airgap-winding arrangement permits the flux density in the airgap to be approximately double that in a conventional machine because there are no teeth to restrict the cross-section of the magnetic circuit. A rather larger radius (about 16%) is possible for airgap-wound rotors because a smooth spinning shaft experiences smaller mechanical stresses than a conventional one. Furthermore the length to diameter ratio can be higher because the whole cross-section contributes to the stiffness whereas in conventional rotors the slotted portion contributes little. The length of the rotor body could be increased by about 43%. These increases in the possible sizes of rotors are explored more fully in sections 2.3.2 and 2.3.3.

The increased flux density and rotor dimensions will permit an increase in rating by a factor of three or four over present designs. Thus ratings of 4 to 6 GVA should be possible using existing materials and without raising current loadings above present levels.

Existing power systems could not tolerate such large ratings because the loss of a single machine would be too large a fractional reduction in generation. The possibility of very

high outputs means that machines of more modest rating can be designed well within the limits of available materials and that there exists a wide choice for the basic parameters. Thus there is considerable scope for optimising the design of say 500 or 1000 MW airgap-wound generators to give a combination of low losses and initial capital cost, high reliability and reactances more suitable for stability.

2.3.2 Calculation of Maximum Possible Radius.

The centrifugal force on the rotor body must be balanced by mechanical stresses within the steel. It can be shown that the maximum stress in a smooth spinning shaft with a central hole occurs in the peripheral direction at the bore and is given by:

$$\rho \omega^2 \left\{ (3+v) r_1^2 + (1-v) r_0^2 \right\} / 4 \quad (6)$$

where ρ = density of the material
 v = Poisson's ratio (typically 0.3)
 r_1 = Outer radius
 r_0 = Radius of central hole

For a derivation of (6) see for example Morley (1940). Taking the safe working stress for rotor steel as 350 MN/m^2 , the density as 7900 kg/m^3 , and Poissons ratio as 0.3, the maximum safe radius is found to be 0.74 m if the radius of the central hole is small.

In practice a hole is bored down the axis of the rotor forging to facilitate the testing of the material, and the detection of flaws. This hole is usually of about 50 mm radius and has very little effect upon the stress. With the advent of new techniques, it is becoming possible to test rotors without central holes. The absence of a hole gives a 50% reduction in the stress, thus solid rotors of up to 1.04 m radius would be possible. However, this stress reduction cannot be relied upon since any flaw near the centre would behave as a hole. Further, forgings with the required properties cannot be produced in such large sizes at present. Therefore, for the purposes of this study, the maximum feasible radius is taken as 0.74 m.

2.3.3 Calculation of maximum possible length.

It can be shown (e.g. Say 1958) that the first critical speed of a rotor w_c is given by:

$$w_c = \sqrt{k/m} \quad (7)$$

where k is an effective stiffness of the rotor and m is an effective mass.

The effective stiffness is proportional to

$$k \propto E.I/l^3 \quad (8)$$

where E is Young's modulus, l is the total length, and I is the moment of area of the cross section, given by:

$$I = \pi r_1^4 / 4 \quad (9)$$

where r_1 is the radius of the steel core. The effective mass is proportional to the actual mass, $\rho l r_2^2 \pi$.

Where ρ is the average density of the rotor and r_2 is the outside radius.

Thus:

$$w_c \propto r_1^2 / r_2 l^2 \quad (10)$$

E and ρ for a slotless rotor would be substantially the same as for a conventional rotor. Typical values of r_1 and r_2 for large conventional rotors are 0.46 m and 0.635 m. Putting $r_1 = 0.74$ m, $r_2 = 0.8$ m, for the slotless rotor, the length which gives the same critical speed as the conventional rotor is 1.43 times the length of the conventional rotor. The ratio of active lengths would be rather higher because the end windings would occupy a smaller portion of the longer slotless rotor. However, the flexibility of the bearings imposes a limit on the rotor mass and it may not be practicable to realise the otherwise extremely long rotors possible with airgap windings.

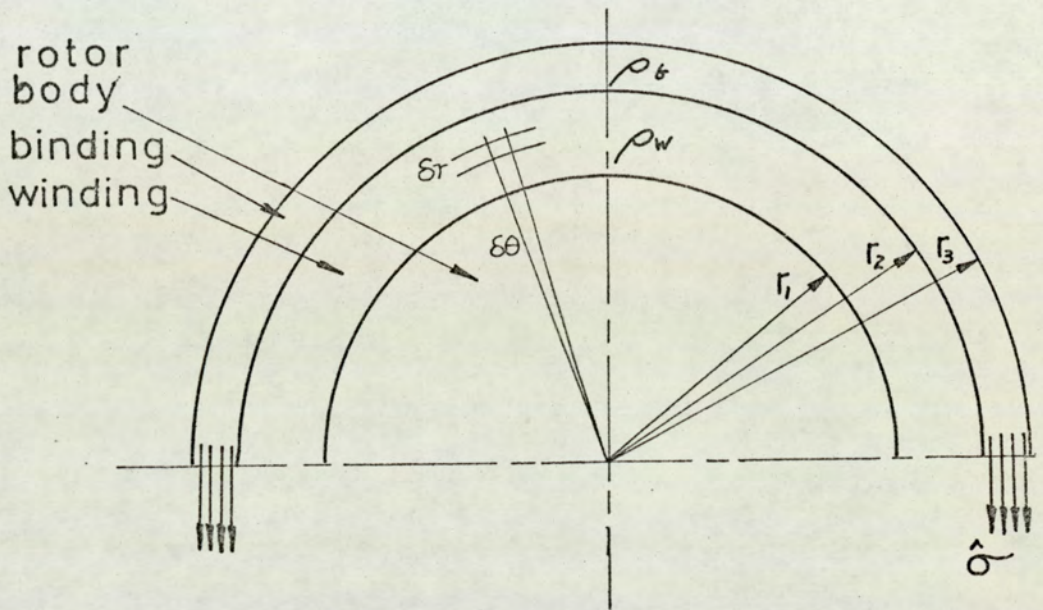
2.4 Feasibility.

The fixing of the windings to the rotor body must be sufficiently strong to withstand the centrifugal forces acting upon the conductors and on the fixing arrangements themselves. (The centrifugal acceleration is typically 6000 g). In this study it is assumed that a binding or cover, possibly made up of separate hoops, is placed over the winding to restrain radial movement in the same way that the overhang of a conventional rotor winding is held by the end bell. The feasibility of this method depends upon the strength of the material and the forces involved.

2.4.1 Calculation of cover thickness needed.

The centrifugal force acting on the field winding of density ρ_w , and on the binding, of density ρ_b , is balanced by hoop stress in the binding. The centrifugal force acting upon the element of conductor shown in fig. 3 is:

FIG. 3. STRESS IN ROTOR BINDING



$\rho_w \cdot l \cdot r \cdot dr \cdot d\theta \cdot r w^2$ integrating over the whole thickness of the winding and cover gives the total radial stress at r_3 needed to balance the centrifugal forces as:

$$\frac{w^2}{3r_3} \left\{ \rho_w (r_2^3 - r_1^3) + \rho_b (r_3^3 - r_2^3) \right\} \quad (11)$$

The average hoop stress in the binding needed to produce this radial stress is:

$$\frac{w^2}{3(r_3 - r_2)} \left\{ \rho_w (r_2^3 - r_1^3) + \rho_b (r_3^3 - r_1^3) \right\} \quad (12)$$

Providing the total depth of the winding and cover is not excessive (i.e. $> 1/3 r_1$) the maximum fraction, A, of this depth, available for the winding is given to within 10% by:

$$A = \frac{\hat{\sigma} / w^2 r_1^2 - \rho_b}{\hat{\sigma} / w^2 r_1^2 - \rho_b + \rho_w} \quad (13)$$

where $\hat{\sigma}$ is the maximum average stress allowed in the binding.

Table 1 gives the maximum allowable stresses and the densities of several promising materials for the rotor cover. In addition to the centrifugal stress in the binding there will be a hoop stress induced by the thermal expansion of the rotor. In the worst case where the cover material is thin, so that the thermal stress in it does not restrain the expansion of the rotor steel, the thermal stress is given by:

$$E_b (\alpha_s - \alpha_b) \Theta \quad (14)$$

where:

E_b is the Young's modulus of the binding,
 α_s and α_b are the coefficients of thermal expansion of the steel and binding material respectively,
and Θ is the difference between the operating temperature and that at which the binding is stress free: 100°C is assumed. This thermal stress is also listed in table 1.

The safe total stress is taken as 37% of the ultimate tensile strength of each material. This is based upon the maximum working stresses used in steels compared with their ultimate strengths. This ratio normally includes a factor of ignorance to allow for stress concentrations near corners. A higher factor might be permitted if the final detailed design retains the uniform cross-section of the binding and smooth stress distribution.

The materials of particular interest are austenitic steel as used in the binding rings of conventional machines and type II carbon-fibre reinforced plastic (C.F.R.P.). The former is a well-understood material; the latter has been described by Ham (1969) and from its properties seems ideally suited to this application. A wound steel strip binding would consist of a continuous strip of austenitic steel, cold drawn to produce

high tensile strength, with a rectangular cross section of (say) 1 mm x 10 mm wound in place over the winding and held by a resin matrix. This material is not very well understood but shows an improvement over homogeneous steel. Its useful strength is a little higher than that of C.F.R.P. but its density is very much higher, therefore C.F.R.P. would be preferred particularly for rotors of large radius. Titanium would show some improvement over austenitic steel were it not for its low Young's modulus which would require the operating stress to be kept low.

Table 1 Properties of some possible binding materials.

Material	Density (ρ_b) tonne/m ³	Safe Stress MN/m ²	Thermal Stress MN/m ²	Centrifugal Stress ($\hat{\sigma}$) MN/m ²
Austenitic Steel	7.9	380	0	380
Wound Steel Strip	7.9	480	0	480
Titanium	4.5	252	23	229
CFRP type I	1.6	380	228	152
CFRP type II	1.55	560	144	416

2.4.2 Choice of Conductor and binding Materials.

The winding density, ρ_w depends upon the conductor material used (the two alternatives studied being aluminium and copper) and upon the subdivision of the winding space between conductor, insulation and coolant ducts. Typically, the mean density of the rotor conductor, insulation and coolant would be 6400 kg/m^3 if copper conductors were used and 2600 kg/m^3 for aluminium.

At some radius, A becomes zero. This is the radius at which the safe working stress is just sufficient to withstand the centrifugal force on the cover itself. This critical radius, r_c , is a characteristic of the cover material alone and is given by:

$$r_c^2 = \frac{\hat{\sigma}}{\omega^2} \rho_b \quad (15)$$

Also for each cover material there exists some radius r_b for which the I^2R loss would be the same in copper as in aluminium because the product of A and the conductivity is the same for each. The loss would be smaller in copper if r_1 is less than r_b and in aluminium for r_1 greater than r_b . r_b is given by:

$$r_b = \frac{\hat{\sigma}}{\omega^2} \frac{(\psi_c - \psi_a)}{(\psi_c \rho_b - \psi_a \rho_b - \psi_c \rho_a + \psi_a \rho_c)} \quad (16)$$

where ψ is conductivity

and suffices a and c refer to aluminium and copper.

$$\text{taking } \psi_a = 3.33 \times 10^7 \text{ siemen/metre}$$

$$\psi_c = 5.00 \times 10^7 \text{ siemen/metre}$$

$$\rho_a = 2200 \text{ kg/metre}^3$$

$$\rho_c = 6000 \text{ kg/metre}^3$$

produces the values in table 2 for r_b with different binding materials. The critical radius is also tabulated.

Table 2

Binding Material	r_b mm	r_c mm
Austenitic Steel	547	694
Wound Steel Strip	614	780
Titanium	495	713
C.F.R.P. Type I	484	975
C.F.R.P. Type II	803	1638

Typically, rotor radii for large airgap-wound machines will be 0.5 to 0.7 m, so that if type II C.F.R.P. is used for the cover, copper will be the better choice of conductor material. For the other binding materials the breakeven radius, r_b , is within the typical range therefore the loss will not be greatly affected by the choice of conductor. However, the depth of binding for aluminium will be less than for copper and the cost of this expensive component will be rather less. The breakeven radius for minimum cost will therefore be less than that derived above for minimum loss. On the other hand the poor mechanical properties of pure aluminium will probably preclude its use. The high strength alloys of aluminium are unsuitable because of their low conductivities.

2.5 Calculation of Losses.

The losses considered are:

- (i) I^2R losses in the rotor and stator windings.
- (ii) Eddy current loss in the stator winding.
- (iii) Iron loss in the stator core.
- (iv) Bearing frictional loss.

The copper losses can be treated accurately with quite simple calculations. Iron loss is a non-linear phenomenon which cannot be treated simply with good accuracy. However an approximate analytical treatment is presented which gives results in a suitable form for optimisation. The frictional loss in the bearings is taken as proportional to the weight of the rotor. This is reasonable because the necessary bearing surface area for a given pressure is proportional to the rotor weight.

2.5.1 Copper Losses.

2.5.1.1 Expressions for I²R losses

If the stator winding is considered to be "smoothed out" around the airgap as shown in fig. 4, the I²R loss can be expressed as:

$$P_S = \frac{(2\pi r_1 J_S / \sqrt{2})^2 (1+\lambda_s)}{2\pi (r_1 + g) d_s k_s \sigma_s} \quad (17)$$

The terms $(1+\lambda_s)/2\pi (r_1 + g) d_s k_s \sigma_s$ express the total resistance of the stator winding with all the conductors in parallel, assuming the winding has a mean radius of $(r_1 + g)$. The r.m.s. current loading is $J_S/\sqrt{2}$ and $2\pi r_1 J_S/\sqrt{2}$ is the sum of the r.m.s. currents in the conductors. The number of turns is irrelevant unless the space factor k_s is affected.

Thus:

$$P_S = \frac{J_S^2 \pi r_1 (1+\lambda_s)}{(1+g/r_1) d_s k_s \sigma_s} \quad (18)$$

Similarly the rotor I²R loss is:

$$P_R = \frac{J_R^2 \pi r_1 (1+\lambda_R)}{d_R k_R \sigma_R} \quad (19)$$

The mean radius is taken as r_1 in this case.

2.5.1.2 Eddy Current Loss.

The stator winding is in the main alternating magnetic field and will be subject to an eddy-current loss. This loss can be limited by subdividing the conductors and transposing the strands.

It can be shown (e.g. Carter 1954) that the loss per unit volume of conductor is:

$$\frac{B^2 w^2 x^2 \sigma_s}{24} \quad (20)$$

where x is the transverse width of the conductor if it is of rectangular cross-section.

Around each strand will be a thin layer of insulation of thickness $t/2$, therefore the space factor of the winding will contain a term $1/(1+t/x)$. It would be unwise to attempt to reduce the eddy current loss by using very fine strands because the reduced space factor would lead to increased I^2R loss. In fact an optimum exists and is discussed in 4.3.

In addition to the above source of eddy current loss, the stray tangential fields in the airgap will give rise to losses. The stray field at the stator winding is due mainly to the stator current and has a magnitude of approximately $\mu_0 J_s$ at the top of the winding and decreases approximately linearly to zero at the iron surface.

The total eddy current loss per unit volume of copper in the active region is, therefore:

$$\frac{w^2 \sigma_s}{24} \left\{ B^2 x^2 + \frac{\mu_0^2 J_s^2 y^2}{3} \right\} \quad (21)$$

where y is the width of the strands in the radial direction and the $1/3$ factor arises from the linear variation of the stray field.

Typically, $B = 2\text{T}$, $x = 2\text{mm}$, $J_s = 3 \cdot 10^5 \text{ kA/m}$ and $y = 8 \text{ mm}$. The terms $B^2 x^2$ and $\mu_0^2 J_s^2 y^2 /$ are, therefore, typically, $1.6 \cdot 10^{-5}$ and $3.2 \cdot 10^{-6}$ respectively. For the sake of simplicity the second term is neglected as are the effects of harmonics in the waveform of the main field (which can be made small if the field winding is suitably distributed) and the eddy current loss is taken as:

$$P_E = \frac{B^2 w^2 x^2 \sigma_s}{24} 2\pi (r_1 + g) l d_s k_s \quad (22)$$

2.5.1.3 Removal of Copper Losses.

It is assumed that both windings are cooled internally by a fluid flowing in ducts with velocity V and raised in temperature by an amount θ during its passage. The passages for the stator winding coolant are assumed to be rectangular tubes interspersed with the strands and the total cooling requirements of the winding are assumed to be met by adjusting the number of ducts provided. The total cross-sectional area of each duct is taken as twice the area of the passage itself. Thus the total area of winding occupied by the cooling ducts is:

$$2 (P_S + P_E) / s\rho V\theta \quad (23)$$

where s is the specific heat of the fluid and ρ is its density.

$$\text{For water, } s\rho = 4.18 \cdot 10^6 \text{ J/m}^3 \text{ }^\circ\text{C} \quad (24)$$

The rotor winding does not need to be stranded, therefore, the coolant may be in direct contact with the conductor and the area needed would be:

$$P_R / s\rho V\theta \quad (25)$$

However, P_R is distributed in a four-pole pattern around the rotor and the cooling must be sufficient to cope with the maximum loss densities which are twice the mean. Thus an area of:

$$2P_R / s\rho V\theta \quad (26)$$

is allocated to rotor coolant.

Throughout the study it has been assumed that the stator winding would be cooled by water as in present machines. Both water and hydrogen gas are considered for the rotor

cooling. Conventional machines usually employ hydrogen at pressures of 3 to 4 atmospheres, however, water cooling schemes for these machines are being developed.

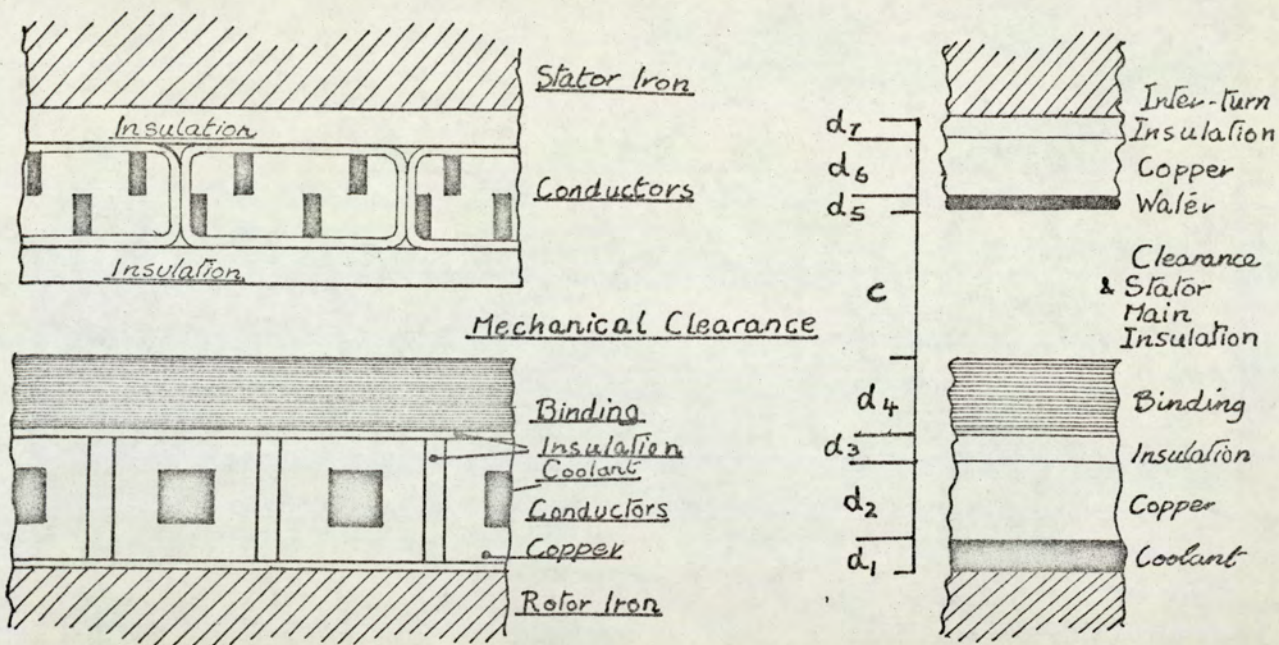
2.5.1.4 Allocation of Airgap Space.

The choice of winding depths was made on the basis of reducing the total cost of the copper losses and the materials to a minimum. All the materials in table 1 are very expensive. The total cost of the windings themselves is smaller and is less dependent on the individual winding depths. In the following treatment, therefore, this cost is considered invariant and the optimum subdivision is taken as that which gives the minimum cost of binding material and copper losses.

For the purpose of analysis the airgap is divided into eight regions.

- d_1 = Average depth of rotor water ducts
- d_2 = Average depth of rotor copper
- d_3 = Average depth of rotor insulation
- d_4 = Average depth of rotor binding
- c = Depth of stator main insulation and mechanical clearance
- d_5 = Average depth of stator coolant
- d_6 = Average depth of stator copper
- d_7 = Average depth of interturn insulation.

This subdivision is illustrated in fig. 4.



approximate physical arrangement

subdivision into equivalent layers

FIG.4. SUBDIVISION OF THE AIRGAP

The following constraints are imposed upon the choice of the eight depths.

- (i) They add up to g , the airgap.
- (ii) As shown in section 2.4.1, the rotor winding depth, $d_1 + d_2 + d_3$, occupies a fraction A of the depth $d_1 + d_2 + d_3 + d_4$.
 A is of the form $k / (k + \rho_w)$ where ρ_w is the average density of the winding region.
- (iii) The heat removed by the stator water is equal to the total loss in the stator winding.
- (iv) As condition (iii) but for the rotor coolant.
- (v) The stator interturn insulation thickness is specified

$$(d_5 + d_6) / (d_5 + d_6 + d_7) = \text{constant } (k_{s_0})$$
- (vi) Similarly $(d_1 + d_2) / (d_1 + d_2 + d_3) = k_{R_0}$
- (vii) A minimum practical value is assumed for c (8 mm insulation each side of stator winding + 34 mm clearance = 50 mm).

These seven conditions reduce the number of independent variables from eight to one. The parameter chosen to be independent for the optimisation of the subdivision of the gap is $d_5 + d_6 + d_7$, the depth of the stator conductors d_5 .

Algebraic manipulation of the seven conditions leads to expressions for the costs in terms of d_5 as follows:

Cost of Stator I^2R + eddy current loss

$$C_S = k_1 \left\{ k_{50} d_5 - \frac{k_{50} d_5 + \sqrt{k_{50}^2 d_5^2 - k_3}}{k_2} \right\} \quad (27)$$

Cost of Rotor I^2R loss + binding material

$$C_R = k_4 \left\{ \frac{(g-c-d_5)}{k_5} \pm \sqrt{\frac{(g-c-d_5)^2}{k_5^2} - k_6} \right\} \quad (28)$$

$$+ k_7 \left\{ \frac{(g-c-d)}{k_5} \pm \sqrt{\frac{(g-c-d_5)^2}{k_5^2} - k_6} \right\}$$

where

$$k_1 = C_L \pi (r_1 + g) s \rho_c V \theta$$

$$k_2 = 2 \left\{ B^2 w^2 x^2 \sigma_s (1-t/x) 1/12 s \rho_c V \theta + 1 \right\}$$

$$k_3 = 2J_s^2 (1+\lambda_s) k_2 / \left\{ (1+g/r_1)^2 (1-t/x) s \rho_c V \theta \sigma_s \right\}$$

$$k_4 = \pi r_1 s \rho_c V \theta \cdot C_L + a' c'$$

$$k_5 = 2(a' + 1/k_{R0})$$

$$k_6 = 2d' (b' + 1/k_{R0}) / k_5$$

$$k_7 = b' c' d'$$

$$a' = (\rho_1 - \rho_3 + \rho_3/k_{R0}) / (\hat{\sigma}/w^2 r_1^2 - \rho_4)$$

$$b' = (\rho_2 - \rho_3 + \rho_3/k_{R0}) / (\hat{\sigma}/w^2 r_1^2 - \rho_4)$$

$$c' = 2\pi r_1 (1+\lambda_B) \rho_4 C_B$$

$$d' = J_R^2 (1+\lambda_R) / s \rho_c V \theta$$

The \pm sign in equation (28) represents two solutions to conditions (ii) and (iv). If the sign is negative, a small fraction of the rotor conductor is occupied by coolant, therefore, the copper section is large and the loss is low; however, the average density is high so that a thick binding is needed. A

positive sign indicates a smaller copper section, larger coolant ducts and a thinner binding. The cheapest solution has large copper area if $k_4 - k_7/k_6$ is positive and small copper area if negative.

Similarly there are two ways of dividing the stator conductors between copper and water, however, the solution with high copper and low water content is unconditionally cheaper.

The total cost $C_S + C_R$ can be minimised numerically quite simply to find the optimum value of d_s . Then from the values of d_s , C_S and C_R the other depths can be found from the seven conditions and are:

$$d_7 = k_{SO} d_s \quad (29)$$

$$d_5 = C_S / k_1 \quad (30)$$

$$d_6 = d_s - d_5 - d_7 \quad (31)$$

$$d_1 = \frac{(g-c-d_s)}{k_5} + \sqrt{\left\{ \frac{(g-c-d_s)}{k_5} - k_6 \right\}} \quad (32)$$

with the sign determined by the sign of $k_4 - k_7/k_6$

$$d_4 = \left\{ \frac{\rho_1 + \rho_3 - \rho_3/k_{RO}}{\delta/w r_1^2 - \rho_4} \right\} d_1 + \left(\frac{\rho_2 + \rho_3 - \rho_3/k_{RO}}{\rho_1 + \rho_3 - \rho_3/k_{RO}} \right) \frac{J_R^2 (1 + \lambda_R)}{\sigma_R S Q V \theta d_1} \quad (33)$$

$$d_3 = (1 - k_{RO}) (g-c-d_s - d_4) \quad (34)$$

$$d_2 = g-c-d_s - d_4 - d_3 - d_1 \quad (35)$$

In some cases, the minimum practical value of c is not the best because both C_R and C_S have separate minima at some values of $(g-c-d_s)$ and d_s respectively. If the gap is larger than the sum of the minimum practical clearance and these two optimum depths, then the minimum total cost is obtained by using the optimum depths and adjusting c .

The optimum values are found from equations (27) and (28) by differentiation and equating the result to zero; this gives:

$$\sqrt{k_3/k_2(k_2-2)} / k_{s0}$$

$$d_{s_{opt}} = \frac{(k_3-1)}{2} \sqrt{\frac{k_2 k_3 (k_3-2)}{k_{s0}}} \quad (36)$$

$$(g-c-d_s)_{opt} = \frac{k_5}{2} \left\{ k_6 \sqrt{\frac{k_4}{k_7}} + \sqrt{\frac{k_7}{k_4}} \right\} \quad (37)$$

The following procedure was used to determine numerically the optimum depths for the windings of the machines described in chapter 3.

- (i) Evaluate the constants k_1, \dots, k_7
- (ii) Evaluate $d_{s_{opt}}, (g-c-d_s)_{opt}$
- (iii) Check whether $d_{s_{opt}}, (g-c-d_s)_{opt}$ can be accommodated in $g-c$ for $c > c_{min}$
- (iv) If so set $d_s = d_{opt}$
 $(g-c-d_s) = (g-c-d_s)_{opt}$
- (v) If not set $c = c_{min}$, minimise $c_s + c_R$
- (vi) From $d_s, (g-c-d_s)$ evaluate d_1, \dots, d_7

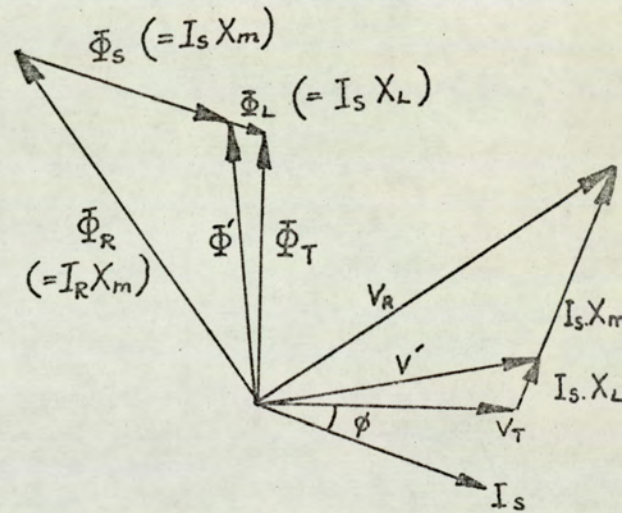
The constants k_1 to k_7 are functions of quantities which are all known with the exception of J_R , the rotor current loading. This is a function of the machine reactances and the stator loading and is derived below.

2.5.1.5 Electric Loadings.

The electric loading of the rotor J_R is found in terms of the stator loading J_S by considering the phasor diagram of synchronous machines, fig. 5, for rated voltage, current and power factor.

FIG. 5. PHASOR DIAGRAM OF A SYNCHRONOUS MACHINE

- V_T - Terminal voltage 1.0pu
- I_S - Stator current 1.0pu
- I_R - Rotor current
- Φ_R - Flux due to I_R
- Φ_S - Flux due to I_S
= armature reaction
= $I_S X_m$
- Φ_L - Stator leakage flux
- Φ_T - Total flux linking stator
- Φ' - Main Flux
- V' - Voltage induced by main flux
- V_R - Voltage due to rotor field alone
- X_m - Magnetising reactance
- X_L - Leakage reactance



It can be seen from the diagram that

$$V_R^2 = (V_T + I_S X_S \sin \phi)^2 + (I_S \cos \phi)^2 \quad (38)$$

where $X_S = X_m + X_L$ is the synchronous reactance

$$\therefore V_R^2 = 1 + X_S^2 + 2X_S \sin \phi \quad (39)$$

Therefore the field current referred to the stator is

$$I_R^2 = (1 + X_S + 2X_S \sin \phi) / X_m^2 \quad \text{p.u.} \quad (40)$$

The base value of I_R being 1.0 p.u. stator current.

Since J_S is defined in terms of the rotor radius and I_R has been referred to the stator winding, the above expression for I_R can be written in terms of J_R and J_S where J_R is

referred to the rotor radius thus

$$J_R = \frac{J_S}{X_m} \sqrt{(1+X_S^2 + 2X_S \sin \phi)} \quad (41)$$

It is convenient to neglect the leakage reactance and write

$$J_R = J_S \sqrt{(1+1/X_m^2 + 2 \sin \phi / X_m)} \quad (42)$$

The error introduced depends upon the leakage and magnetising reactances. The error in the term k_6 will be negative and is tabulated below for a typical range of reactances.

Table 3 Error in k_6 due to setting $X_S = X_m$

		X_L			
		.04	.08	.12	.16
X_m	0.5	-4%	-8%	-12%	-16%
	1.0	-4%	-8%	-11%	-14%
	1.5	-4%	-7%	-10%	-12%
	2.0	-3%	-6%	-8%	-11%

The error is therefore quite small and the approximation is acceptable for an initial estimate of the optimum subdivision of the airgap.

2.5.2 Iron Loss.

2.5.2.1 Calculation of magnetic fields in the Iron.

If the stator iron were magnetically linear and sufficiently laminated to render eddy currents negligible, the vector potential field within the iron would be Laplacian i.e.

$$\nabla^2 \underline{A} = 0 \quad \text{where} \quad \underline{B} = \text{curl } \underline{A} \quad (43)$$

Further, if axial fluxes near the ends are ignored, the vector potential is everywhere axial so that:

$$\nabla^2 A_z = 0$$

which implies that A_z is of the form:

$$A_z = (a_n r^n + b_n / r^n) \cos n \theta$$

For simplicity, the distribution of current in the airgap is assumed sinusoidal, therefore:

$$a_n = b_n = 0 \quad \text{for all } n \neq 1$$

Now, since A_r and A_θ are everywhere zero, the radial and tangential flux densities are:

$$\begin{aligned} B_\theta &= -\partial A_z / \partial r \\ &= -(a - b/r^2) \cos \theta \end{aligned} \quad (44)$$

$$\begin{aligned} B_r &= (\partial A_z / \partial \theta) / r \\ &= -(a+b/r^2) \sin \theta \end{aligned} \quad (45)$$

If it is assumed that the permeability of the iron is high, it follows that no flux will pass round the outside of the core therefore the radial field just inside the outer boundary will be everywhere zero.

$$a = -b/r_3^2 \quad (46)$$

where r_3 is the outer radius, the inner radius being r_2

The total flux per metre length, Φ , carried by each side of the core is the difference in vector potential between r_2 and r_3 thus:

$$\begin{aligned}\Phi &= b \left\{ \frac{-r_3}{r_3^2} + \frac{1}{r_3} \right\} - b \left\{ \frac{-r_2}{r_3^2} + \frac{1}{r_2} \right\} \\ &= -b (r_3^2 - r_2^2) / r_3^2 r_2\end{aligned}\quad (47)$$

Φ is given by the total radial flux entering the core at r_2 , which is approximately equal to the flux leaving the rotor.

$$\therefore \Phi = Br_1 \quad (48)$$

thus :

$$b = -Br_1 r_2 r_3^2 / (r_3^2 - r_2^2) \quad (49a)$$

$$\text{and } a = Br_1 r_2 / (r_3^2 - r_2^2) \quad (49b)$$

The maximum radial and tangential flux densities, Br_{\max} , $B\theta_{\max}$, occur at the inner surface of the core, r_2 , and have magnitudes:

$$Br_{\max} = Br_1 / r_2 \quad (50a)$$

$$B\theta_{\max} = \frac{-Br_1}{r_2} \frac{r_3^2 + r_2^2}{r_3^2 - r_2^2} \quad (50b)$$

2.5.2.2 Assessment of Non-linear effects.

This linear model implies large circumferential flux densities near the inside of the core and saturation will be important. For example typical values might be:

$$\begin{aligned} B &= 2.0T \\ r_1 &= 0.7m \\ r_2 &= 0.875m \\ r_3 &= 1.75m \end{aligned}$$

and the corresponding B_{max} would be 2.67 Tesla which is considerably higher than the saturation flux density of steel. The maximum radial field in this case would be 1.60 Tesla which would not cause severe saturation. An approximate illustration of the effect of saturation is given in fig. 6a, 6b. The field near the inside of the core is limited to the saturation flux density and the field further out is increased by a constant factor over the value for the linear case so that the total flux remains unchanged. It can be seen that only a small fraction of the core volume saturates. Therefore, the linear model may be used for iron loss calculations without excessive errors in the total core loss figure.

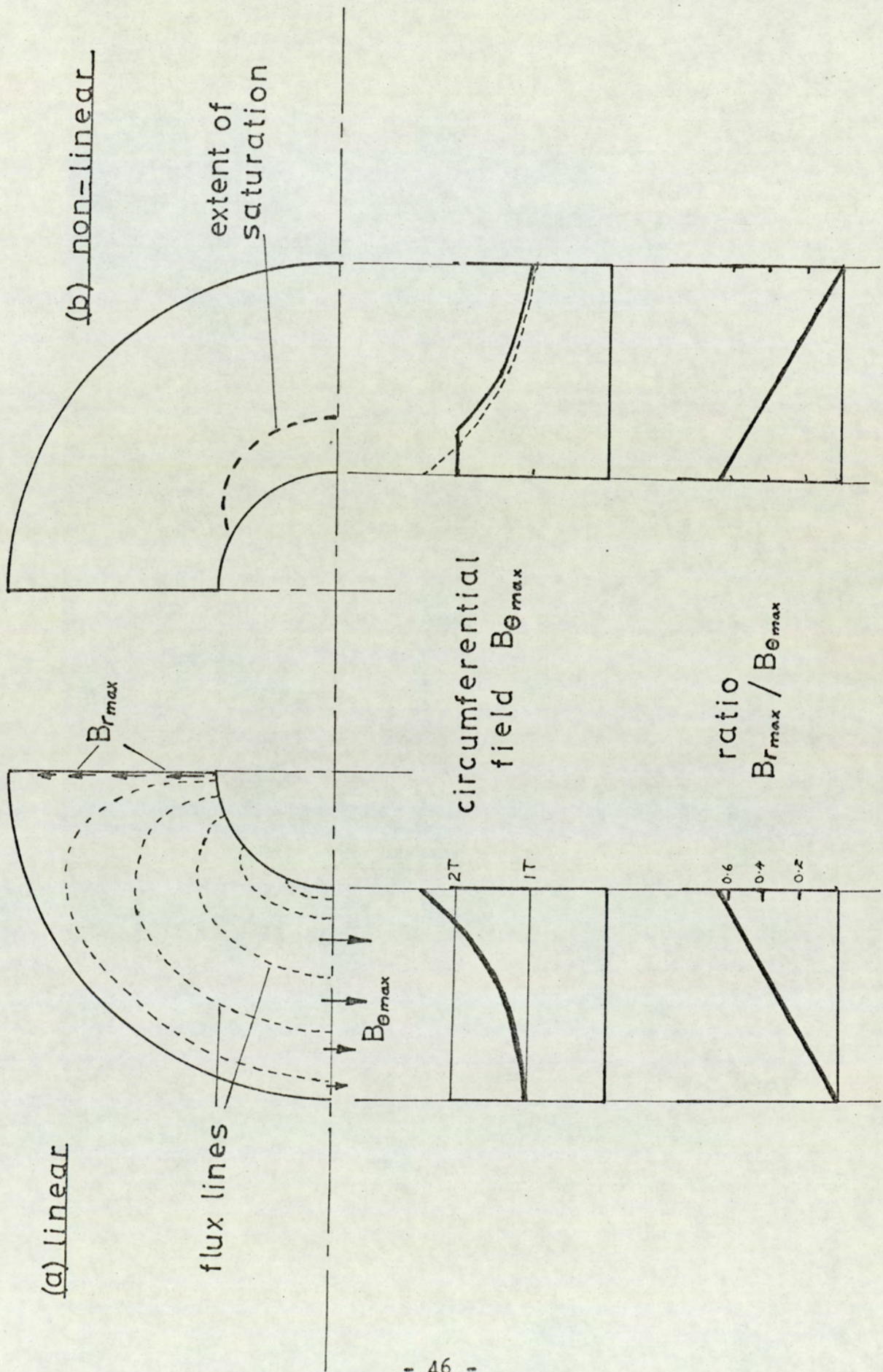


FIG. 6. STATOR CORE FLUX DISTRIBUTION

2.5.2.3 Total Core Loss.

The loss per cubic metre at 50Hz depends upon the type of steel used and the two components of the field. The curves for a typical 3% Si grain-oriented steel (Unisil) are given in fig. 7. The relative magnitudes of B_r and B_θ vary through the core. A pessimistic "average" curve $P = 1.5 \cdot B_\theta^2$ W/kg ($= 11.5 \times B_\theta^2$ kW/m³) is shown and is used below in the loss calculation.

The loss in a cylindrical shell of thickness δr is:

$$2\pi r \delta r l B_\theta^2 \cdot 11.5 \quad \text{kW} \quad (51)$$

The total loss in the core is:

$$23 \pi l \int_{r_2}^{r_3} r B_\theta^2 dr \quad \text{kW} \quad (52)$$

Substituting for B_θ and integrating, the loss is:

$$23 \pi l (B \cdot r_1)^2 \left\{ \frac{1}{2} \frac{r_3^2 + r_2^2}{r_3^2 - r_2^2} + \frac{2 r_3^2 r_2^2}{(r_3^2 - r_2^2)^2} \ln (r_3/r_2) \right\} \text{kW} \quad (53)$$

The function of r_3 and r_2 in brackets is plotted in fig. 8 in terms of r_3/r_2 . The weight of the stator core is also plotted in terms of (r_3/r_2) , the full expression for the stator core weight being:

$$\rho_c \pi r_2^2 l (r_3^2/r_2^2 - 1) \quad (54)$$

Only the term $r_3^2/r_2^2 - 1$ is plotted.

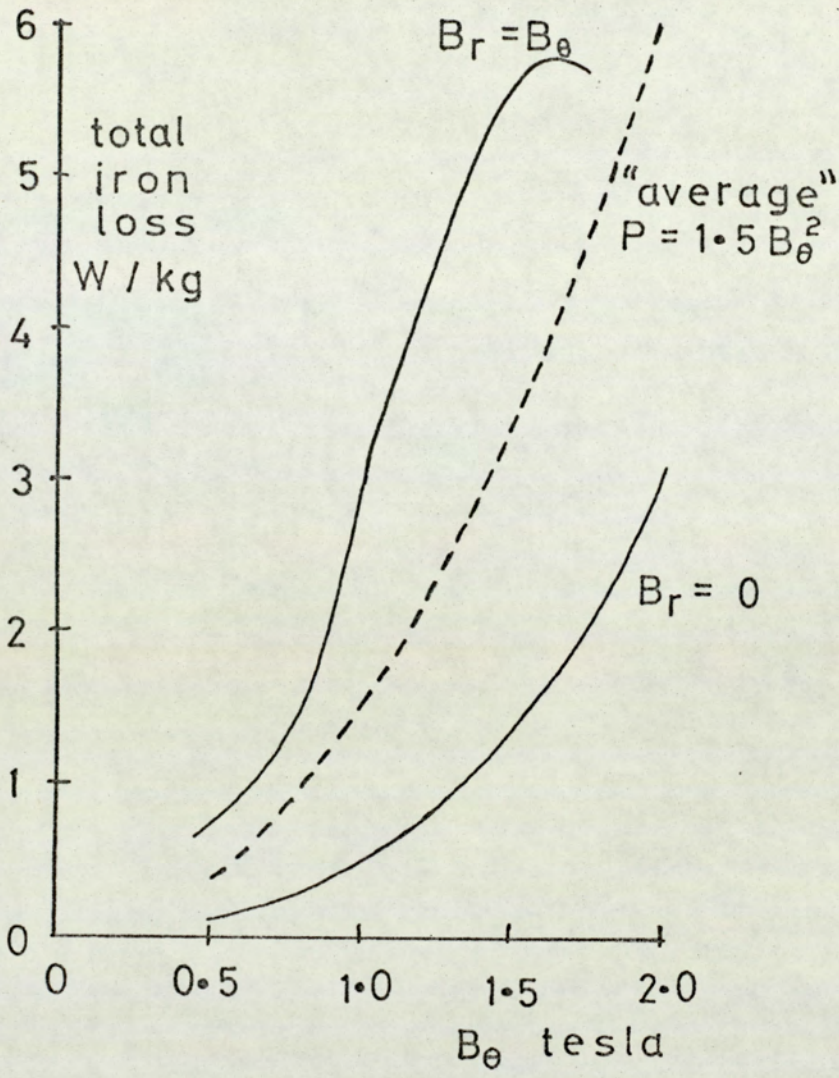


FIG. 7. LOSS IN A TYPICAL CORE STEEL
AT 50 Hz

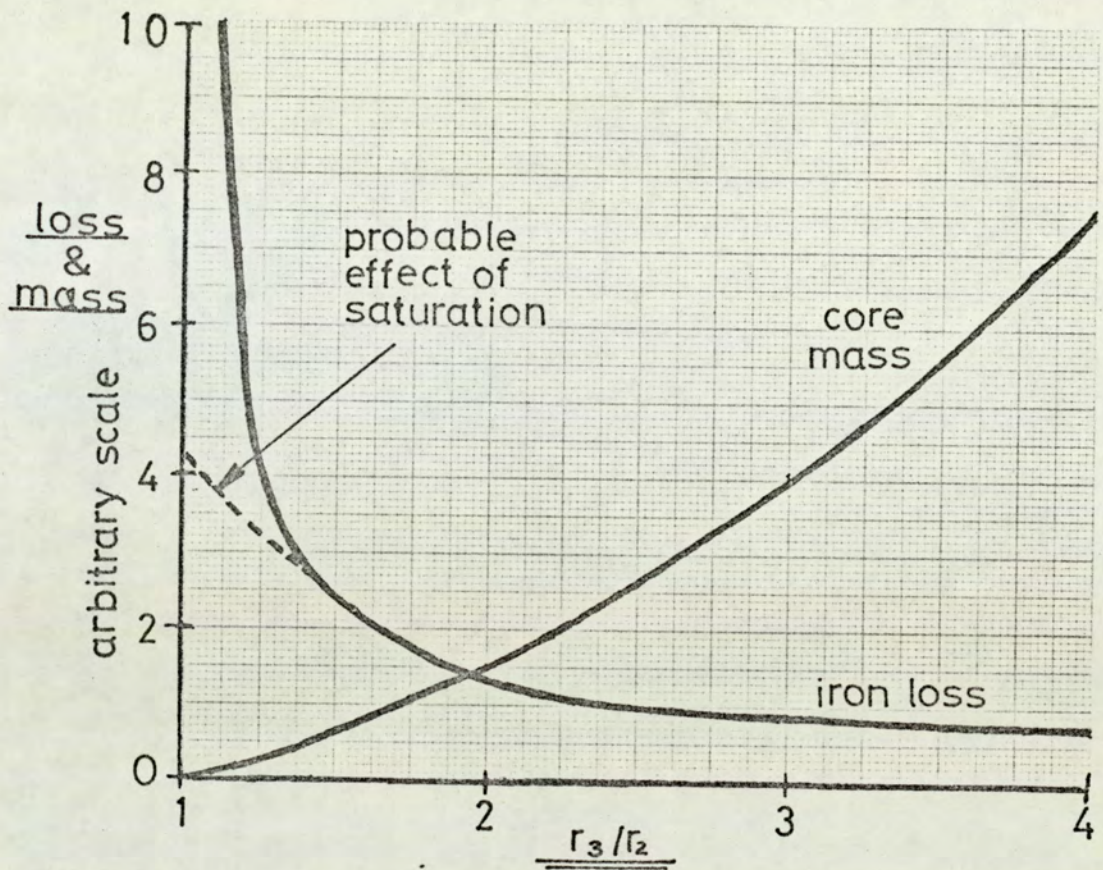
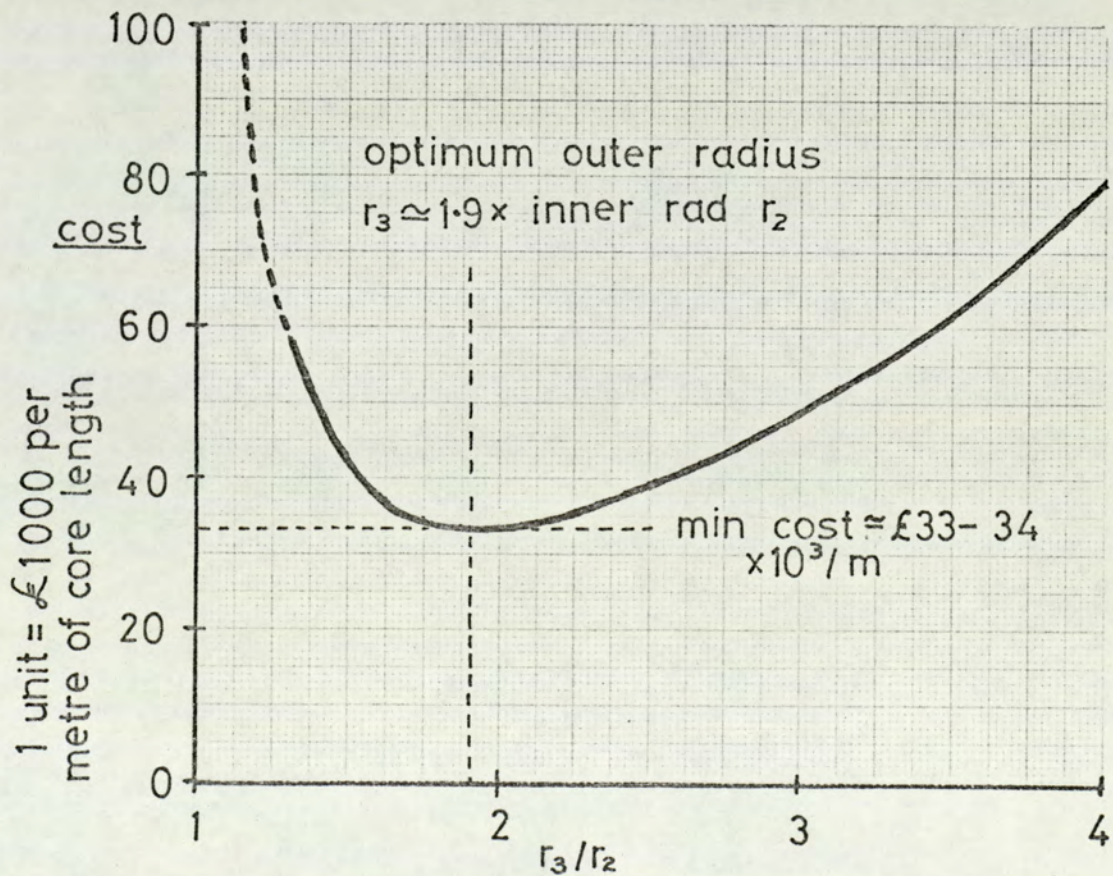


FIG.8. STATOR CORE LOSS & MASS (above)

FIG.9. COST OF LOSS & MATERIAL (below)



2.5.2.4 Optimisation of Core depth.

The core depth can be chosen so that the total cost of material and losses is a minimum. Taking the material cost to be £250 per tonne, and the capitalised value of generator loss to be £100/kW, then for the typical case used previously where:

$$\begin{aligned} B &= 2.0 \text{ T} \\ r_1 &= 0.7 \text{ m,} \\ r_2 &= 0.875 \text{ m;} \end{aligned}$$

1 unit on the loss axis represents £14,200 per metre of core length and one unit on the weight axis represents £4,600 / metre length. The total of these costs is plotted against r_3/r_2 in fig. 9. The optimum ratio r_3/r_2 is 1.9 in this case, and the minimum cost is about £34,000 per metre of core length. These figures depend upon the radii r_1 and r_2 , the flux density, B , and the specific costs of material and loss, C_m and C_L . It can be shown by differentiation of eqn (53) that the optimum ratio $x = r_3/r_2$ is given by:

$$\frac{(x^2+1)}{(x^2-1)^3} \ln x = \frac{0.166}{B^2} \left(\frac{r_2}{r_1}\right)^2 \frac{C_m}{C_L} \quad (55)$$

where C_m is expressed in £/tonne

C_L is expressed in £/kW

and B is expressed in T

The density of laminated core steel is taken as 7.65 tonne/m³.

However, a significant reduction in the weight of the core and hence in the ease of handling can be achieved with a very small cost penalty by making the ratio rather less than the optimum because the total cost curve is quite flat over a wide range near the optimum.

2.5.3 Bearing Loss and Rotor Weight.

The loss in bearings is approximately proportional to the weight of the shaft and rotor to be supported. This is because the required area of support is, for a given pressure, proportional to the weight. (See for example Salisbury 1950).

The mass of the rotor depends to some extent upon the mass of the end shafts and couplings and upon the axial length required at the ends of the body to accommodate the end turns and connections for coolant and current. For the purposes of the design studies the end turns are assumed to require an axial distance equal to the radius of the rotor body, 200 mm is assumed for the connections; and the shafts, couplings etc. are assumed to weigh 5 tonnes. The total weight of the rotor follows from the dimensions in the active region.

The bearings of a slotless machine would be of substantially conventional design. The bearing loss in conventional 500 MW machines with rotors weighing about 80 tonnes is usually between 400 and 800 kW. A pessimistic figure for the bearing loss is taken as 10 kW per tonne of total rotor weight.

The capitalised value of this loss is of the same order as the cost of the rotor forging and is an important component of the total cost to be minimised.

2.6 Choice of Overall Machine Shape.

Using the above formulae for losses, and those for the basic machine reactances given in appendix 4, various possible designs of airgap-wound machines may be compared. A design for a given rating can be represented by four independent quantities if we assume that the airgap subdivision and the stator core depth are optimised. The quantities regarded as independent for the outline studies in chapter 3 are the rotor radius, stator current loading, airgap flux density and the machine magnetising reactance. The length, airgap, winding thicknesses, losses, weights and costs can all be determined from the four original numbers. The terminal voltage and current may be fixed at a later stage by the choice of the number of turns per phase in the armature winding. The designs given in the next chapter were found simply by choosing the cheapest from many possibilities. The ability to specify a design by only four numbers makes this simple approach possible.

2.6.1 Computer Program for Optimisation of Machine Designs.

The program is arranged to produce by means of "DO" loops a large number of designs based upon different sets of values for the four independent variables r_1 , B , J_s and X_m and specified values for the constants S , $\cos \phi$, k_{so} etc. An approximate formula for X_m :

$$X_m \simeq \frac{\mu_0 J_s}{B \ln (1+g/r_1)} \quad (56)$$

is used to determine an approximate value of g which is then used to give approximate values for the mean radii of the two windings. These radii and the value found for g are used to obtain a new value of X_m and values for X_g , X_e , X_L and X_s . From J_s , $\cos \phi$, X_s and X_m a value is found for J_R .

The optimum value of d_s is found by using a repeated bisection technique to determine the value of d_s for which the derivative of the cost of binding and losses with respect to d_s is zero. The same method is used to find the optimum ratio of the inner to outer core radius, by finding the solution to equation (55).

From the results of the two iterative sections the losses, weights, reactances and costs of each design are evaluated and printed. The program could be extended to select the cheapest from the large number of designs produced. However, cost is not the sole factor involved in the choice of design and it is of interest to note the penalty incurred by deviations from the optimum design. Such changes may be needed to improve the reactances of the machine for example.

CHAPTER 3.

OUTLINE DESIGN STUDIES.

- 3.1 Specification.
- 3.2 Features considered.
- 3.3 660 MW designs with water-cooled rotors.
 - 3.3.1 Optimum design.
 - 3.3.2 Effect of design changes.
 - 3.3.3 Leakage reactance and forces during faults.
 - 3.3.4 Choice of design variables.
 - 3.3.5 660 MW designs with gas-cooled rotors.
- 3.4 Upper limit design.
- 3.5 100 MW design.
- 3.6 Range of viable ratings.

3.1 Specification.

The specification for each of the following studies contains only those parameters necessary to ensure compatibility with an existing power system. This allows full use to be made of the new features of the layout in optimising the design for minimum cost. For the airgap-wound generator to fit into an existing power system it is necessary to specify the required power output, the power factor and a range of synchronous and transient reactances compatible with stability. In general, lower values of these reactances than those of conventional large machines would be desirable. Further, the sub-transient reactance should be high enough to restrict fault currents to a safe level determined by the strength of the winding attachment arrangements.

The studies are based upon the following specifications:

- (i) 660 MW, 0.85 p.f. (777 MVA)
- (ii) 3350 MW, 0.85 p.f. (3950 MVA)
- (iii) 100 MW, 0.85 p.f. (118 MVA)

In each case the synchronous reactance should be less than 2.0 p.u. and the transient reactance less than 0.4 p.u.

3.2 Features Considered.

An optimum design was chosen from the many possibilities on the basis of minimum total cost, however, this choice may be modified by considerations of reactances etc. Obviously it would be impossible in this study to include every item, for example, factory overheads, in calculating the total cost. Nevertheless the major components of the cost can be estimated.

The material costs considered are:

- (i) Rotor steel (£500 - 850 / tonne depending upon total mass of steel).
- (ii) Rotor and stator copper (£2 /kg).
- (iii) Rotor and stator insulation (£5 /kg).
- (iv) Rotor binding or cover material
 - (C.F.R.P. £25 /kg).
 - (Steel £2.5 /kg).
- (v) Stator iron (£250 /tonne)

Losses are accounted at £100 /kw.

The losses considered are:

- (i) Rotor and stator I^2R losses.
- (ii) Stator eddy current loss.
- (iii) Stator iron loss.
- (iv) Bearing friction.

Both steel and type II C.F.R.P. have been considered for the binding material. In all cases studied it was found that a steel binding would cost approximately the same as a carbon fibre binding because the lower specific cost of steel is compensated by its higher density and the need for a greater thickness of steel than carbon fibre. The rotor I^2R loss is

higher if the binding is steel because of the smaller depth available for conductor.

The rotor winding is of copper in all the designs described below; however, some 660 MW designs were prepared in outline with aluminium rotor windings. The total cost of loss and material for the cheapest of these designs was slightly less than for the cheapest of the designs using copper. In addition the total loss is considerably (about 1MW) less for aluminium than copper. However, the total weight of the aluminium design is greater because aluminium, being not so good a conductor as copper, must operate at a lower current density, therefore, the best design using aluminium has a larger airgap, larger radius and lower flux density than the best design for copper. Therefore, the aluminium design must have a greater active volume and total mass. Although the cost of loss and materials is slightly less for aluminium, the total cost, including the items omitted so far would be rather less for the copper design because of the much smaller quantity of material to be processed and hence the smaller manufacturing charge. A crude attempt is made in section 3.3.2 to allow for this cost. This naturally favours machines of high specific output.

Most of the designs presented have water cooling of both rotor and stator windings, however, a selection of the more promising 660 MW gas cooled designs is given. Since gas is a less effective coolant than water it imposes a restriction on the current density. Thus, gas cooling leads to higher cost and mass in the same way as the use of aluminium conductors, however, it also causes increased loss whereas aluminium does not. A possible gas cooling scheme is described in chapter 4.

3.3 660 MW Designs with Water-Cooled Rotors.

3.3.1 Minimum Cost Design.

A large number (72) of designs were produced by computer using the expressions for loss and methods of optimising depths derived in chapter 2. Each design is based upon specified values of rotor radius, r_1 , flux density, B , magnetising reactance, X_m , and current loading, J_s . The range $r_1 = 0.5$ to 0.8 m, $B = 1.5$ to 2.0 T, $X_m = 0.5$ to 1.0 p.u, $J_s = 300$ to 400 kA/m was investigated. The consideration of the design constraints in section 2.2 justifies the choice of range in r_1 , B and J_s . The variation of goodness factor with airgap (section 2.1) suggests that such comparatively low reactances as 0.5 to 1.0 are appropriate and this is borne out by the results of the study. The design which emerged as the cheapest is described in outline by the principle features below and by the cross section shown in fig. 10 .

Rating	777 MVA	0.85 p.f.
Flux density	2.0 T	} Referred to surface of rotor steel
Stator Current Loading	300 kA/m	
Rotor Current Loading	633 kA/m	
Rotor Steel Radius	600 mm	
Active Length	3.644 m	
Airgap	171 mm	
Rotor winding depth	55.8 mm	
Rotor binding depth	36.6 mm	
Stator winding depth	29.0 mm	
Stator outer radius	1.46 m	
Rotor winding space factor	0.67	
Stator winding space factor	0.444	

The parameters taken as constant for the purpose of deriving the above optimum values are:

Minimum practical depth of clearance plus main stator insulation	50 mm
------------------------------------------------------------------	-------

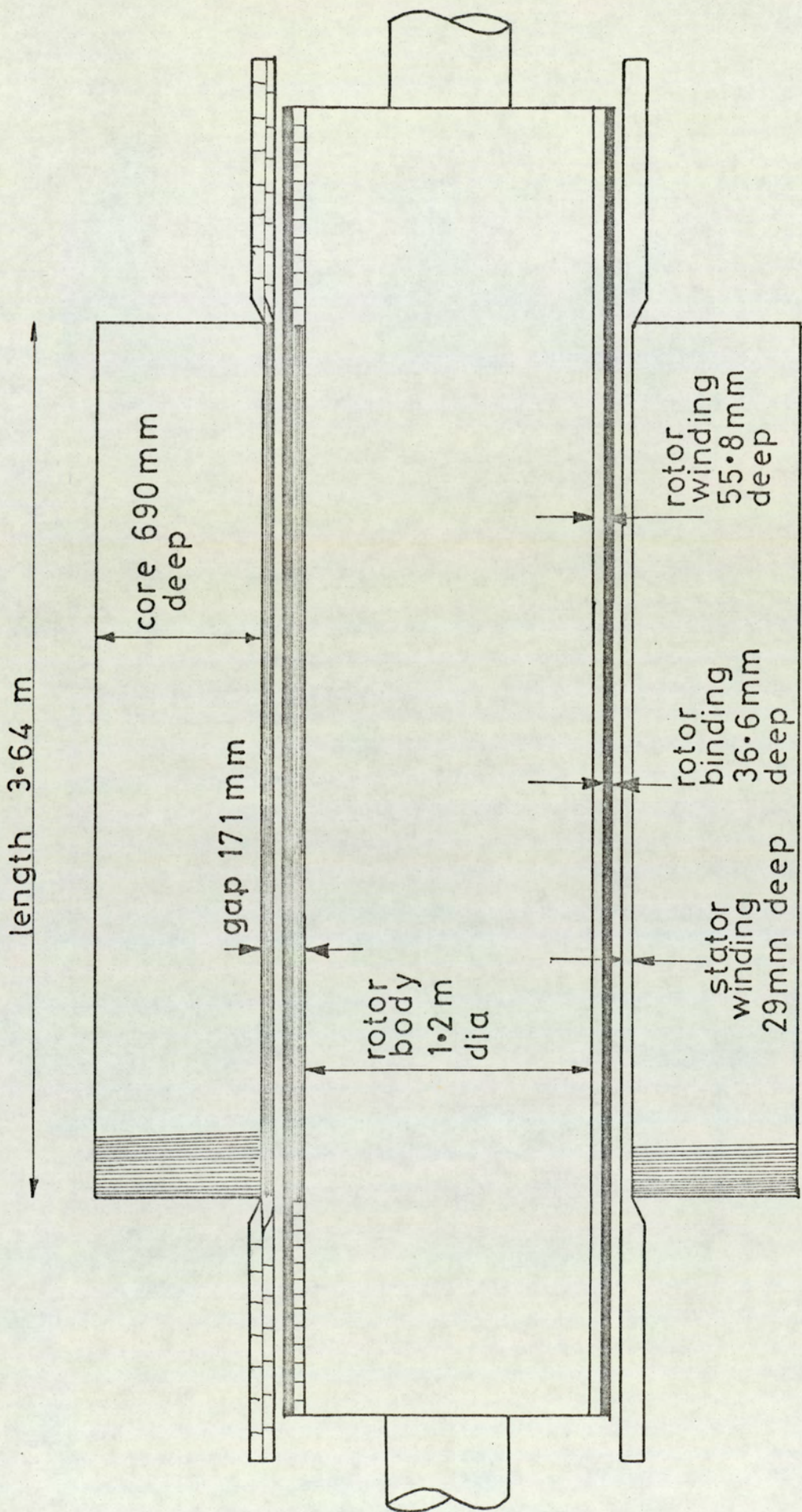


FIG.10. CROSS - SECTION OF OPTIMUM 660 MW MACHINE (scale 25:1)

Water velocity in windings	1.5 m/s
Temperature rise	40 °C
Stator conductor strand width	2 mm
Thickness of strand insulation (each side of each strand)	0.1 mm
Rotor space factor neglecting duct area - $(d_1 + d_2) / (d_1 + d_2 + d_3)$	0.75
Stator space factor neglecting ducts and strand insulation	0.6
Copper resistivity	2.10^{-8} ohm-m
Density of Carbon fibre	1.55 tonne/m ³
Stress in binding	$4.16 \cdot 10^8$ N/m ²

The reactances of this design are:

Synchronous Reactance	0.791 pu
Leakage Reactance	0.048 pu
Transient Reactance	0.064 pu

The losses are:

Stator I ² R	2130 kW
Eddy current loss	748 kW
Rotor I ² R	2130 kW
Iron loss	596 kW
Bearing friction	621 kW
Total	6225 kW

The weights and material costs for the major components are listed below.

<u>Component</u>	<u>Mass (tonne)</u>	<u>Cost (£k)</u>
Rotor Steel	53.6	30.9
Rotor Copper	6.60	13.2
Rotor Insulation	0.69	3.5
Rotor binding	1.16	29.1
Stator Conductor	3.87	7.75
Stator Insulation	2.03	10.1
Stator Iron	135	33.7
Total	<u>202</u>	<u>128</u>

The cost of fabrication and of the minor components will increase the total cost of the machine to perhaps ten times the basic material cost. These manufacturing costs will depend mainly upon the detailed design and are not included at this stage.

3.3.2 Effect of Design Changes.

It is of interest to note the penalty incurred by using other dimensions or loadings than the optimum. Fig. 11 - 13 show how the cost, loss, weight and the transient and sub-transient reactances are affected by deviations away from the optimum radius, flux density and magnetising reactance.

Clearly for this rating, the cost, loss and reactances do not depend critically upon the choice of X_m , B and r_1 . The effect of changing the electric loading is shown in table 4 in which the optimum design is compared with two possible designs using 400 kA/m. The losses are higher for the 400 kA/m designs but the lower material costs compensate to some extent. The bottom row of table 4 gives adjusted figures for the total cost which make some allowance for the manufacturing process. These figures are obtained by weighting the material costs according to table 5.

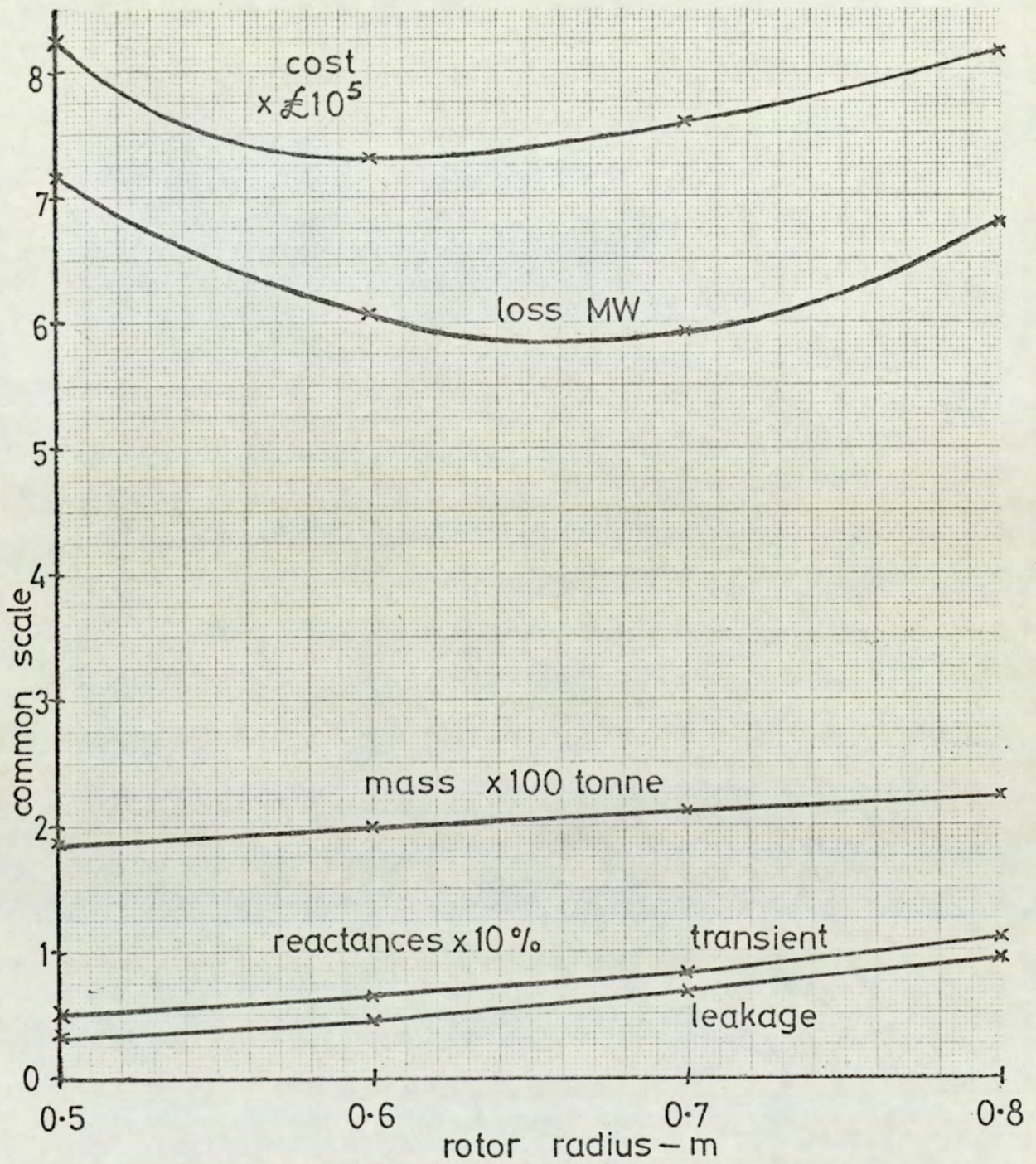


FIG. 11. VARIATION OF MACHINE PARAMETERS
WITH ROTOR RADIUS 660 MW, 0.85 pf

C.F.R.P. binding, water cooled rotor.

$B = 2T$, $J_s = 300 \text{ kA/m}$, $X_m \approx 0.75 \text{ p.u.}$

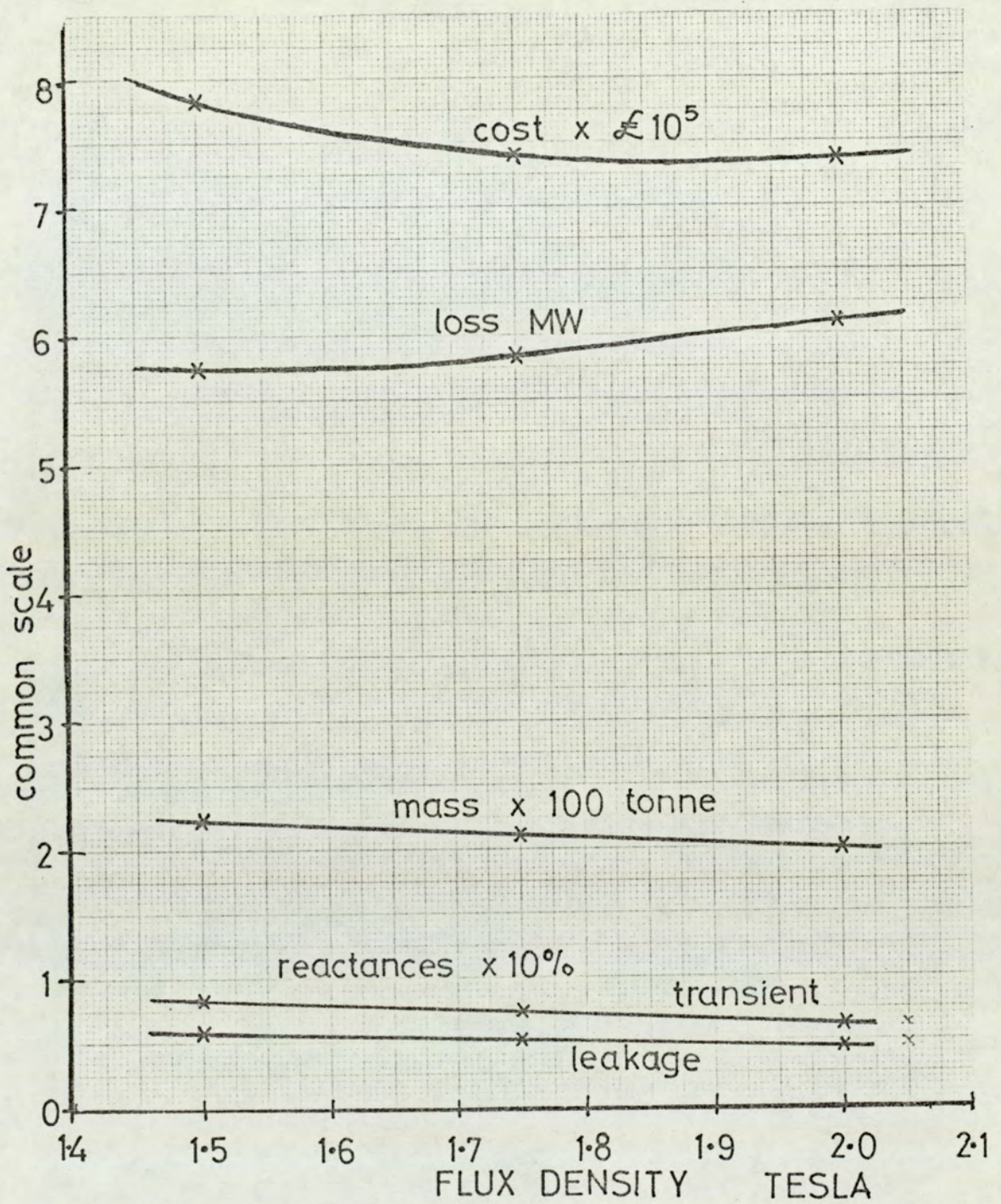


FIG.12. VARIATION OF MACHINE PARAMETERS

WITH FLUX DENSITY 660 MW, 0.85 pf.

$J_s = 300$ kA/m, $r_l = 0.6$ m $X_m = 0.75$ p.u.

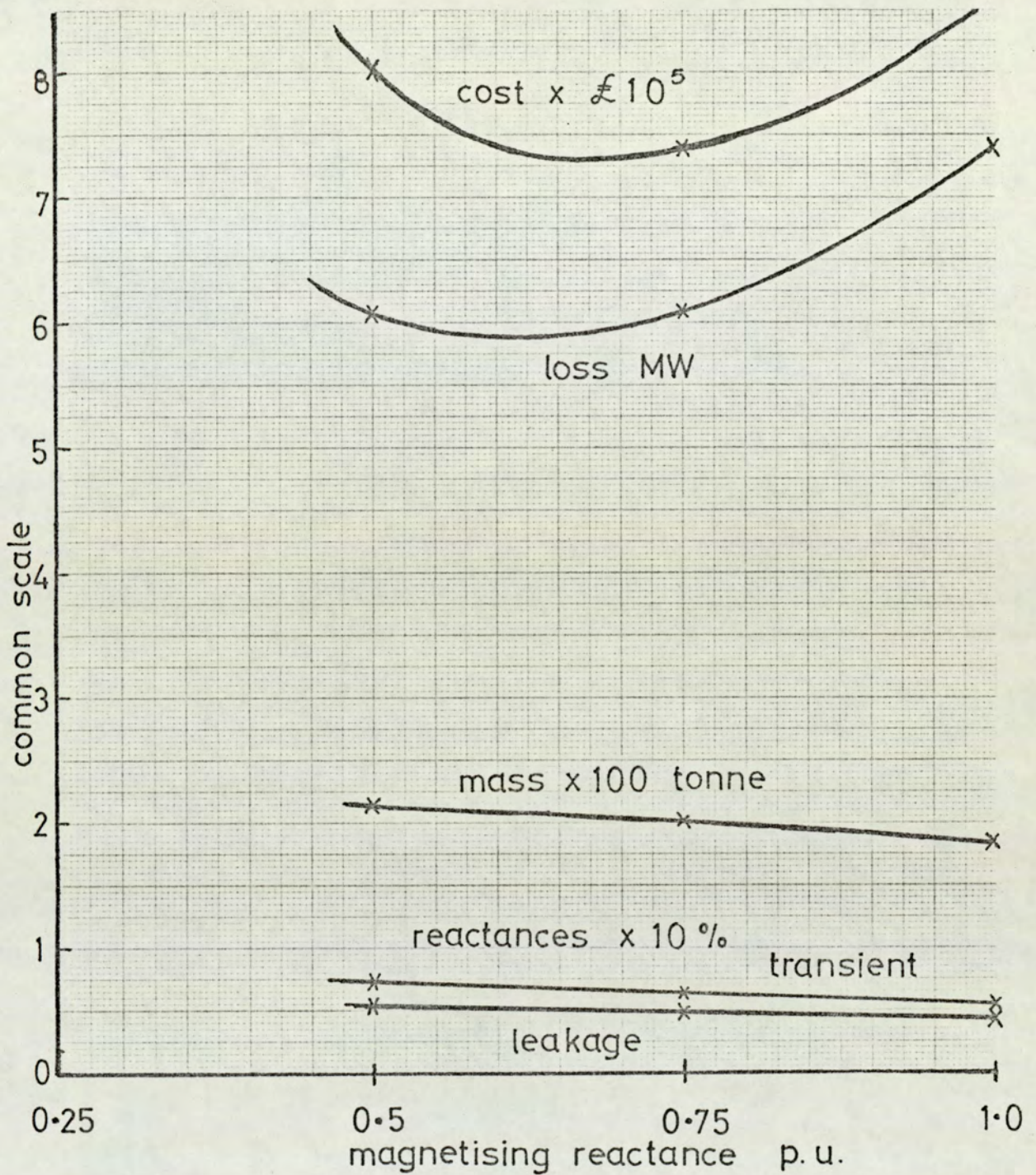


FIG.13. VARIATION OF MACHINE PARAMETERS

WITH MAGNETISING REACTANCE 660 MW, 0.85 p.f.

$J_s = 300 \text{ kA/m}$, $B = 2 \text{ T}$, $r_i = 0.6 \text{ m}$

Table 4

Comparison of alternative 660 MW designs.

Feature	1 (Optimum)	2	3	
Electric Loading	300	400	400	kA/m
Flux Density	2.0	1.75	2.0	T
Length	3.644	3.124	2.733	m
Rotor Radius	0.6	0.6	0.6	m
Magnetising Reactance	0.743	0.988	0.991	p.u
Transient Reactance	0.064	0.11	0.099	p.u
Leakage Reactance	0.048	0.084	0.078	p.u
Total Weight	202	167	159	tonne
Total Loss	6.224	6.391	6.939	MW
Total Cost	750,000	763,000	797,000	£
Adjusted Total Cost	1,155,000	1,168,000	1,136,000	£

Table 5.

Weighting factors used to allow for manufacturing costs.

Item	Weighting Factor
Rotor Steel	4
Stator Iron	3
Insulation	6
Copper	3
Carbon Fibre	5

3.3.3 Leakage Reactance and Forces during faults.

The adjusted total costs of the three designs are so close that the choice between them may be made on technical rather than economic grounds. The ability of the machine to withstand the high forces during faults is most important and calls for a moderately high sub-transient reactance to limit fault current to a tolerable level.

The leakage or sub-transient reactances of the 400 kA/m designs are higher and will more effectively limit fault currents than that of the 300 kA/m design despite the higher steady state base current. For example it is 18% less for the 2T, 400 kA/m design and 25% less for the 1.75T, 400 kA/m design compared with the 2T, 300 kA/m design. These figures correspond to reductions in end winding forces of 33% and 54% respectively. The forces occurring on the airgap portion depend upon the distribution of the leakage reactance as demonstrated in appendix 2. Comparative figures for the three designs are given in table 6 for faults occurring at the generator terminals and at the transformer terminals. A leakage reactance of 15% is assumed for the transformer.

Table 6 Comparison between fault forces for various designs.

Design				Terminal Fault		Transformer Fault	
Js kA/m	B T	r, m	Xm p.u.	End Winding Region	Active Region	End Winding Region	Active Region
300	2	0.6	0.74	100%	100%	100%	100%
400	1.75	0.6	0.99	46%	69%	127%	96%
400	2	0.6	0.99	67%	90%	134%	115%
300	2	0.7	0.74	51%	81%	83%	92%
400	1.75	0.7	0.99	29%	55%	97%	85%
400	2	0.7	0.99	33%	70%	101%	101%

For comparison a conventional machine would have 12% end winding force for a terminal fault and 43% for a transformer fault. The stress at the stator bore represented by 100% in the active region is 23.6 MN/m (see appendix 2).

The last three designs in table 6 are obtained by increasing the radius of the first three; this increases the airgap and the leakage flux in the active region and increases the end winding leakage reactance. The forces are thereby reduced, particularly in the most critical area, the end windings, during a terminal fault. The total cost after the adjustment to allow for manufacture is increased by about £150,000 by the change in radius, but the total loss is slightly less.

In general, the leakage reactance can be increased by increasing the rotor radius or the airgap. The former is more effective as can be seen from table 6. Considering the third design; a 17% increase in r , halves the force on the end winding whereas a similar increase in g (changing from 2.0 to 1.75 Tesla, causes a 16.5% increase in g) reduces this force by 31%.

Increasing the rated electric loading J_s also increases the leakage reactance (as shown by table 4) and reduces the fault

forces. However, during steady-state operation the forces are higher and the conductors are more likely to suffer metal fatigue and eventually to crack. This is a severe problem on present machines operating at about 300 kA/m, so that higher values of J_s must be accompanied by improved end winding supports.

3.3.4 Choice of Design variables.

Table 6 lists six designs. The first three (0.6m radius) are preferable on economic grounds, the others (0.7m radius) are preferable on the grounds of fault current limitation. The choice of radius will depend upon the feasibility of restraining the higher forces in the cheaper designs or of preventing terminal faults by using enclosed leads between the generator and the transformer.

On economic grounds there is little to choose between the 300 and 400 kA/m designs. The lower figure would be preferred technically because of the lower steady state end winding vibration. The higher figure gives smaller forces during faults but the forces can be as effectively reduced by using a larger radius.

The flux densities and magnetising reactances given in table 6 are chosen on economic grounds. It can be seen from fig. 12 that reducing the flux density will increase the material cost. The adjusted cost would be increased considerably (by £100k at 1.75T, £280k at 1.5T) for a very small increase in leakage reactance. It can be seen from fig. 13 that any reduction in X_m from the optimum would result in a severe cost penalty.

The preferred design, therefore, is the optimum cost design whose parameters are given in section 3.3.1. Should the low sub-transient reactance be a major drawback, the most suitable remedy is to use a larger radius.

3.3.5 660 MW designs with gas cooled rotors.

The total adjusted costs for 660 MW machines with gas cooled rotors appear to be rather higher than for those with water cooled rotors because a larger duct area is required in the rotor winding making the loss higher. The gas cooling is impossible if the rotor winding current density is too high, so it is necessary to use larger airgaps and lower flux densities to keep the current density within the capacity of the gas cooling system.

The assumptions made for the calculations are that the space factor, k_{RO} , of the rotor winding is 60%, the remaining 40% being occupied by 25% insulation and 15% by a labyrinth of passages leading from a space beneath the winding to the airgap. This space is assumed to be of a depth suitable for delivering the required quantity of gas from the end of the rotor to the winding. The gas is assumed to be hydrogen at an absolute pressure of 4 bar travelling at 100 m/s in the space and with a temperature rise of 60°C. Thus 1 m³ may absorb 5 kJ of heat. The equations used for the optimisation of the airgap subdivision are the same as those used for the water cooled rotor machine but with different constants for the rotor and stator cooling systems.

The following designs, Table 7, emerged as the cheapest and appear to be quite attractive technically. However they have higher costs compared with the water-cooled designs.

Table 7 Gas Cooled 660 MW Designs.

Stator water flowing at 1.5 m/s, 40°C temp. rise;
 Rotor gas flowing at 100 m/s in sub space, temp. rise 60°C,
 400 kN/m² abs. (1 m³ absorbs 5 kJ)

Design	1	2	3	4	5	
Radius	0.6	0.6	0.7	0.7	0.7	m
Gap field	2.0	1.5	2.0	1.5	1.75	T
Stat load	400	400	300	300	400	kA/m
Mag react	0.48	0.73	0.49	0.74	0.74	pu
X'd	11.8	13.3	9.1	10.0	15.2	%
X" d	9.1	9.9	7.3	7.8	12.5	%
airgap	392	338	3.21	279	327	mm
Outer rad	1.70	1.49	1.84	1.62	1.76	m
Length	2.73	3.64	2.68	3.57	2.30	m
Rotor Load	1146	875	845	646	884	kA/m
Rotor mass	59.6	66.9	71.6	82.2	65.4	tonne
Stator mass	126	119	152	143	114	tonne
Rotor wdg depth	214	176	156	130	156	mm
Rotor bdg depth	92.4	73.0	85.5	69.9	83.2	mm
Stat wdg depth	35.4	38.8	29.3	29.0	37.9	mm
Rotor space factor	0.38	0.36	0.32	0.31	0.31	-
Stator space factor	0.44	0.48	0.44	0.44	0.48	-
Rotor Fe wt	43.3	51.3	58.1	69.1	53.5	tonne
Rotor Cu Wt	11.9	11.2	9.0	8.7	7.9	tonne
Rotor Ins Wt	2.2	2.2	2.0	1.9	1.8	tonne
Rotor bdg wt	2.23	2.15	2.49	2.46	2.21	tonne
Stator Cu Wt	6.6	8.2	5.6	5.6	7.6	tonne
Stator Ins wt	3.1	3.4	3.0	3.1	3.2	tonne
Xe	5.8	5.8	5.2	5.2	9.2	%
Xg	3.3	4.2	2.2	2.7	3.3	%
Rot I ² R	2651	2394	2854	2452	2967	kW
Stat I ² R	4355	3812	3085	3338	3678	kW
Eddy	877	742	727	513	682	kW
Iron	526	458	643	564	460	kW
Friction	596	669	716	822	654	kW
Total loss	9004	8077	8026	7690	8443	kW
Total cost	1635	1563	1596	1589	1568	k£

Rotor Winding—15% gas ducts, 25% insulation,
 rest occupied by sub slot gas duct and copper
 Stator winding—8 mm insulation to core and to gap,
 40% of periphery is interturn insulation,
 remainder copper strands 2 mm thick and strand insulation .2mm.

3.4 Upper Limit Design.

It was seen that a wide choice exists between various 660 MW designs. We shall now examine a design which offers little scope for variation. If every dimension and loading is set at the upper practical limit, the designer may choose only the magnetising reactance. The basic dimensions and loadings are therefore:

$$\begin{aligned} B &= 2T \\ r_1 &= 740\text{mm} \\ l &= 12\text{m} \\ J_s &= 300 \text{ kA/m} \\ \text{Rating} &= 3950 \text{ MVA (3350 MW at 0.85 pf)} \end{aligned}$$

If an electric loading of 400 kA/m were permitted the rating could be increased to 5250 MVA 4450 MW.

This is basically a lengthened version of the 660 MW, 300 kA/m, 2T, 0.7m design for which the optimum magnetising reactance was 0.75 p.u. we may, therefore, safely assume that the optimum X_m is again 0.75 p.u. which requires the airgap to be 211 mm. The optimum stator winding depth is approximately 40 mm for a water flow velocity of 1.5 m/s and temperature rise of 40°C. The airgap is allocated in the following manner:

Stator winding depth	40 mm
Space factor	0.405
Strand width	2.0 mm
Main stator insulation	8 mm thickness each side of winding
Mechanical Clearance	34 mm
Rotor winding depth	64 mm
Space factor	0.549
Rotor binding depth	57 mm

The reactances are:

Magnetising	0.74
Transient	0.042
Sub-transient	0.026

The losses, masses and costs are given in table 8.

Table 8 Losses, Weights and Costs for 3350 MW Machine.

Region	Loss kW	Weight tonne	Matl cost £k	Adjusted Cost £k
Stator Iron	2980	673	168	802
Stator Copper	I R: 5070 Eddy 3870	15.3	31	987
Stator Insulation	-	7.6	38	228
Rotor Iron	Bearing loss 2230	200	181	946
Rotor Copper	7460	20.9	42	876
Rotor Insulation	-	2.7	13.5	8.1
Rotor Binding	-	6.51	163	815
Total	21,620	926	636.5	4735

The high efficiency and low cost of this machine are attractive features, the total cost being 1.41 £/kW compared with 1.74 £/kW for the 660 MW machine and typically 2-3 £/kW for large conventional machines.

The high mass and low sub-transient reactance are major drawbacks. The former is a result of the extremely high rating and it cannot be reduced significantly. The low sub-transient reactance is more serious and could be increased by using a larger electric loading or lower magnetising reactance as discussed in connection with the 660 MW machine.

3.5 100 MW Design.

For this relatively small rating a large number of good designs could be produced giving low loss and total cost. The following design was chosen from many for illustration because of its low cost, comparatively high leakage reactance and low current loading which simplifies the necessary end bracing.

Rating	118 MVA,	0.85 pf
Synchronous Reactance		0.81 p.u.
Transient Reactance		0.081 p.u.
Sub-transient Reactance		0.068 p.u.
Stator Current Loading		200 kA/m
Rotor Current Loading		426 kA/m
Flux density		1.5 T
Rotor radius		0.5 m
Active length		1.59 m
Airgap		125 mm
Outer radius of stator iron		1.07 m
Stator winding depth		22.3 mm
Space factor		0.503
Strand Width		2.0 mm
Rotor winding depth		36.3 mm
Space factor		0.704
Rotor binding depth (carbon fibre)		16.5 mm
Clearance and main insulation		50 mm
Rotor mass		24.9 tonne
Stator mass		31.2 tonne
Rotor I ² R loss		656 kW
Stator I ² R loss		610 kW
Eddy current loss		130 kW

Iron loss	120 kW
Bearing friction loss	249 kW
Total loss	1764 kW
Total adjusted cost	333 k£

Lower values of stator current loading would result in an unacceptably low leakage reactance. The choice of J_s is therefore a compromise between limiting the end winding vibration and limiting the effects of fault current.

3.6 Range of Viable Ratings.

The specific power and cost of the three design studies are used to construct fig. 14 which shows roughly the expected values of these parameters over a wide range of ratings. By extrapolation it can be inferred that the specific cost will be excessive for machines much smaller than about 100 MW. This is caused partly by the increasing importance of the end turn loss as the machine gets shorter and partly by the cost of materials in the end region. The reduced specific output is caused by using lower flux densities and current loadings than in the larger machines and by the higher relative amount of material in the end region.

It would be possible to overcome these tendencies by reducing the rotor radius but the sub-transient (i.e. leakage) reactance would become intolerably small.

Thus the lower limit to the range of ratings in which slotless machines may be usefully employed is about 50 to 100 MW. The upper limit has been considered previously and is 3 to 3.5 GW for currently available materials and modest electric loadings.

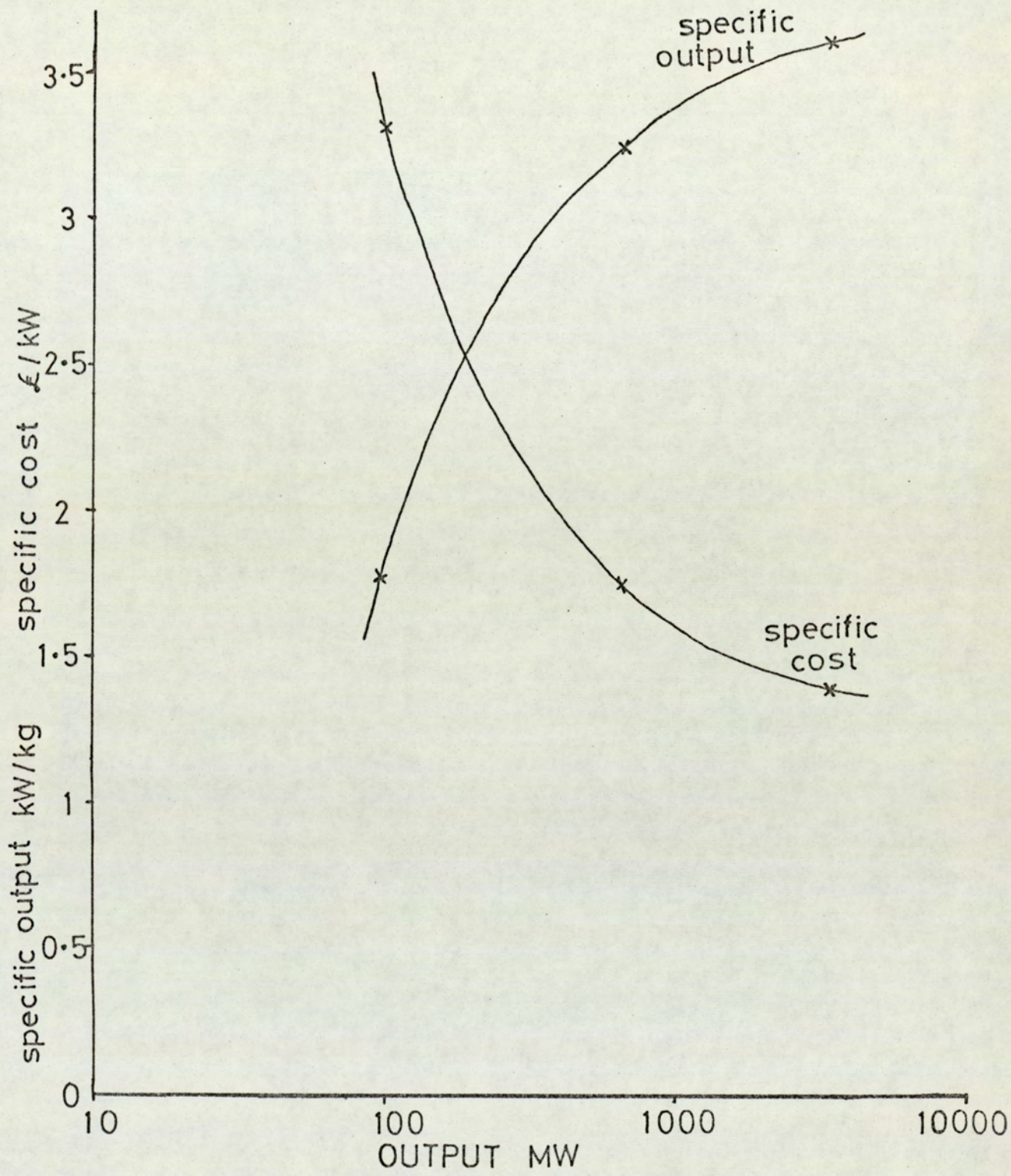


FIG.14. EFFECT OF RATING ON TOTAL MASS & COST

Chapter 4.

Detailed Design.

- 4.1 Winding Arrangements
 - 4.1.1 Stator windings
 - 4.1.1.1 Three-phase interspersed windings
 - 4.1.1.2 Twelve-phase windings
 - 4.1.1.3 Stator winding end turns
 - 4.1.2 Rotor windings
 - 4.1.2.1 Single layer concentric windings
 - 4.1.2.2 Double layer concentric windings
 - 4.1.2.3 Double layer helical windings
- 4.2 Attachment of windings
 - 4.2.1 Stator windings
 - 4.2.2 Rotor windings
 - 4.2.2.1 Radial forces
 - 4.2.2.2 Tangential forces
- 4.3 Stator conductor design
- 4.4 Cooling arrangements
 - 4.4.1 Cooling system requirements
 - 4.4.2 Stator core cooling methods
 - 4.4.3 Stator winding cooling
 - 4.4.4 Rotor cooling system
 - 4.4.5 Overall cooling system

4.1 Winding Arrangements.

4.1.1 Stator Winding.

The factors to be considered in selecting a winding arrangement are:

- (i) Fundamental winding factor
- (ii) Space harmonic content
- (iii) Formation of end turns
- (iv) Ease of attachment to the iron
- (v) Utilisation of winding space

For a high utilisation of the space and for mechanical strength, a single-layer arrangement is preferred because less insulation is required. The quantity of inter-turn insulation needed depends partly upon the voltage appearing between adjacent turns. It is prudent therefore to avoid the mixing of phases; that is to keep the number of conductors adjacent to ones of different phase to a minimum. Phase mixing is useful, however, in reducing space harmonics and is equivalent to short pitching in a conventional double-layer winding.

Two basic types of winding are of interest: three-phase windings with phase mixing (or interspersed) and twelve-phase windings without phase mixing (sometimes known as six-phase or split three-phase windings).

4.1.1.1 Three-phase Interspersed Windings.

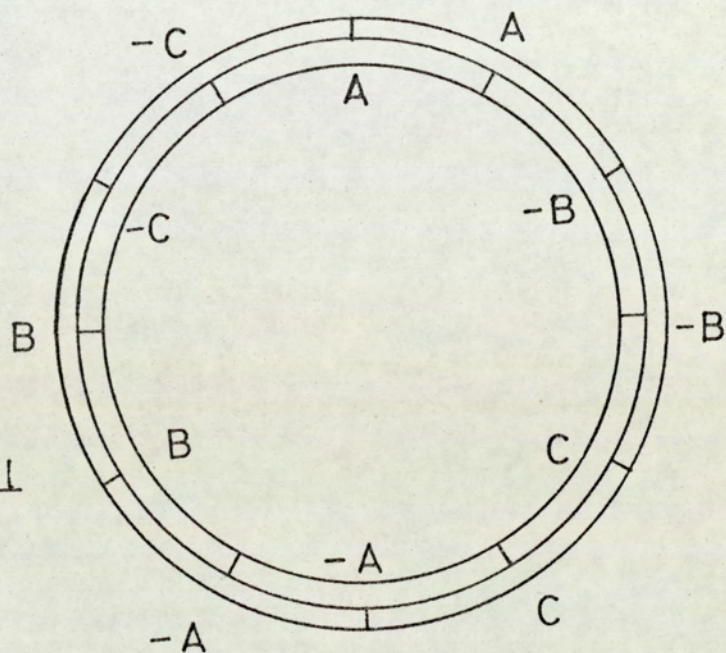
Figs. 15 and 16 illustrate the development of the single-layer interspersed winding from the conventional two-layer short-pitched winding. If the conductors are interleaved in groups rather than singly, the amount of inter-turn insulation needed is slightly less. The form of interleaving can be described using Chalmers' (1964) notation, in which the groups of conductors in one phase belt are denoted by the numbers of conductors in the separate groups. For example fig. 16a is denoted 1-1-4-1-1 whereas fig. 16b is 2-4-2.

Clearly many variations of this type of winding are possible. The fundamental and harmonic winding factors of a number of promising versions are given in table 9, along with those for a conventional $5/6$ -pitch 60° -spread winding in the limiting case of an infinite number of slots (conductors) per pole and phase. The only windings with lower harmonics than the conventional winding have large numbers of turns and will produce high voltage and require thick insulation. Types 1-4-1, 1-5-1, 1-1-4-1-1 and 1-1-5-1-1 offer suitable compromises between harmonics and insulation requirements. The stray loss induced in the rotor by the fields of the harmonic components of the winding is also listed in table 1 for typical machine dimensions.

Some of the interspersed arrangements give a considerable reduction in this loss. The calculation of rotor surface loss is given in appendix 3.

FIG 15 SHORT-PITCH WINDINGS

(a) two-layer conventional type



(b) single layer type showing overlapping phase bands

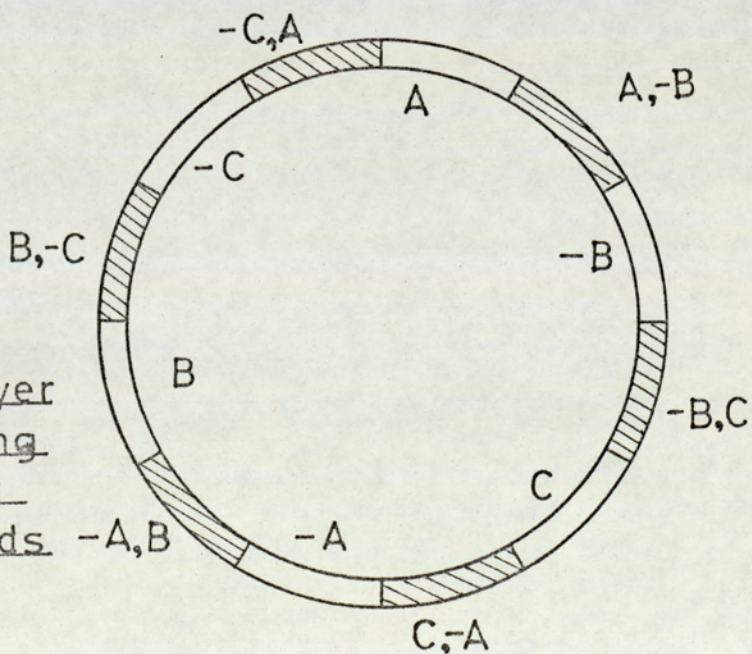
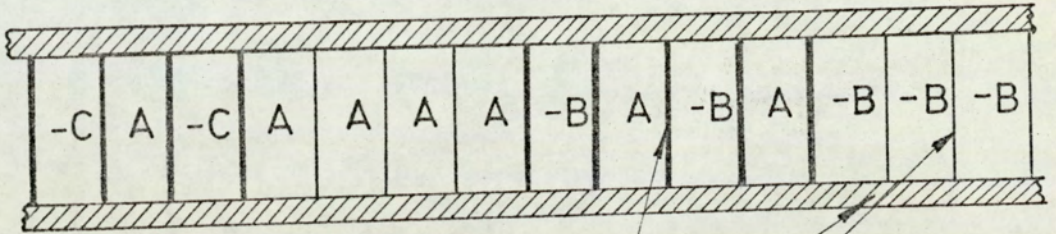
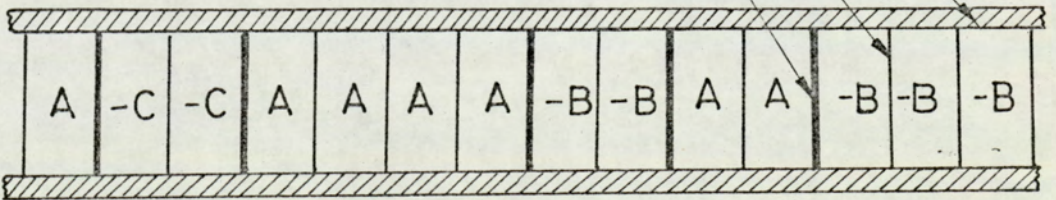


FIG 16 INTERLEAVED WINDINGS .

(a) fully interleaved



main insulation
inter-turn insulation
inter-phase insulation



(b) interleaved groups

Table 9.

Winding Factors of Interspersed Windings and
Corresponding Loss in a Typical Machine

Type	1	5	7	11	13	loss W/m ²
1-3-1	0.913	0	0.108	0.208	0.208	11 940
1-4-1	0.926	0.055	0.043	0.146	0.168	8 390
1-5-1	0.934	0.089	0	0.100	0.127	12 130
2-5-2	0.903	0.040	0.152	0.232	0.219	20 040
2-7-2	0.920	0.031	0.072	0.074	0.018	8 570
2-9-2	0.930	0.074	0.019	0.122	0.147	9 880
2-11-2	0.936	0.102	0.016	0.081	0.109	14 780
3-10-3	0.918	0.021	0.083	0.183	0.196	9 230
3-11-3	0.922	0.039	0.062	0.163	0.182	8 260
3-13-3	0.929	0.068	0.027	0.129	0.154	9 160
3-14-3	0.931	0.079	0.013	0.114	0.140	10 590
1-1-4-1-1	0.906	0.013	0.100	0.104	0.049	6 210
1-1-5-1-1	0.916	0.023	0.067	0.108	0.081	4 370
1-1-6-1-1	0.924	0.051	0.038	0.100	0.091	5 640
1-1-7-1-1	0.929	0.073	0.014	0.087	0.090	8 330
1-2-4-2-1	0.903	0	0.052	0.038	0.121	2 040
1-2-5-2-1	0.912	0.024	0.041	0	0.065	1 710
1-2-6-2-1	0.919	0.044	0.028	0.022	0.026	3 070
1-2-7-2-1	0.924	0.062	0.013	0.032	0	5 310
5/6 pitch 60° spread						
Many conductors	0.923	0.052	0.037	0.088	0.074	4 860

4.1.1.2 Twelve-Phase Windings.

The three-phase arrangements all have one or more of the following drawbacks:

- (i) Space harmonics producing high stray loss in the rotor surface.
- (ii) Large numbers of turns producing high voltage and needing excessive insulation.
- (iii) Complicated mixing of phases giving poor space utilisation.
- (iv) Poor fundamental winding factor (~ 0.9 in some cases) giving reduced specific output.

This justifies examination of a radical alternative such as the twelve-phase arrangement.

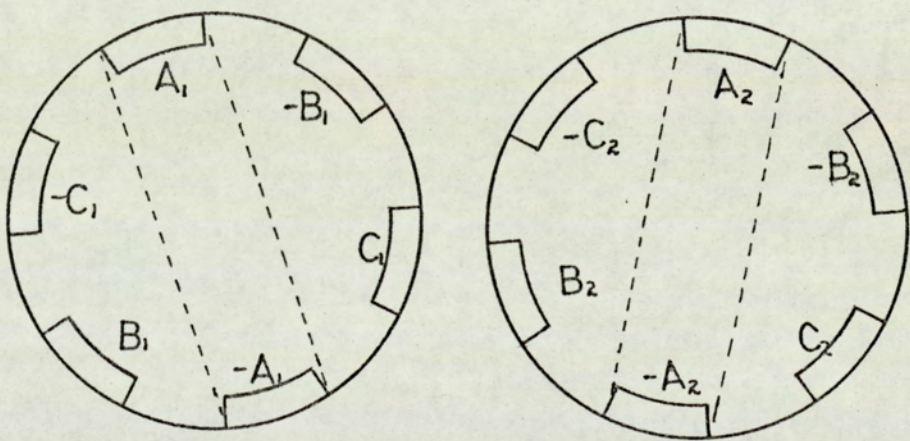
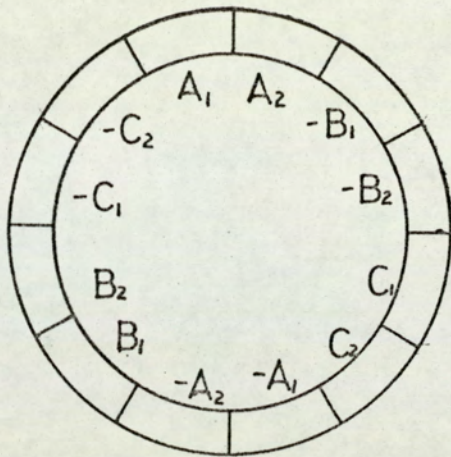
Robert, Dispaux and Dacier (1966) suggested that the losses in conventional machines might be reduced by using a twelve-phase winding. In airgap-wound machines it can be shown that there are additional benefits.

The twelve-phase winding consists of two three-phase windings each with full-pitch coils of 30° spread. The two windings are separated by 30° spatially and produced output voltages differing by 30° in phase. Fig. 17 illustrates this combination.

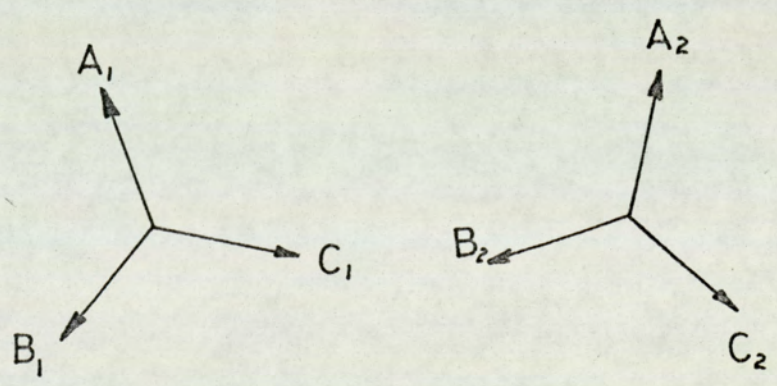
The two sets of three-phase output voltages and currents can be combined at the generator transformer into a single set by passing one through a star-delta transformer and the other through a star-star or delta-delta transformer. Appendix 1 examines a number of possible variations on this basic transformer arrangement.

The simple arrangement shown in fig. 17 embodies all the advantages of the twelve-phase winding. The fundamental winding

12-phase arrangement



3-phase components



output voltage

FIG. 17. TWELVE-PHASE WINDING

factor is very high (0.989). The harmonic content is low (5th and 7th are absent, 11th and 13th winding factors are 9.1% and 7.8%). The space utilisation can be rather better than for three-phase windings because a given output can be achieved with a lower terminal voltage. The output current is restricted by the design of generator leads and transformers. Also more economical use can be made of the trough and lid fixing arrangement described in 4.2.1.

The principal disadvantage of the twelve-phase system is the duplication of the leads and transformer. For machines of less than 500 or 660 MW rating this would be a severe penalty and would outweigh the benefits. However, for larger ratings the possibility of splitting the leads and transformer into smaller units might be welcomed and could be a positive advantage.

The choice of stator winding is clear. For large ratings the twelve-phase type is preferable. For smaller ratings the three-phase type, although not the best technically, gives the lowest overall cost. The dividing line is the maximum rating for which a single three-phase transformer could be built.

4.1.1.3 Stator Winding End Turns.

As the conductors of a conventional machine emerge from the end of the core, the space left by the teeth allows a sharp bend to be made, which is essential to keeping the end turns short. With an airgap winding it is necessary either to introduce gaps between conductors at the ends or to use a different form of end winding from the conventional involute type.

The concentric arrangement proposed by Davies (1967) does not require such gaps but requires the conductors to be formed into rather complicated shapes and is only applicable to three-phase windings.

Gaps can be introduced conveniently by bending alternate conductors inward or out to form a second layer, each with gaps, the end winding could then be similar to a conventional one. This is illustrated in fig. 18.

For ease of assembly it is wise to build the winding as a small number of blocks or modules. This can be done if the conductors are bent in groups (as in fig. 19) rather than individually and if the cone angle of the end winding is small, or, preferably, zero. Figs. 19 and 20 illustrate such an end winding arrangement and fig. 21 is a connection diagram for two phases of such a winding with 48 conductors. The phases are denoted as $A_1, B_1, C_1, A_2, B_2, C_2$, to identify the two three-phase sets. This arrangement employs 24 coils, each phase consisting of two coils which may be connected in series or parallel. This type would be equally suitable for a three-phase winding although complications could arise with interspersing of the phases.

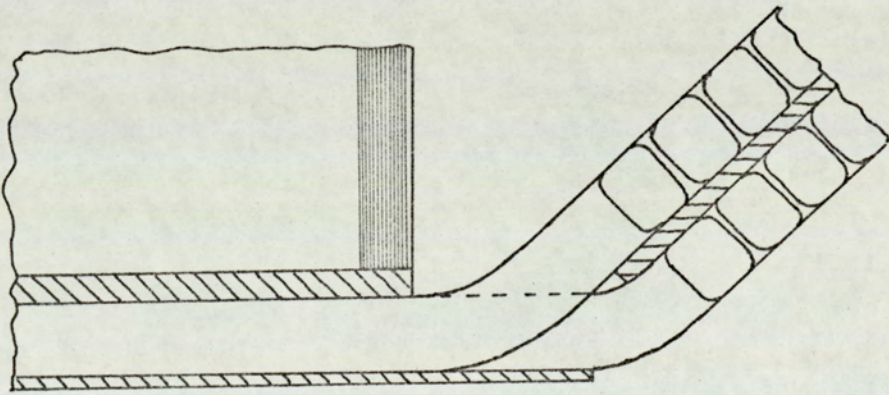
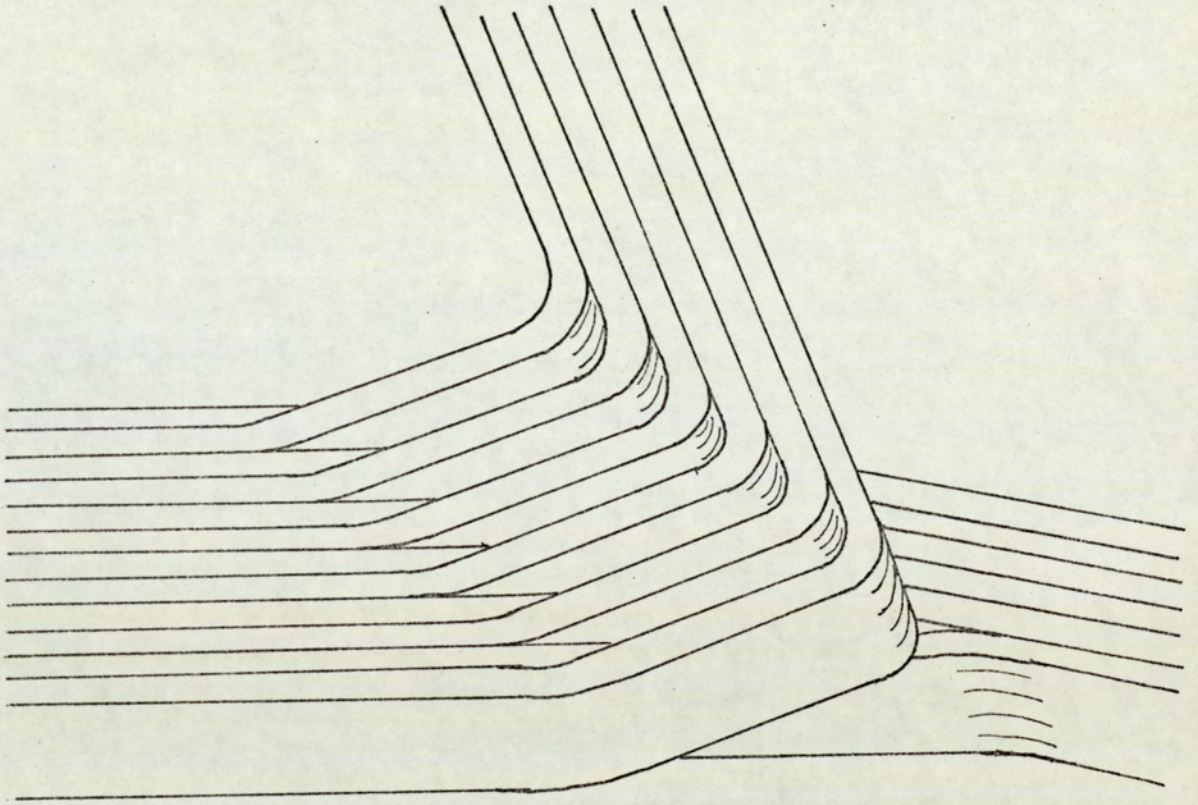


FIG 18 A METHOD OF FORMING END TURNS

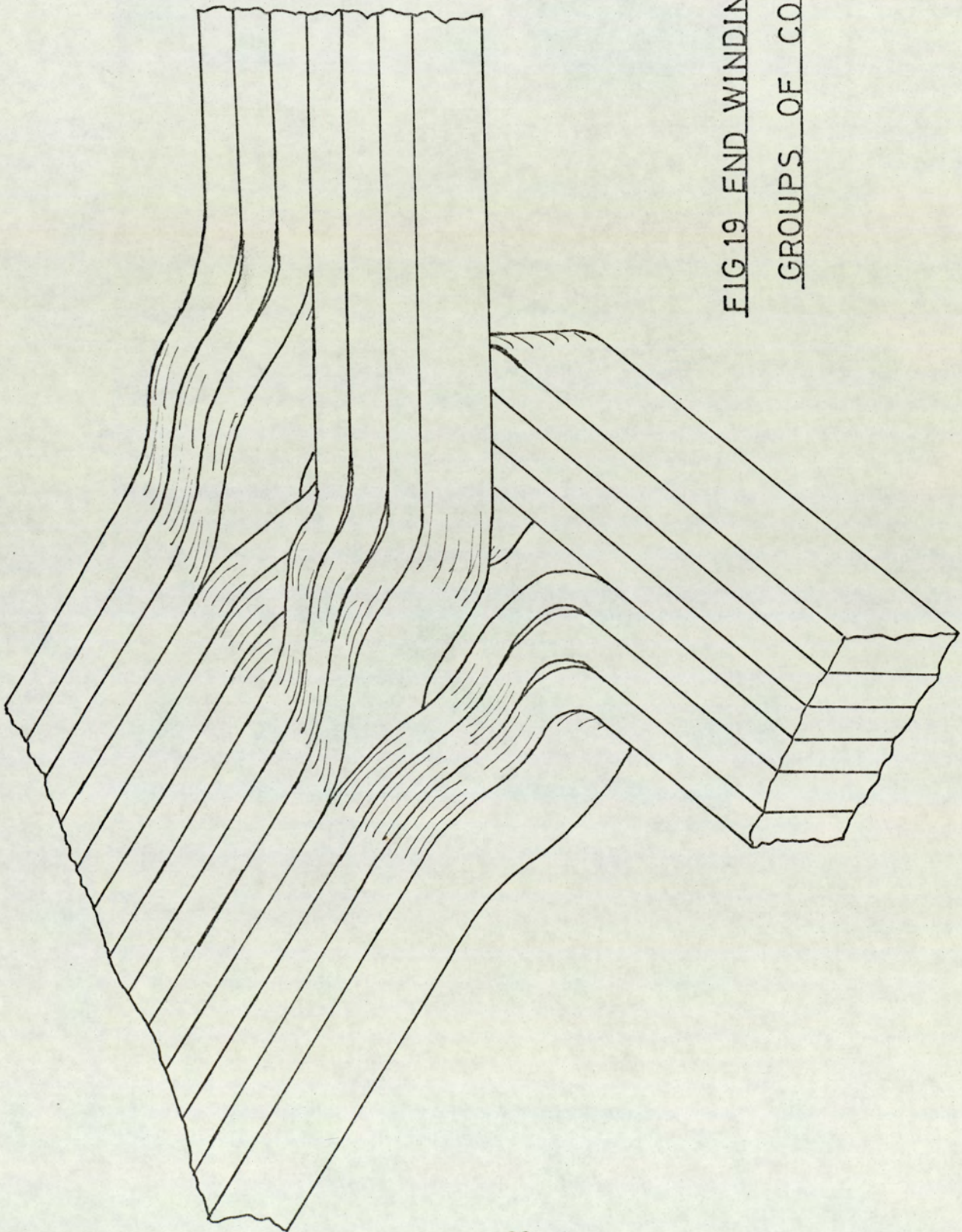
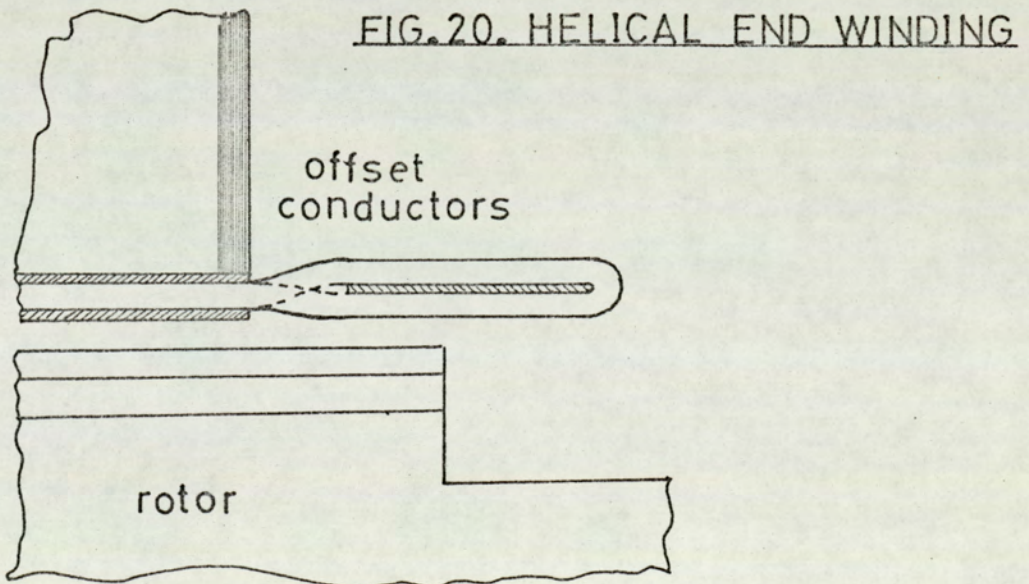


FIG 19 END WINDING FORMED BY
GROUPS OF CONDUCTORS

4.1.2 Rotor Windings.

The rotor winding should be reasonably free from harmonics which could induce voltages in the stator and should generate the fundamental m.m.f. using minimum total ampere turns. A uniform distribution of conductor around the rotor surface would produce a uniform mechanical loading on the binding. Means of connecting several paths in parallel would give some electrical damping in the quadrature axis. The arrangement of the end turns will determine the ease with which coolant can be fed to the conductors for direct liquid cooling.

Three basic types of field winding are examined on the basis of the above requirements.



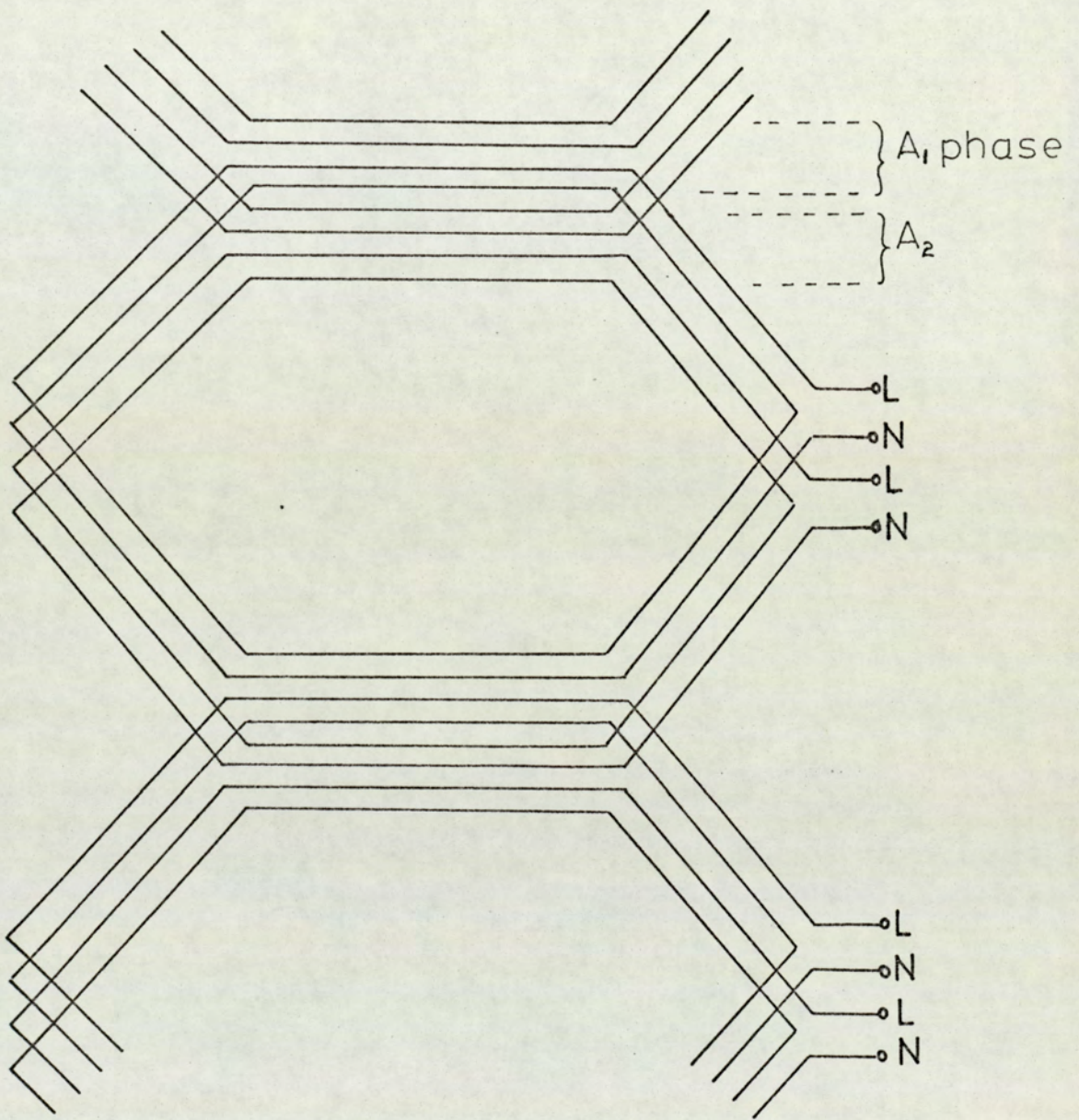


FIG. 21. CONNECTION DIAGRAM FOR TWELVE
-PHASE WINDING

1.2.1 Single Layer Concentric Windings.

The simplest form of this type of winding consists of two flat spiral coils as shown in the development diagram fig. 22. The main problem is the provision of connections to the centre of each coil. If a damper circuit has to be incorporated in the rotor, it could take the form of a continuous sleeve over the field winding; it could then serve the purpose of transferring current between the coil centres or to the end of the rotor. One alternative is to locate the leads in grooves in the rotor surface, but this would be unsatisfactory because of the stress concentrations which would arise in both the body and cover of the rotor.

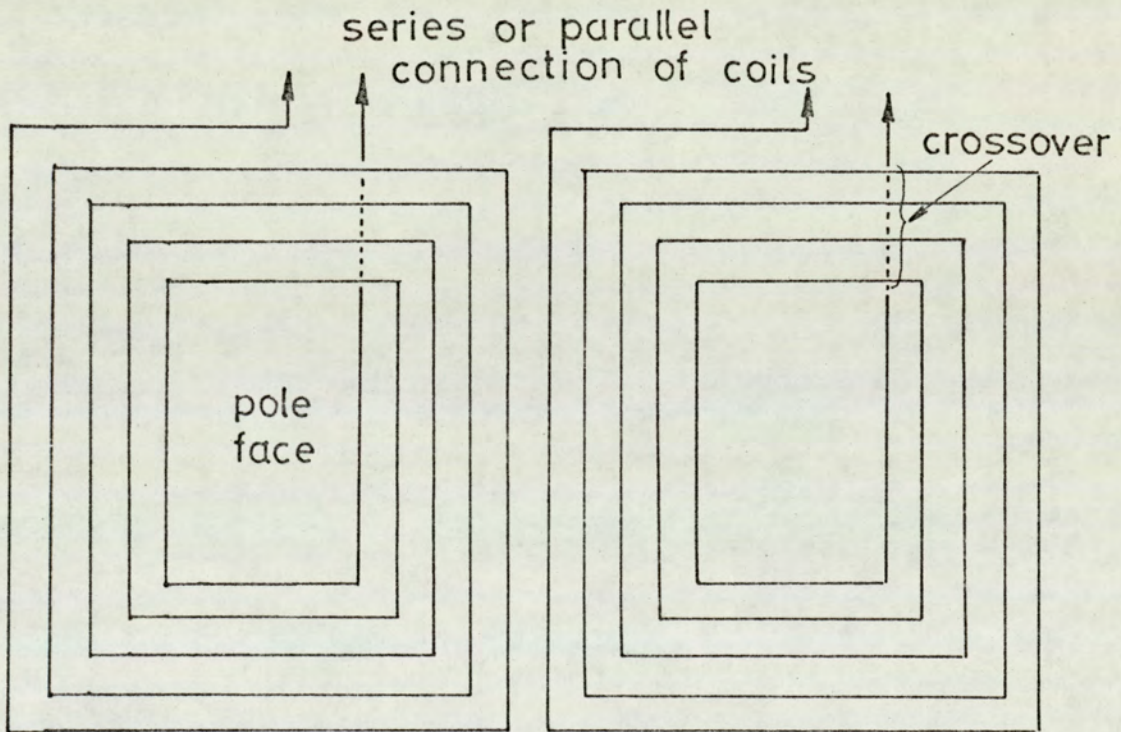
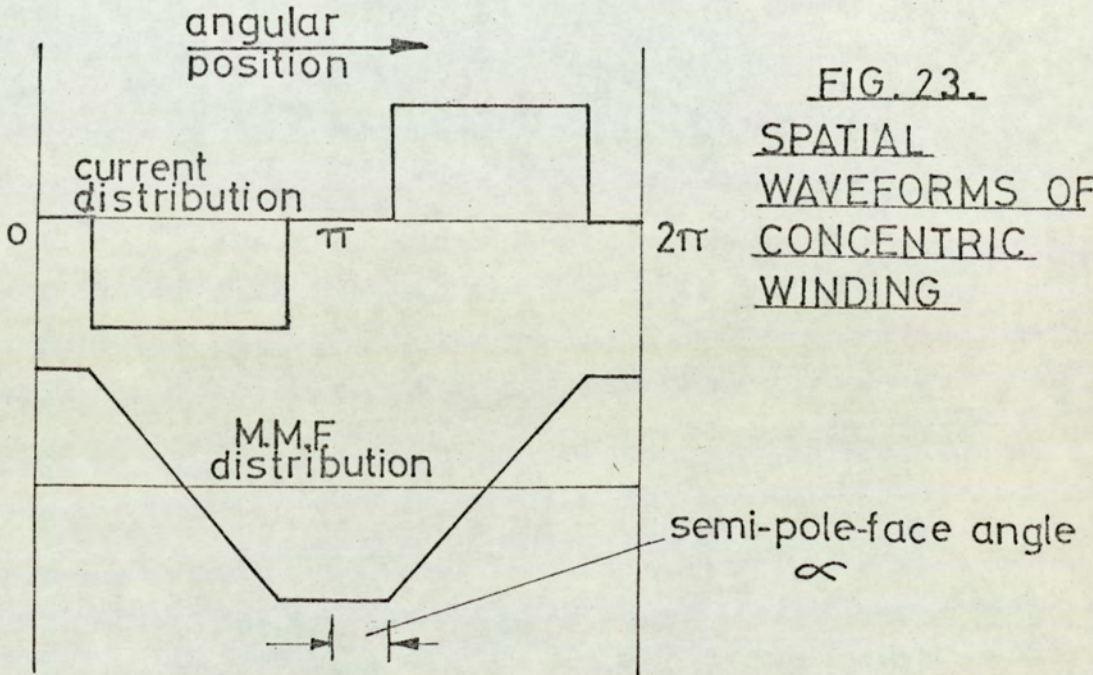


FIG.22. DEVELOPED DIAGRAM OF CONCENTRIC SINGLE-LAYER ROTOR WINDING

The current and m.m.f distributions around the rotor surface are shown in fig. 23. The space harmonics content is high but by suitable choice of the semi-pole-face angle α , those which

could induce armature voltages can be limited to a tolerable level. Indeed the field windings of conventional machines give the same distributions without generating excessive harmonic armature voltages.



The geometry of the end turns makes the design of a direct liquid cooling circuit difficult, because supply pipes must pass under or over the outer end turns to reach the inner turns of the coil. This presents the same problem as the inner electrical connection. Indirect liquid cooling or gas cooling however will avoid the problem.

Although it uses simple coil shapes, the single layer concentric winding may be very complicated at the ends so it will be suitable only if a damper circuit together with gas or indirect liquid cooling were employed.

4.1.2.2 Double layer Concentric Windings.

If two concentric coils are mounted one above the other, the electrical connections at their centres may be made by connecting them in series so that no cross-overs would be needed. The top and bottom windings could be displaced by a small angle which would reduce the space harmonic content and allow the choice of semi-pole face angle to be made on the basis of minimising the copper loss.

The problem of feeding liquid coolant to the conductors is more severe than in the single-layer winding because there must be more pipes of smaller cross-section and routes must be provided to both top and bottom layers.

The distribution of the mass of the winding contains smaller discontinuities if the two layers are displaced. This will reduce the concentrations of stress in the binding.

The two-layer concentric winding is somewhat more promising than the single-layer type but still presents difficulties of coolant connections if direct liquid cooling is to be used.

4.1.2.3 Double-Layer Helical Windings.

This type of winding is essentially the same as a three-phase armature winding of zero cone angle. The mass is uniformly distributed. The harmonic content, with currents flowing in the phases equal to the instantaneous values of a balanced three-phase set, is very low in comparison with conventional field windings. Damper action in both axes can be obtained by arranging each phase as two parallel paths, as is common in armature windings, and the external parallel connection of two of the phases provides further damping. Since each half turn passes between the "noses" of the two end windings, coolant can be fed into each conductor without the need for pipes to cross over the end turns. Thus this type of winding is more readily adapted to direct liquid cooling.

Space must be provided at the ends for the conductors to bend. The solution proposed for the stator is not acceptable here because of the restricted depth available beneath the binding. The only solution which does not involve increasing the depth of the winding at the ends is to reduce the width of the conductors at the ends thereby forming gaps between adjacent conductors. This is feasible for the field winding conductors because they do not need to be subdivided and transposed, but will result in an increased loss in the end turns.

An incidental benefit of the helical winding is that it could provide excitation in any direction and might be used as a form of divided-winding rotor (see Soper & Fagg 1969).

Clearly the helical winding has many potential advantages for slotless rotors over the more conventional concentric types. These arise largely out of the need to keep the total thickness of the winding and its coolant feed pipes to that of the active part of the winding.

4.2 Attachment of Windings.

4.2.1 Stator Windings.

The stator windings must be secured to the core sufficiently firmly to withstand the electromagnetic forces which could occur under fault conditions. The magnitude of these forces are calculated in appendix 2. The most severe type of fault, a sudden short circuit at the generator terminals, is very rare owing to the enclosed design of modern generator leads, and most specifications do not require machines to withstand them. Faults at or near the output terminals of the generator transformer are more common but less severe. The transformer leakage reactance helps to limit the current, therefore, the forces are less than if the fault were at the machine terminals. Typically, the forces during a transformer fault are four to five times the steady stator forces which correspond to a stress between the stator windings and core of approximately 300 kN/m^2 .

A number of arrangements have been proposed for restraining the winding. In one arrangement, fig. 24, suggested by Davies (1968), the windings are held between two concentric insulating cylinders to form an integrated structure which can be inserted as a single piece and glued in position.

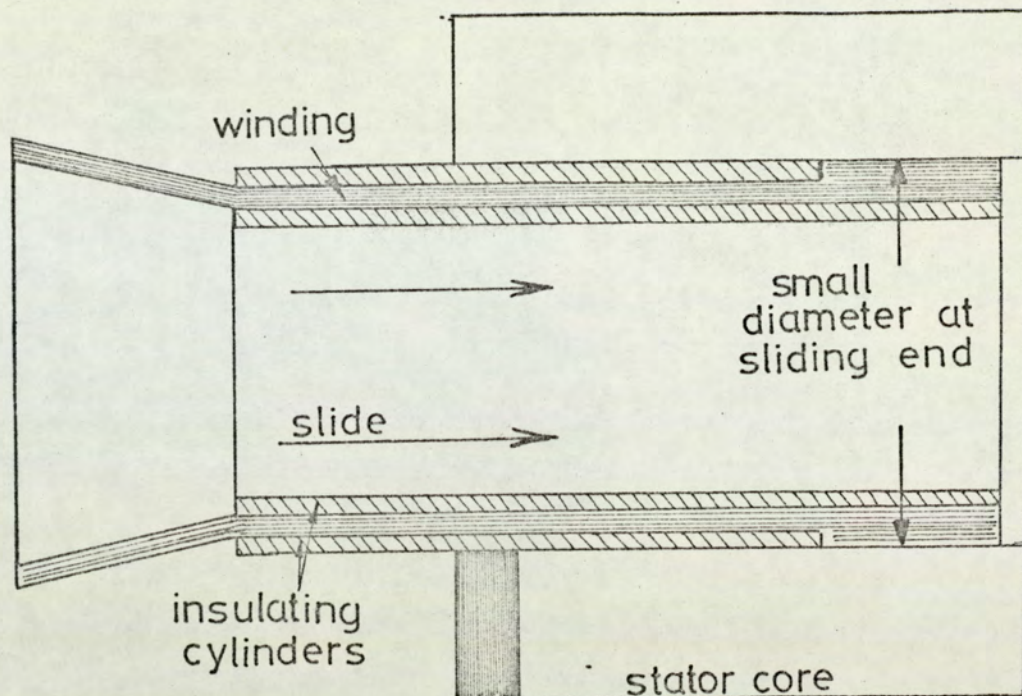


FIG.24. INSERTION OF COMPLETE WINDING INTO STATOR CORE

Another scheme, proposed by Reece and Preston (1972), is illustrated in fig. 25. The winding is divided into groups of conductors, each group being enclosed by an insulating shell formed from a trough and a lid of laminated reinforced material. The protruding ends of the troughs and lids are located in notches in the core and wedges are driven between adjacent shells to form an arch-bound structure. This structure provides good insulating properties, in addition to its good mechanical properties, due to the laminar structure of the materials and the long creepage paths between the conductors and the core.

A major problem requiring solution is the flexure of the stator core due to the magnetic force of the main field. The movement of the core can be as high as 0.1 mm from its mean position; over the lifetime of the machine this could cause serious mechanical damage to the insulating system.

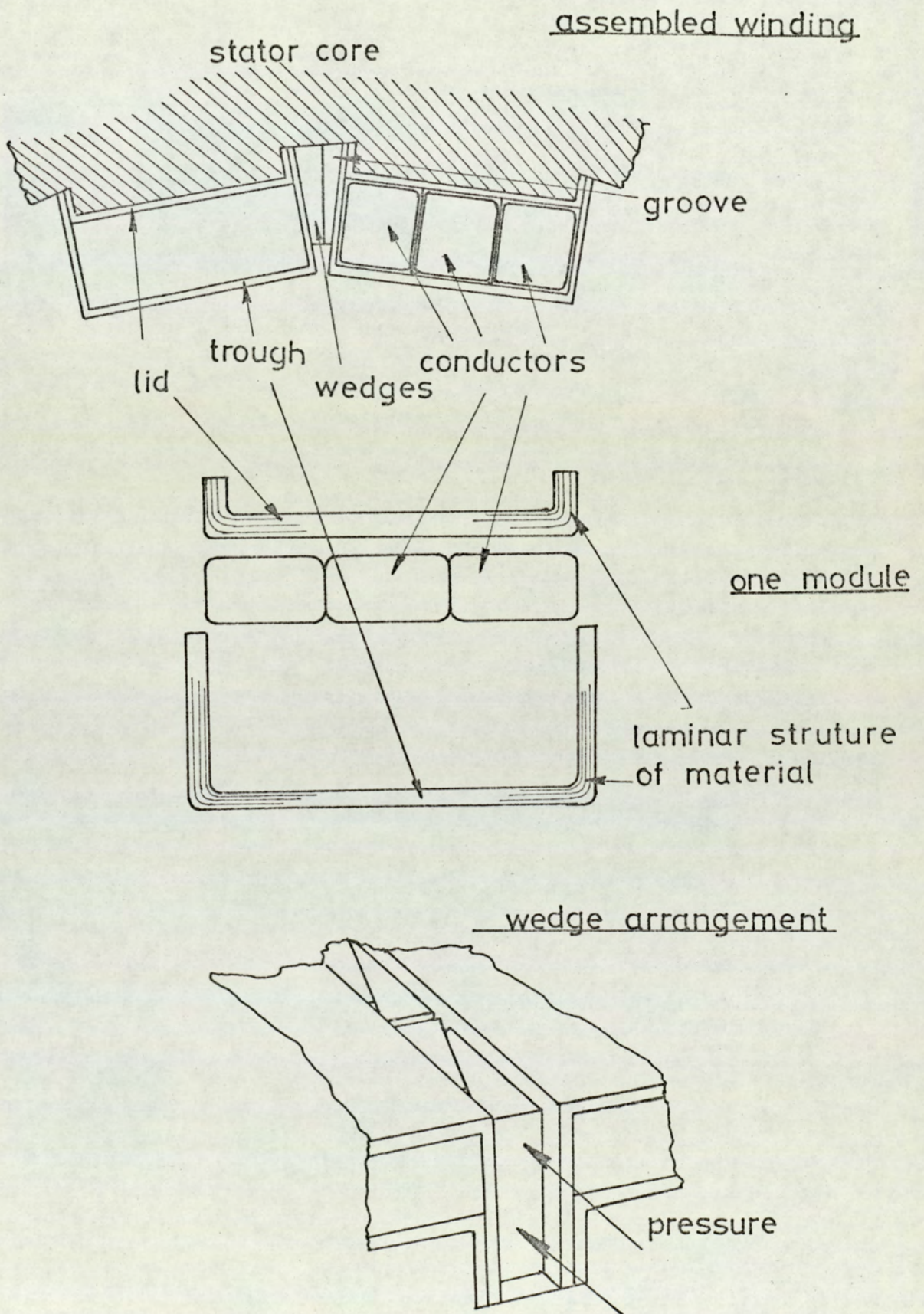


FIG. 25. TROUGH & LID SYSTEM FOR STATOR WINDING

4.2.2 Rotor Windings.

4.2.2.1 Radial Forces.

The rotor windings are subject to both tangential and radial forces. The radial forces have been considered in chapter 2. The rotor cover is stressed tangentially to balance the centrifugal forces acting on the conductors and on the cover itself. Differential thermal expansion between the rotor and its cover causes an additional component of hoop stress in the cover, which has been allowed for in the calculations of the cover thickness needed. Thermal expansion will also tend to cause an axial differential strain between the rotor and the cover and could result in serious damage to a continuous cover of composite material by separating the fibres. With other types of cover, the insulation of the windings may be damaged. Some means should be provided to allow the cover to take up the strain. The simplest solution would be to build the cover from a set of hoops, which would also permit a gas cooling system to be employed for the rotor windings. - See section 4.4.

4.2.2.2 Tangential Forces.

The tangential forces on the rotor winding balance the torque exerted by the prime mover. The resultant stress between the windings and the rotor body has an average value given by:

$$P/w.2\pi r_1^2 l.$$

which is of the order 10^5 to 10^6 N/m². Under fault conditions the stress could be up to 10 times higher.

Fig. 26 illustrates a possible arrangement for transferring this force to the rotor body. Over the active length of the rotor, strips of metal (e.g. high strength aluminium alloy) are interspersed with the field winding conductors and are either embedded in shallow grooves in the rotor body, or welded to the surface. The end turns of the field winding are not subjected to tangential forces, therefore, the strips need not extend into the end turns.

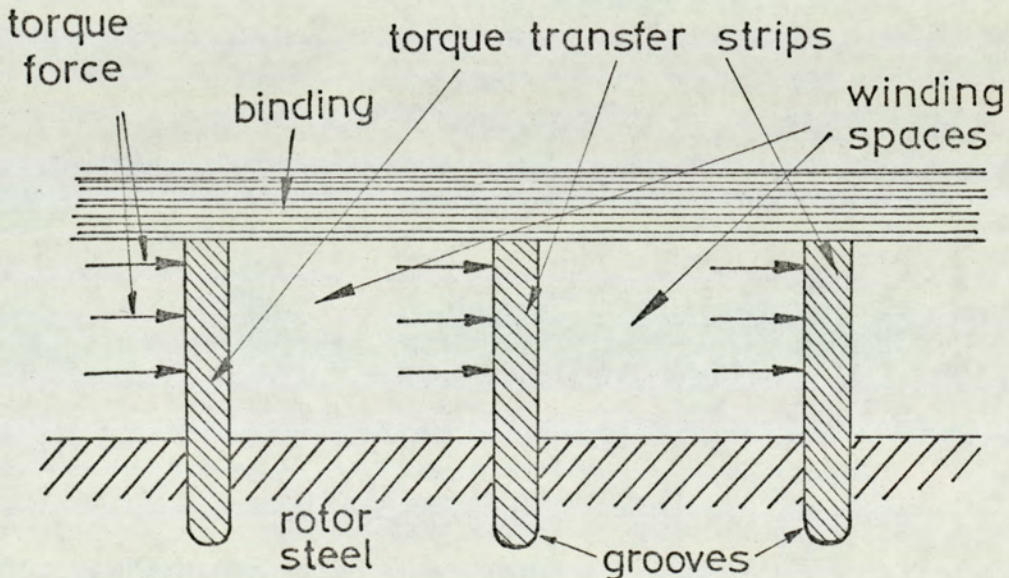


FIG.26. A POSSIBLE METHOD OF SUPPORTING ROTOR WINDING AGAINST TORQUE FORCES

4.3 Stator Conductor Design.

The stator conductors must be divided into thin strands to reduce the loss caused by eddy currents inducted by the oscillations of the main field in the airgap. Each strand must be insulated from the others and the strands must be transposed. Similarly in conventional machines the stator conductors consist of transposed strands to reduce the loss caused by slot leakage fields.

If the harmonics of the field waveform are neglected the loss per unit volume of copper is given by:

$$B^2 w^2 x^2 / 24 \rho$$

for rectangular strands

where B is the maximum radial flux density at the stator winding, x is the tangential width of the strands and ρ is the resistivity of the material. (For proof see for example Carter, 1954).

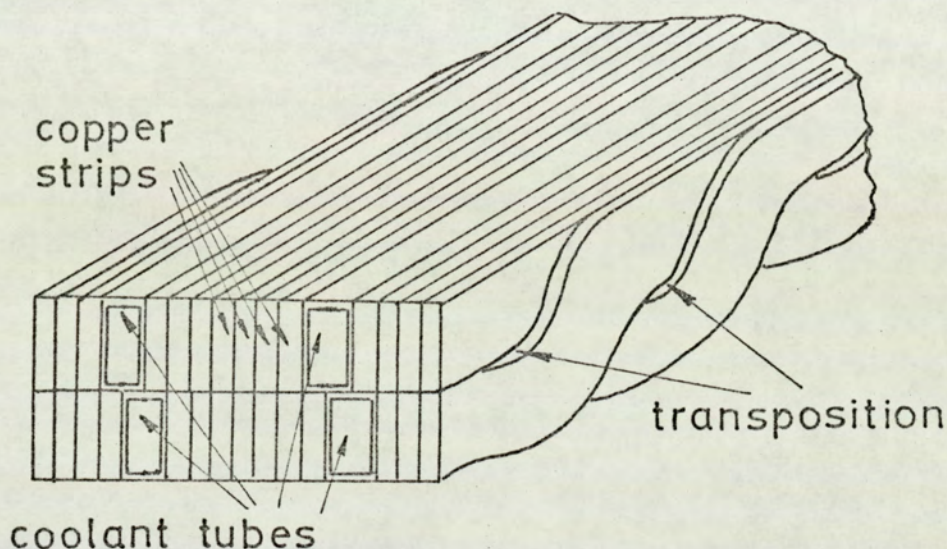
The insulation round each strand cannot in practice be made thinner than about 25μ . Therefore if the strands are very thin the strand insulation will occupy a significant fraction of the total conductor section and the I^2R loss will be increased. Clearly there is an optimum strand width. If the strands are rectangular the space factor will vary as $x/(x+t)$ where t is the thickness of insulation between adjacent strands. It can be shown that the optimum strand width (excluding insulation) is approximately:

$$(12J_s^2 \rho^2 t / B^2 w^2 k_s^2 d_s^2)^{1/3}$$

Where k_s is the space factor found by ignoring the strand insulation d_s is the depth of the winding, and J_s is referred to the same radius as B. The optimum width is in the range 0.4 to 1.0 mm for typical values of B, J_s , k_s , d_s .

One possible design of conductor is similar to the Roebel bars used in conventional machines and consists of rectangular copper strips interspersed with stainless steel water tubes and is shown in fig. 27.

FIG. 27. WATER-COOLED ROEBEL BAR



The strips are twisted together so that over the full length of the machine each occupies every position in the cross section and no differential voltage is induced between strands to cause circulating currents.

In practice it is extremely difficult to build such a conductor from strips smaller than 1.5 to 2.0 mm, therefore, strips rather thicker than the optimum must be used at the expense of increased loss. A strip thickness of 2 mm was assumed in the loss calculations in chapter 3.

4.4 Cooling Arrangements.

4.4.1 Cooling System Requirements.

The quantities of heat to be removed from the various parts of the machine are of the same order as those for a conventional machine of the same rating. Some typical values are given below for a 660 MW slotless design and for a 500 MW conventional machine which is currently in operation using a combination of direct water and direct hydrogen cooling.

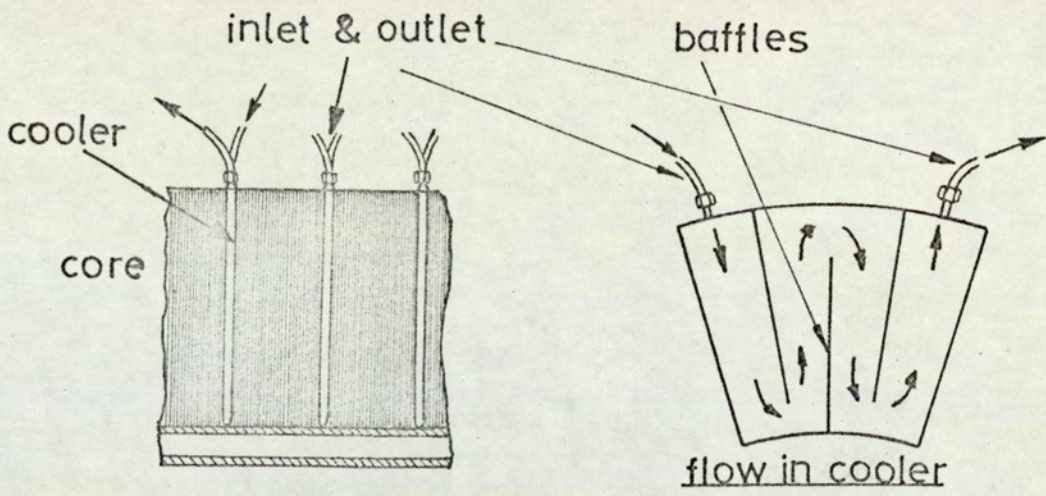
	<u>660 MW</u> <u>Slotless</u> <u>Machine</u>	<u>500 MW</u> <u>Conventional</u> <u>Machine</u>
Stator Copper Loss	2.9 MW	2.0 MW
Rotor Copper Loss	2.1 MW	2.0 MW
Iron Loss	0.6 MW	0.6 MW

Clearly the same cooling techniques used for the 500 MW machine should be adequate for a 660 MW slotless machine.

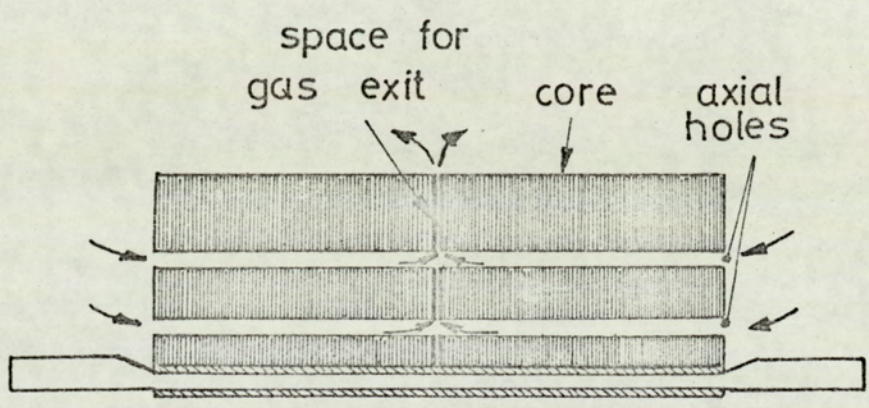
4.4.2 Stator Core Cooling Methods.

Although the iron loss in the slotless machine is similar to that in the conventional machine, its removal should be somewhat easier because its distribution is more uniform. In conventional machines the iron loss is largely concentrated in the teeth where the coolant passages must be restricted to provide the maximum magnetic cross-section.

The conventional arrangement of cooling passages where gas passes radially through the core to or from the airgap would be impossible in a slotless machine since the stator winding and its insulation will prevent gas flow between the core and the gap. Two alternative arrangements are shown in fig. 28 a and b. In type (a) Cooling pads are interspersed with the laminations. This arrangement lends itself readily to liquid cooling which could be integrated with the water cooling system for the stator winding and possibly rotor winding, thus reducing the size of heat exchanger needed, or eliminating the need for the heat exchanger and for hydrogen as an operating atmosphere. In type (b) the coolant is passed axially along the core; gas or water could be used. Some conventional machines use this basic arrangement with gas coolant, and it has proved successful.



(a) coolers interspersed with laminations



(b) axial coolant passages

FIG.28. METHODS OF COOLING STATOR CORE

4.4.3 Stator Winding Cooling.

The slotless arrangement presents no need for or any benefit from a change from the highly successful direct water cooling scheme adopted for most large conventional machines. However, if for any reason oil is considered a more suitable coolant for the stator core and the rotor winding it could easily be used for the stator winding too and the cooling systems could be combined.

4.4.4 Rotor Cooling System.

Most conventional rotors are cooled by hydrogen although direct water cooling systems are under development. Liquid cooling has the attraction of avoiding the need for a high pressure atmosphere of hydrogen in the machine and a heavy casing to contain explosions. The problems include the feed and extraction of liquid to and from the rotating member, and the high pressure at the periphery caused by the rotation. For example, the water pressure at the rim of a rotor of 0.7 m radius would be approximately 25 MN/M^2 . Any slight defect in the connections would soon leak under such pressure and damage to the electrical insulation would result. This problem might be avoided by using oil instead of water.

The problem of feeding and extracting liquid coolant has been overcome in practice by means of a concentric arrangement of inlet and outlet pipes shown schematically in fig. 29. A novel arrangement suggested by Aichholzer (1971) can handle very large quantities of water.

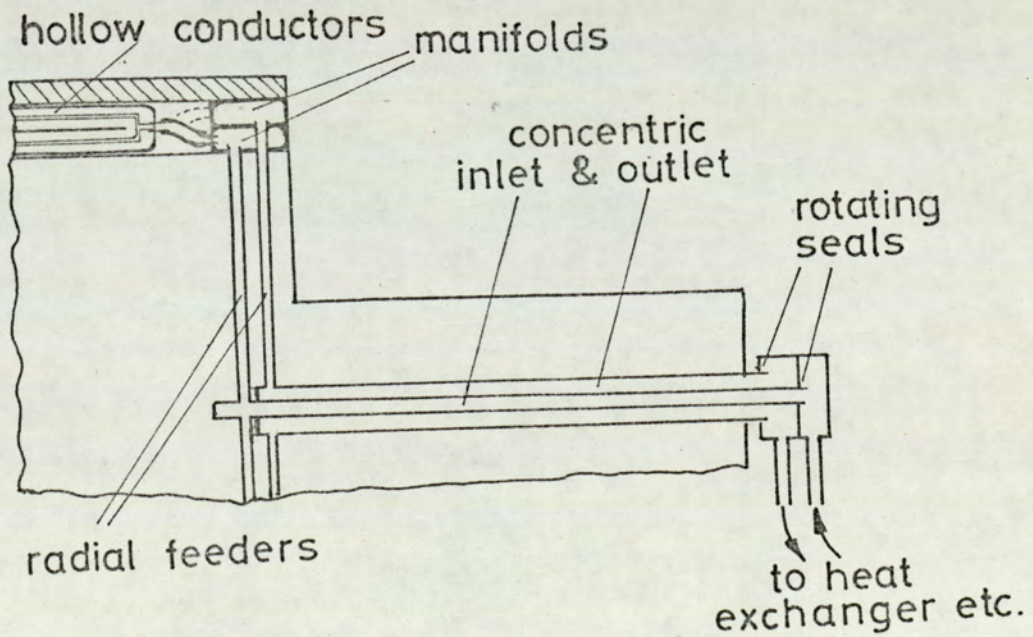
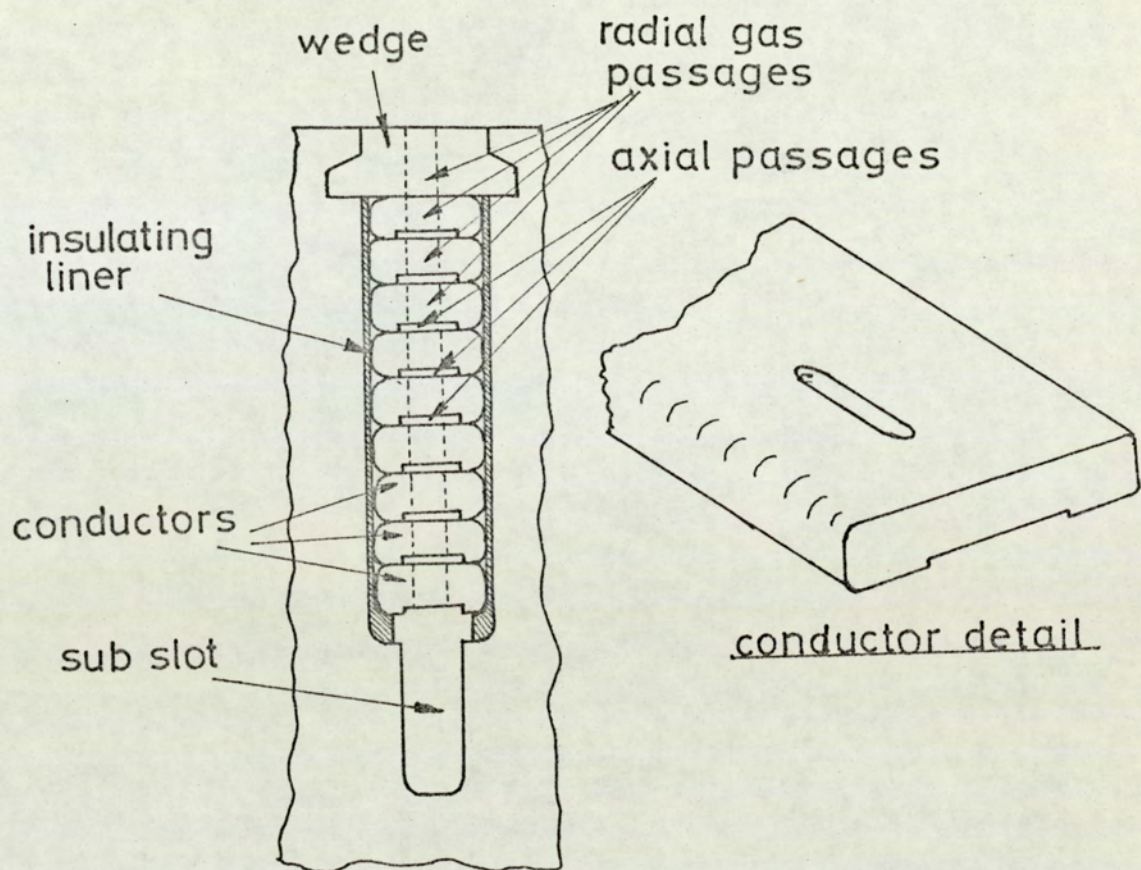


FIG.29. WATER COOLING SCHEME FOR ROTOR

Gas cooling would avoid both problems and allows greater freedom in the design of the winding layout (see 4.1.2). The system used in conventional machines can be adopted to a slotless rotor with slight modification. Fig. 30 illustrates one possible arrangement of the winding with its fixing arrangements which would allow gas to pass from a space beneath the winding through a labyrinth of radial and axial passages, formed in the conductors, to the top of the winding. The passage into the airgap is then between the hoops which make up the binding. A more detailed account of rotor gas cooling systems can be found in "Turbine Generator Engineering".



CONVENTIONAL ARRANGEMENT

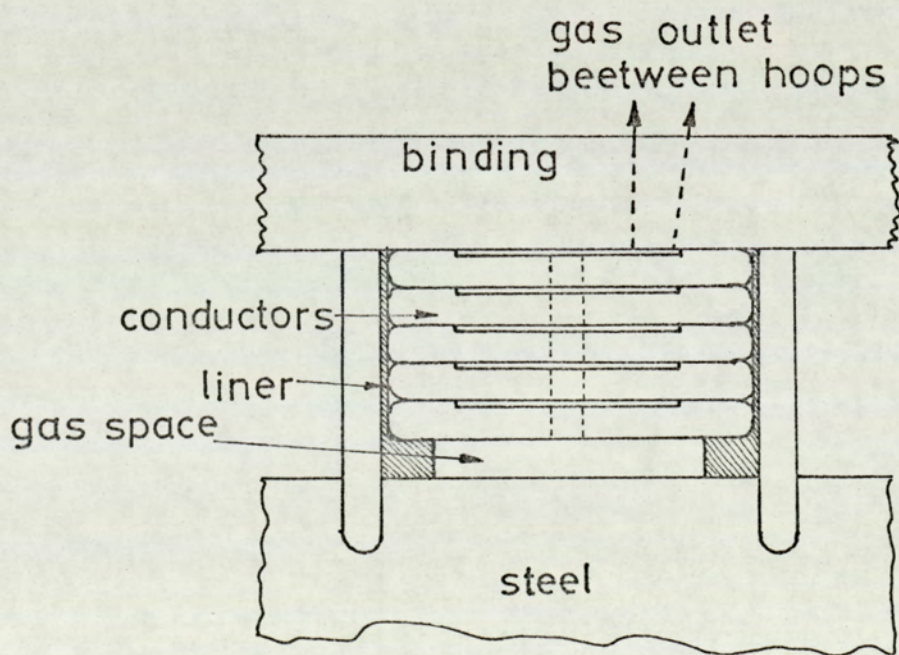


FIG.30. POSSIBLE ADAPTATION OF CONVENTIONAL GAS COOLING SCHEME

4.4.5 Overall cooling system.

It can be seen from the above that the cooling of airgap-wound machines presents no special problems. Conventional methods should be adequate and are quite suitable for the slotless geometry. Fig. 31 shows one possible layout of slotless machine with conventional cooling. More advanced techniques such as water or oil cooling of the rotor and of the stator core are also feasible.

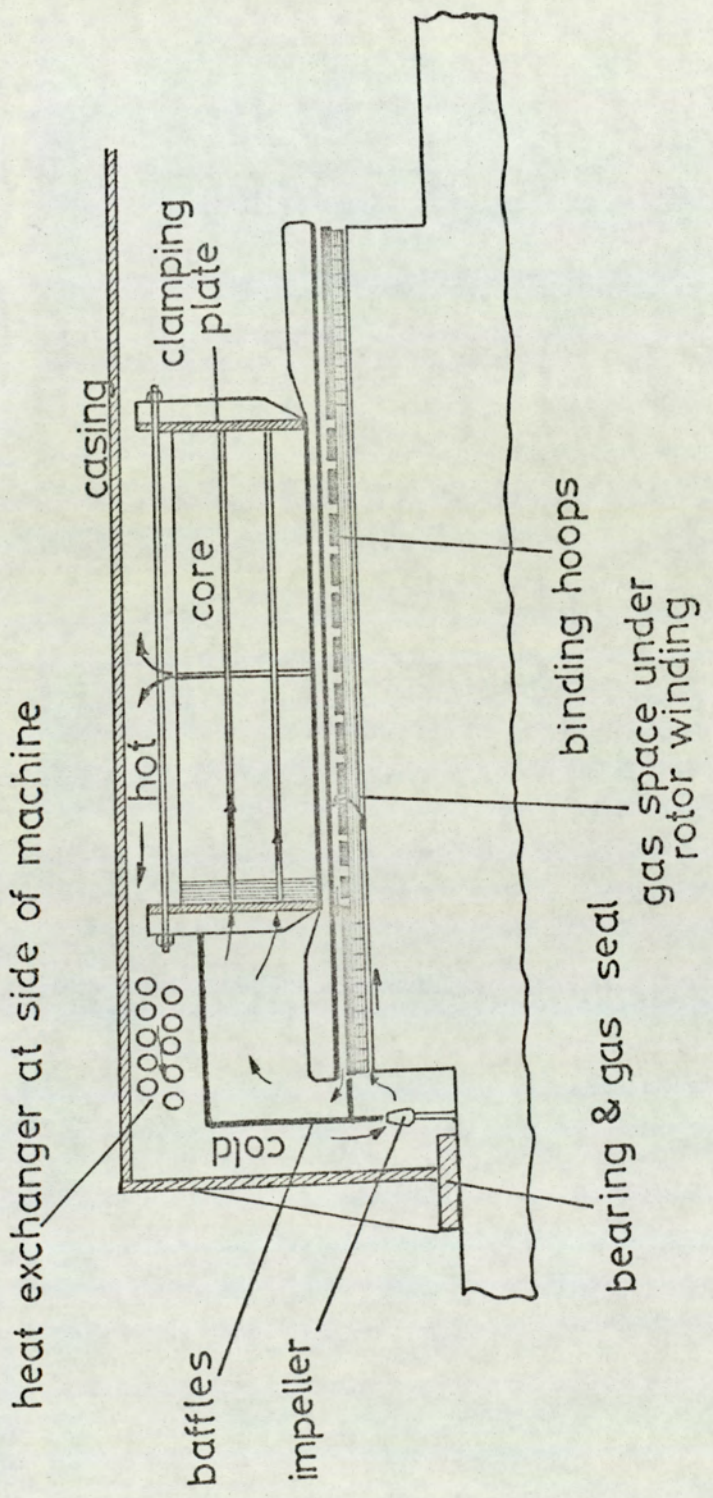


FIG. 31. GAS CIRCUIT FOR COOLING ROTOR WINDING
& STATOR CORE

Chapter 5.

Discussion.

- 5.1 Feasibility of airgap-wound generators
- 5.2 Comparison between slotless and conventional machines.
 - 5.2.1 Technical comparison
 - 5.2.2 Economic comparison
 - 5.2.2.1 Initial cost
 - 5.2.2.2 Losses
 - 5.2.3 Overall comparison
- 5.3 Further development
 - 5.3.1 Outstanding problems
 - 5.3.2 Prototype machine
- 5.4 Review of previous work
 - 5.4.1 Aichholzer
 - 5.4.2 A.S.E.A.
- 5.5 Comparison with superconducting machines
 - 5.5.1 Description of proposed superconducting machine
 - 5.5.2 Quantitative design for comparison
 - 5.5.3 Equivalent slotless machine
 - 5.5.4 Comparison
 - 5.5.4.1 Cost
 - 5.5.4.2 Development
 - 5.5.5 Alternative types of superconducting machine

Discussion.

5.1 Feasibility of Airgap-wound Generators.

It has been shown in chapters 1 and 2 that ratings above about 2 GVA are not possible unless new materials become available, new ways of restraining and winding vibration are found, or the conventional type of design is abandoned. The airgap-wound machine is similar in many respects to the conventional type, therefore most of the components can be designed and built to operate reliably using established methods. Four areas of novelty can be identified.

(i) The finely stranded stator conductors immersed in a strong magnetic field.

(ii) The stator insulation system which must provide mechanical support.

(iii) The rotor winding support system. The binding will probably be made of a carbon-fibre composite - a novel material.

(iv) The rotor cooling system which will be influenced by the design of the support system.

Possible designs of stator conductors, stator insulation, rotor cooling systems and rotor support systems have been given in chapter 4. None of these components poses insurmountable problems and the feasibility of slotless machines is in little doubt.

5.2 Comparison between Slotless and Conventional Machines.

5.2.1 Technical Comparison.

The technical merits and de-merits of the airgap-wound machine compared with the conventional variety are summarised in table 10. Perhaps the most important difference between them is the simplicity of the slotless machine compared with the intricate shape of the conventional machine. This will be reflected in almost every aspect of the design and construction. For example, the prediction of the stray field near the end of the stator core will be made easier by the simple boundary shapes. Such predictions are most important because this region is difficult to cool and excessive stray loss there could result in the permanent de-rating of the generator.

Table 10.

Technical Comparison between Slotless and Conventional Machines.

Feature	Slotless	Conventional	Remarks
Development Potential	5 GVA	2 GVA	
Synchronous Reactance	0.5 to 1.0 p.u. (typical)	2.0 to 3.0 p.u. (typical)	Slotless machine more stable
Sub-transient Reactance	0.05 to 0.008 p.u. (typical for 660 MW)	0.2 p.u. (typical for 660 MW)	Severe fault currents in slotless machine
Power/Weight Ratio	3kW/kg	1.5 to 2.0 kW/kg	Transport to site & foundation design easier
Overall length	7 m (660 MW)	11 m (660 MW)	Eases critical speed problems
Stator core loss density	Higher at bore than outer parts	Heavily concentrated in teeth	Core hot-spot temp lower in slotless m/c
Stator core end loss	High gap field (2T) smooth geometry	Low gap field (1T) complex geometry	Not conclusive - slotless easier to screen
Rotor surface loss	Large gap, smooth rotor	Small gap, slotted rotor	Slotless m/c has lower loss & higher negative sequence I_2^2t capacity.
Stator core vibration	High field thick core	Low field thinner core	No large difference
Rotor steel stresses	Smoothly distributed	Heavy stress concentrations near teeth	Maximum stress lower in slotless rotor
Constructional Problems	<p>Application of Windings & Binding to rotor.</p> <p>Rotor balancing.</p> <p>Rotor threading with small clearance & avoiding damage to stator winding & rotor binding.</p> <p>Construction of stator conductors</p>	<p>Machining rotor slots</p> <p>Threading the long rotor.</p> <p>Provision of end screens to cover the teeth.</p> <p>Clamping slotted stator laminations to a uniform pressure.</p>	

5.2.2 Economic Comparison.

5.2.2.1 Initial Cost.

The cost of a slotless rotor would be similar to the cost of a conventional one because the high cost of the binding would be offset by the savings due to its smaller size and simpler construction. For example a conventional 660 MW rotor costs approximately £300,000 and the cost of an equivalent airgap-wound rotor would be about £330,000 based on the figures for the £660 MW design given in chapter 3.

The cost of an airgap-wound stator should be considerably less than its conventional counterpart because:

- (i) It is lighter therefore building and material costs are less.
- (ii) Being lighter it may be possible to house the core directly in the outer casing rather than use the "caged core" form of assembly.
- (iii) No material is wasted by punching slots.
- (iv) Much less insulation is required, but this is offset by the higher cost of building the more finely divided conductors.

The reduced length and weight of the machine as a whole will give some savings in the cost of the generator foundations and in the cost of the power station building.

5.2.2.2 Losses.

In a conventional machine the stray load loss is a significant part of the total loss. (For a 660 MW machine it is about 2 to 2.5 MW and the total loss is 9 to 9.5 M). This loss is caused by stray fields in the end region, harmonic and negative sequence fields in the airgap, cross magnetisation of the stator teeth and eddy current loss in the stator conductors due to the slot leakage field. In a slotless machine the stray load loss should be rather less (probably about 1 MW for the 660 MW machine of chapter 3) because the large airgap and smooth rotor surface will reduce rotor surface loss, cross-magnetisation of teeth is eliminated, and the eddy current loss due to leakage fields will be small owing to the small depth and length of the stator winding. A loss saving of about 2.2 MW is to be expected this represents an equivalent capital saving of £220,000.

5.2.3 Overall Comparison.

Economically the slotless machine offers savings totalling perhaps £400,000 for a 660 MW machine. Its main technical attractions are its low weight and simple construction. The major drawbacks are the low sub-transient reactance and the rotor balancing and threading problems.

At the 660 MW level therefore the slotless arrangement is a very attractive alternative to the conventional machine.

5.3 Further Development.

5.3.1 Outstanding Problems.

The areas in which further work is required include:

(i) Study of fringe fields at the end of the stator core, and design of screens or flux diverters to reduce eddy current heating due to axial fields. This problem exists in conventional machines but the geometry is different and the field lower.

(ii) Study of the fault performance, particularly the voltages induced in the field winding by the sudden change in armature current and the effect this has upon the excitation system.

(iii) Detailed analysis of the stresses in the rotor binding caused by rotational forces on the steel body, the winding and the binding; and due to thermal expansion both radially and axially.

(iv) Vibration of the stator core due to the force exerted by the airgap field. This "ovalising" force and the resulting deflection could cause wear of the stator insulation.

5.3.2 Prototype Machine.

At some stage during development it will be necessary to build an airgap-wound machine of sufficient size to provide a realistic test of the unconventional components and to gain experience in operating machines of low reactance. The 100 MW design given in chapter 3 could form the basis for a prototype; it would be large enough to give realistic testing conditions whilst not requiring such a large capital outlay as a 500 or 660 MW prototype. In addition it might be installed in a gas turbine power station which would further reduce the investment compared with a large steam driven machine.

It is a useful feature of the fully slotless machine that it is feasible in sizes below 100 MW. The airgap-wound stator machine becomes impractical below about 500 MW so that a prototype would require a very large capital investment.

5.4 Review of Previous Work.

5.4.1 Aichholzer.

Aichholzer (1972) describes a fully slotless generator of 2 G.V.A. 0.98 p.f. rating with a terminal voltage of 60 kV.

The rotor steel core is of fairly small diameter and has a very thick winding of aluminium held in place by a steel binding. The airgap is very large, consequently the field of 2.2T in the rotor steel is reduced to about 1.0T at the stator winding. The stator winding is a three phase type. The high terminal voltage calls for a large volume of stator insulation and a poor space factor for the stator winding results.

The small rotor diameter, large airgap, aluminium rotor winding and the poor fill factor, combine to produce a machine of high loss. The efficiency is quoted as 98.6% which gives the total loss as 28 MW. Of this 28 MW, 17 MW is dissipated in the rotor winding. The author describes in great detail a novel device for delivering large quantities of cooling water to the rotor to remove this high loss.

Clearly, improvements to Aichholzer's design could be made by using a copper rotor winding and the optimisation procedures outlined in this thesis, in particular the rotor loss may be considerably reduced and the drastic measures taken for cooling would be unnecessary.

5.4.2 Allmanna Svenska Elektriska Aktiebolaget(A.S.E.A.)
(Sweden).

In a British patent application, (A.S.E.A. 1965) a form of slotless stator machine is described. A conductor based upon this patent has been constructed and has proved successful.

A salient pole slotless rotor is suggested, to take advantage of the improved magnetic capacity of the stator core. This approach seems quite promising because it gives a reduction in the magnetic airgap whilst retaining a large volume to accommodate the rotor winding.

The rotor winding is cooled by water and is arranged concentrically, consequently the ends are rather complicated. The conductors are made of copper and the binding is steel. The stator conductors are inserted as groups between narrow teeth protruding from the stator core. These teeth perform the function of restraining forces and are too small to have any significant effect upon the magnetic field.

This design is basically similar to that considered in the present work and similar methods of optimisation would be applicable.

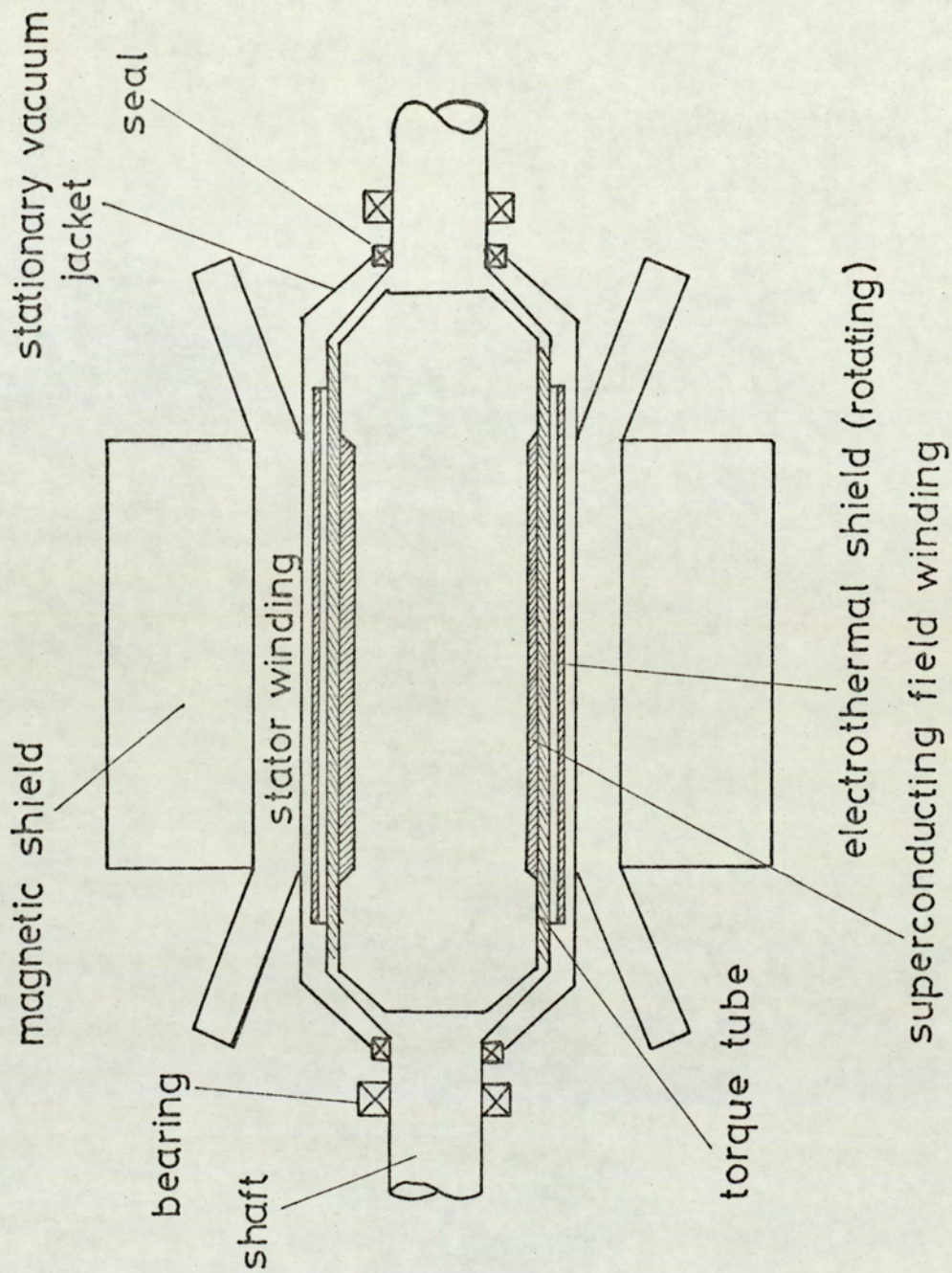


FIG 32
GENERAL LAYOUT OF
ROTATING - FIELD
SUPERCONDUCTING
GENERATORS

5.5 Comparison with Superconducting Machines.

5.5.1 Descriptions of Proposed Superconducting Machine.

Most proposals for generators in the 2000 MW + range incorporate superconductors (e.g. Appleton & Anderson 1972). The favoured arrangement being as shown in fig. 32 with a rotating superconducting field winding and normal armature.

The engineering problems are severe and include:

(i) Providing adequate screening against the rotating field: suitable iron or copper shields prove either to be heavy or to sustain high loss. (Harrowell, 1972).

(ii) Avoiding heat transfer along the drive shaft: a hollow shaft of fairly large diameter provides the best solution but this may introduce problems in the design of bearings.

(iii) Feeding coolant (at approximately 4 K) into the rotating member.

(iv) Construction of a refrigeration system sufficiently reliable for commercial operation.

The benefits to be gained are reduced loss, weight, cost, and synchronous and transient reactances and the possibility of achieving extremely high outputs - 10 GVA and above has been suggested as possible by Woodson, Smith, Thullen and Kirtley (1971).

5.5.2 Quantitative Design for Comparison.

The following design has been outlined by Thullen, Smith & Woodson (1970) for an 850 MW 0.85 p.f. 60 Hz superconducting generator with an iron screen and forms a useful comparison with slotless machines.

Active length	3.3 m
Inside radius of field winding	0.223 m
J_s referred to this radius (= 942 kA/m referred to mean radius of armature winding, 0.429 m)	1.81 MA/m
Peak magnetic field at mean stator winding radius	1.48 Tesla
Copper & Iron loss	8.5 MW
Synchronous reactance	38%
Transient reactance	25%
Mass of rotor	1.2 tonne
Mass of stator	61 tonne
Output at 3000 r.p.m	708 MW, 834 MVA

Clearly different constraints have been imposed on this design from those imposed on slotless machines; in particular the criterion for choosing J_s was that the transient reactance must not exceed 0.25 p.u. The high stator current loading will probably give rise to serious end winding vibration troubles and may be the cause of the high total loss in the armature.

The flux density at the stator is only 30% of that inside the rotor winding. This is a result of the magnetically open construction which allows much of the flux to bypass the armature winding.

This design might possibly be improved if some further

optimisation procedure were used to select more favourable dimensions and loadings. Nevertheless, the design is attractive, the low weights and reactances being particularly so.

5.5.3 Equivalent Slotless Machine.

A good slotless design for 708 MW 0.85 p. . 50 Hz can be obtained by taking the optimum 660 MW design and increasing the length slightly to increase the output to 708 MW. The following design results from increasing the length of the 660 MW machine with a water-cooled copper field winding, carbon fibre binding and Roebel stator conductors:

Steel radius	0.6 m
Airgap	0.1714 m
Outer stator core radius	0.46 m
Active length	3.91 m
Flux density at rotor steel radius	2.0 T
(= 1.6 T at mean radius of stator winding)	
Stator Current loading	300 kA/m
(= 254 kA/m referred to mean radius of winding)	
Synchronous reactance	81%
Transient reactance	6.4%
Sub-transient (leakage) reactance	4.8%
Stator mass (core only)	145 tonne
Rotor mass (total)	65 tonne
Losses	
Stator I^2R	2220 kW
Rotor I^2R	2240 kW
Iron	640 kW
Eddy Current	890 kW
Friction	650 kW
Total	6640 kW

5.5.4 Comparison.

5.5.4.1 Cost.

The two designs are compared in table 11.

Table 11.

Features of Slotless and Superconducting Machines.

Feature	Slotless Machine	S/C Machine	Remarks
Efficiency	99.1%	98.8%	Cost advantage of £200,000 for slotless machine
Weight	210 tonne	62 tonne	Large cost advantage for S/C machine
Synchronous Reactance	81%	38%	Both attractive particularly S/C machine
Transient Reactance	6.4%	25%	Rather lower than desirable for slotless machine
Transient time constant	180 mS	-	Not defined for a superconducting field winding
Cost of rotor Winding material	£17,000	£40,000	
Cost of rotor structure	£60,000	£120,000	Material cost only for slotless Rotor - Total costs probably comparable.
Cost of stator Materials	£50,000	£15,000	Taken as proportional to weight.

The capital costs of the two machines are similar, however the higher efficiency of the airgap-wound generator gives it an advantage of approximately £200,000. The lower weight of the superconducting machine will compensate for its lower efficiency in reduced transport and foundation costs.

5.5.4.2 Development.

Most of the development required to realise practical airgap-wound generators is in the following areas:

- (i) Design of stator winding insulation and support system.
- (ii) Design of rotor winding attachment cooling and restraint systems.
- (iii) Investigation of thermal expansion effects on the rotor.
- (iv) Investigation of critical speeds.
- (v) Investigation of stray and fringe field effects in the end regions.

For the superconducting machine, the following areas need development:

- (i) Design of slotless stator winding insulation and support system.
- (ii) Design of hollow drive shaft and appropriate bearings.
- (iii) Design of low temperature coolant feed system.
- (iv) Design of attachment and restraint systems for field winding.
- (v) Design of a refrigeration system to meet high standard of reliability.
- (vi) Assessment of end effects.

Clearly much of the development for airgap-wound machines is relevant to the development of superconducting machines.

The slotless layout is similar in many respects to the conventional form therefore the development is restricted to just a few specific design problems. Superconducting generators on the other hand are highly novel and will call for large sums to be spent on development. However, some progress has been made in the development of large superconducting magnets and their

associated refrigeration systems. Thus the slotless machine appears more promising for the next generation of machines in the 1 to 5 GVA range.

5.5.5 Alternative types of superconducting machine.

Other forms of superconducting machine are being studied which might overcome some of the drawbacks of the "conventional" form. In particular the rotating armature version in which the field winding is placed on the stator eliminates many of the stray field problems and needs no rotating cryostat. The field at the armature is not attenuated as in the rotating field type, (from about 5 to 1.5 Tesla) therefore, the power to weight ratio may be higher. The main area for development is the transfer of the power from the rotor - some recent novel forms of brush-slipping assemblies using liquid metals may be of use. Another type (Harrowell 1972) abandons rotary motion altogether, the armature being a set of coils reciprocating in a strong steady field; both field and armature windings may be superconducting the field winding is toroidal therefore there is no stray field. However, the crankshaft and big end bearings may pose severe reliability problems.

An alternative approach to the design of rotating field superconducting machines has been used by Lorch (1971). A superconducting rotor is combined with a conventional 660 MW stator. The cost of the whole machine plus the refrigerator and the losses is about £310,000 less than the equivalent cost for a conventional machine. This arrangement might allow the stator to be uprated to about 1000 MW because the limiting constraints on the conventional machine rotor are removed. The cost saving for a 1000 MW machine with the uprated 660 MW stator is approximately £850,000 compared with a conventional 1000 MW machine.

This form of machine seems an excellent way of achieving

outputs of perhaps 2 G.V.A. and compares well with the slotless machine in every aspect apart from the probable cost of development.

Chapter 6.

Conclusions.

1. It has been shown that the airgap wound or slotless generator is essentially conventional but is potentially able to be developed to capacities about three times higher than is possible with the existing type of machine.

2. A slotless machine would be shorter, lighter, more efficient and cheaper than a conventional machine of the same capacity. For example a 660 MW slotless machine would be 4 to 5 m shorter, 150 tonne lighter, would have a 2MW less loss and would show a total cost saving of about £400,000 compared with a conventional machine.

3. The synchronous, transient and sub-transient reactances are lower than those of conventional machines. Thus the steady state and transient stability margins are higher.

4. It has been shown that the increased ratings and cost savings arise because the use of airgap windings modifies the design constraints in the following ways:

4.1 Higher flux densities may be used.

4.2 Rotor mechanical stresses are reduced, permitting larger diameters.

4.3 Rotor stiffness is enhanced allowing greater lengths to be considered.

5. The feasibility of restraining the rotor windings against centrifugal forces by means of a cover or binding has been demonstrated. The most suitable binding material is type II carbon fibre composite but other materials such as steel may be used at the expense of increased losses.

6. The stator conductors must be made of fine strands to avoid excessive eddy current loss induced by the main airgap field. The optimum width of such strands has been shown to be about 0.5 to 1.0 mm but 2mm strands which would be easier to handle are acceptable.

7. Possible methods of attaching the rotor and stator windings to the steel parts have been described, the preferred method being the trough-lid system. The steady-state forces acting upon the windings are easily constrained but during terminal faults there exist much higher forces which may cause severe damage. However, conventional machines rarely survive such faults.

8. The stator winding may be of either the three-phase or twelve-phase arrangement. For large outputs the simplicity and reduced losses of the twelve-phase winding outweigh the need for a special transformer arrangement. For smaller ratings (less than 660 MW say) the three-phase type is preferable because of the simpler transformer system. The restricted space in the airgap dictates the need for a single-layer stator winding. Possible three and twelve-phase single-layer windings have been described and a method of forming the end turns has been suggested.

9. The rotor winding may be concentric as in conventional machines. An alternative type more suitable for direct liquid cooling has been put forward.

10. The rotor winding could be cooled by gas or liquid. Possible gas and liquid cooling arrangements have been described briefly. The stator winding may be water cooled in the normal way. The stator core could have axial passages to carry cooling

gas similar to the conventional method. An alternative scheme has been proposed using water cooled pads interspersed with the laminations.

11. The optimum way of allocating the available airgap space between the two windings has been found. The factors considered include the I^2R and eddy current losses, the cost of the binding material and the provision of coolant ducts inside the conductors.

12. The optimum stator core thickness has been found which gives the minimum total cost of material and loss.

13. In general a good design for an airgap-wound generator incorporates the following features:

13.1 A short rotor of large diameter.

13.2 A large airgap

13.3 A high flux density

in comparison with a conventional machine and:

13.4 The highest electric loading permissible from considerations of end winding vibration.

Acknowledgments.

The study reported in this thesis was carried out at the Central Electricity Research Laboratories, Leatherhead, Surrey and forms part of the advanced machines work of the Electromagnetics section. Acknowledgment is made to the Central Electricity Generating Board for permission to submit this thesis. Some of the material, notably the design of the stator conductors and their support structure - the trough-lid system stems from a joint study by C.E.R.L. and the Nelson Research Centre (N.R.C.) of G.E.C. Ltd. I wish also to thank Mr. A.B.J. Reece of N.R.C. for allowing the publication of those aspects.

I would like to thank my supervisors Prof. E.J. Davies and Mr. J.G. Steel for their valuable encouragement discussion and constructive criticism throughout the course of the work, and Dr. W.T. Norris who supervised the work in the early stages.

My colleagues at C.E.R.L., Dr. J.L.T. Exon, Dr. M.L.J. Rollason, Mr. R.H. Minors and Mr. R.V. Harrowell have contributed a great deal through day to day discussion.

I wish also to express thanks to my wife for continued patience and encouragement over several years.

Appendices.

1. Generator Transformer Connections for Twelve-Phase Windings
 - 1.1 Twin transformer arrangements
 - 1.2 Single transformer arrangements
2. Forces and Stresses in Stator Winding
 - 2.1 Steady state case
 - 2.1.1 Electromagnetic stress (E.M.S.)
 - 2.1.2 Mechanical stress
 - 2.1.3 Twelve-phase winding
 - 2.2. Fault conditions
 - 2.2.1 Fault current
 - 2.2.2 Electromagnetic stress
 - 2.2.3 Mechanical stress
 - 2.2.4 Methods of Reducing Stress
3. Rotor Surface Eddy Current Loss
 - 3.1 Loss mechanism
 - 3.2 The effect of rotation
 - 3.3 Calculation of harmonic fields
 - 3.4 Example
4. Calculation of Reactances
 - 4.1 Magnetising reactance
 - 4.2 Stator leakage reactance
 - 4.2.1 Airgap leakage reactance
 - 4.2.2 End winding leakage reactance
 - 4.3 Rotor leakage reactance
 - 4.4 Approximate formula for magnetising reactance.

Appendix I

1. Generator Transformer Connections for Twelve-Phase Windings.

The output from a twelve-phase stator winding can be converted to three-phase form for transmission by several types of transformer connection. Each type performs the conversion by phase-shifting one three-phase set of outputs by 30° through a star-delta transformer connection and adding it to the other set. Similar arrangements are used in the converting stations for direct-current transmission links.

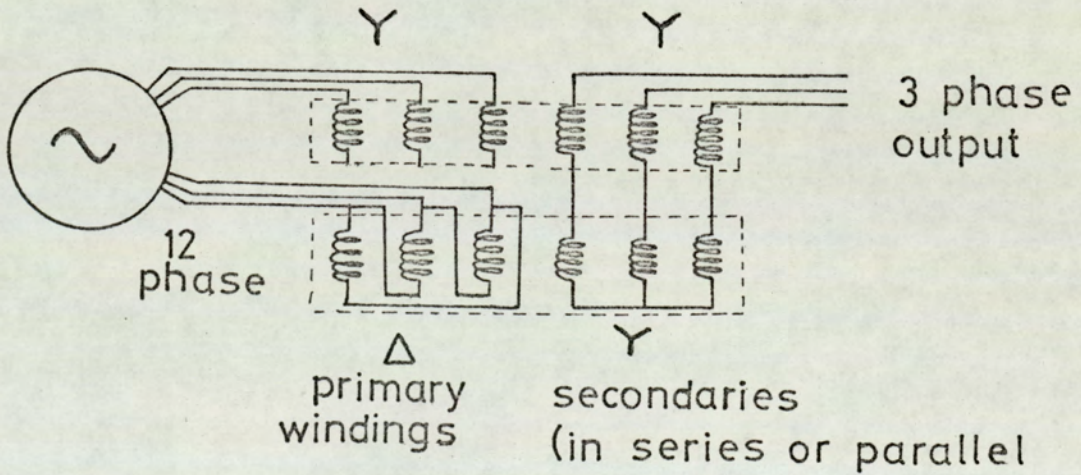


FIG.33. BASIC CIRCUIT DIAGRAM

1.1 Twin Transformer Arrangements.

Although the twelve-phase winding has winding factors of zero for the 5th, 7th, 17th, 19th etc. harmonics, the two component three-phase outputs contain voltages at these frequencies. A star-delta transformer shifts the phases of the harmonics so that the two sets contain 5th, 7th, 17th, 19th harmonic voltages in anti-phase whilst the fundamental, 11th, 13th, 23rd, 25th are in phase. If the two sets are connected in series as in fig. 33, the 5th, 7th, 17th, 19th will cancel and the final three-phase output will contain only fundamental and harmonics of order $12n \pm 1$. However, this arrangement introduces insulation problems for the transformer connected to the transmission lines. Parallel connection of the two transformer outputs is more convenient but the 5th, 7th, 17th, 19th harmonics are effectively short-circuited and harmonic currents flow between the two three-phase outputs of the generator via the transformer, limited only by leakage reactances and the small harmonic magnetising reactance of the generator.

1.2 Single Transformer Arrangements.

In the two arrangements described above the two outputs are added electrically at the transformer output. Each has a counterpart in which the addition is performed within the magnetic circuit of a single transformer with two primary three-phase windings, one star connected the other delta connected. The parallel connection of the secondaries is equivalent to the configuration of fig. 34 in which the primary m.m.f.s are added in series. Harmonic currents flow with this arrangement too and are somewhat higher because the secondary leakage reactance is left out of the circulating path.

The series electrical connection is equivalent to that of figs. 35 and 36 in which the fluxes from each primary are added in parallel. This arrangement overcomes the electrical insulation problem but calls for a rather complicated core geometry if the transformer is to be made as a single unit as in fig. 36 (6 limbs). Three single-phase output transformers arranged as in fig. 35 may be more convenient especially for high power machines for which a single transformer would be impractical anyway. The cores for this system due to Allen (1971) are simple three-limb types and the problems of electrical insulation and circulating harmonic current present in the arrangements of figs. 33, 34 and 36 are avoided; therefore, fig. 35 is the preferred configuration for large outputs.

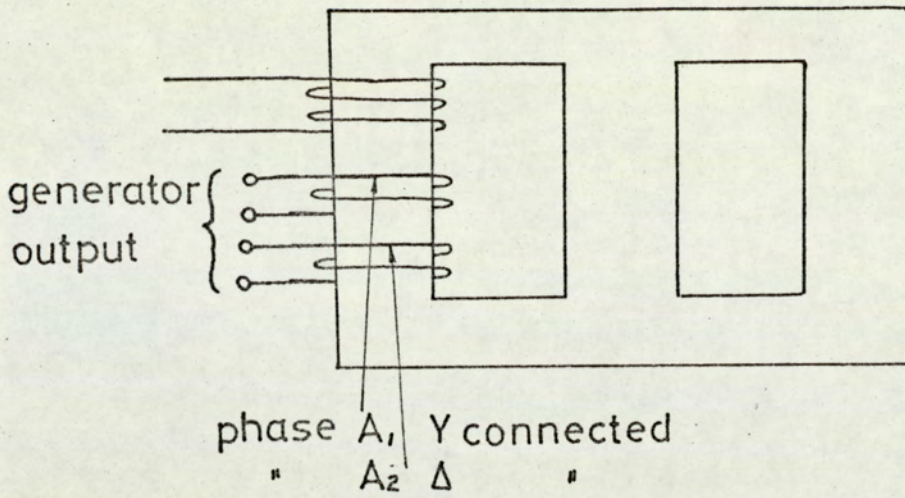


FIG.34. SINGLE TRANSFORMER SYSTEM WITH SERIES MAGNETIC CIRCUITS

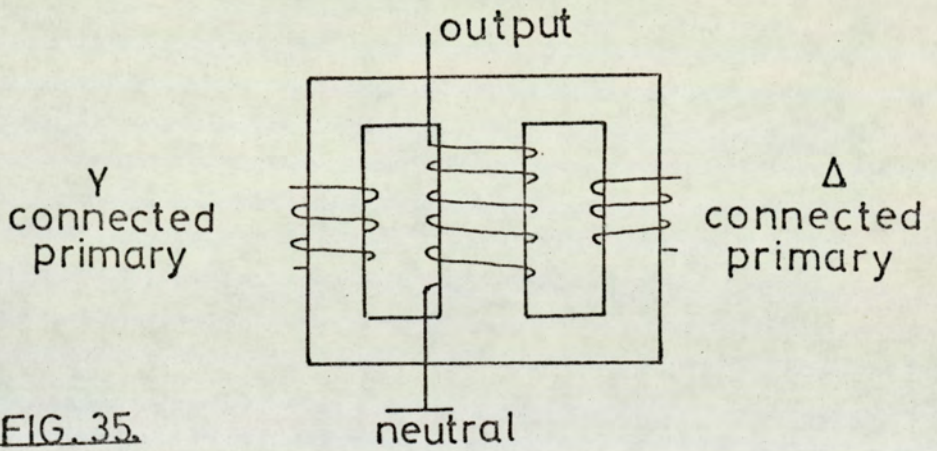


FIG. 35.

ONE PHASE OF 3 TRANSFORMER SYSTEM WITH PARALLEL MAGNETIC CIRCUITS

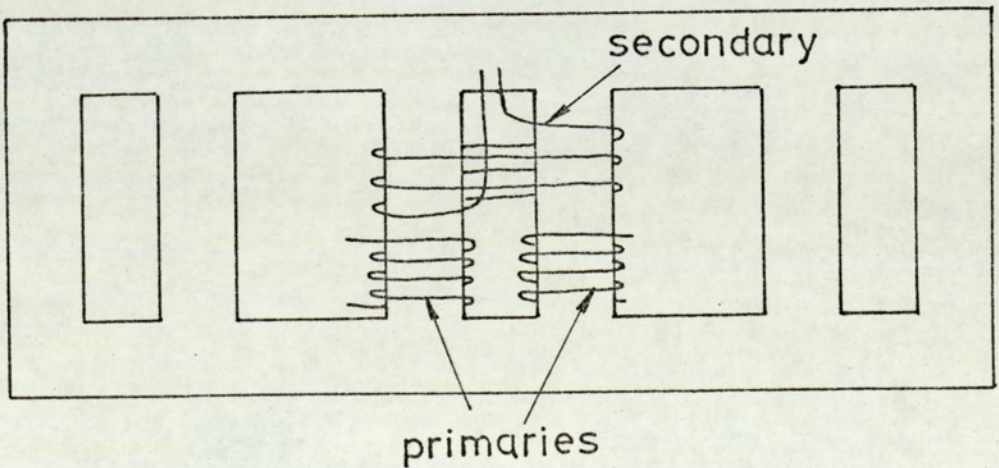


FIG.36. SINGLE CORE VERSION OF ABOVE

Appendix II

Forces and Stresses in Stator Winding Structure.

2.1 Steady state case.

2.1.1 Electromagnetic Stress (E.M.S.)

The total effect of the forces acting upon the stator conductors is to produce a torque on the stator balancing the torque produced by the prime mover (e.g. steam turbine). Therefore, there is a shear stress set up at the interface between the stator core and winding, the average value being given by $P/2\pi wr^2l$, where r is the inner core radius. For the optimum 660 MW design this stress is approximately 155 kN/m^2 .

The stress at any point is the product of the instantaneous local values of the electric loading and radial flux density. Ideally, both these quantities form sinusoidal patterns and their product is sinusoidal but of double frequency and has a mean component. It can be shown that the mean value is $(\cos \phi)/2$ times the peak-peak value, $\cos \phi$ being the power factor. Thus the maximum stress occurring is $1 + 1/\cos \phi$ times the average. (337 kN/m^2 for the 660 MW design). In the zero power factor (z.p.f.) case the mean value is zero and the peak value of the sinusoidal component is given by $BJs/2(1+g/r_1)^2$

2.1.2 Mechanical Stress.

The electromagnetic forces acting on the winding are transferred through the main insulation to the core and through the inter-turn insulation to adjacent conductors. To some extent the electromagnetic stress (E.M.S.) will be attenuated by the more highly loaded conductors transferring force to their less highly loaded neighbours, thus, in effect, reducing the peak value of the sinusoidal part of the stress.

The effect may be analysed by use of the model shown in fig. 37.

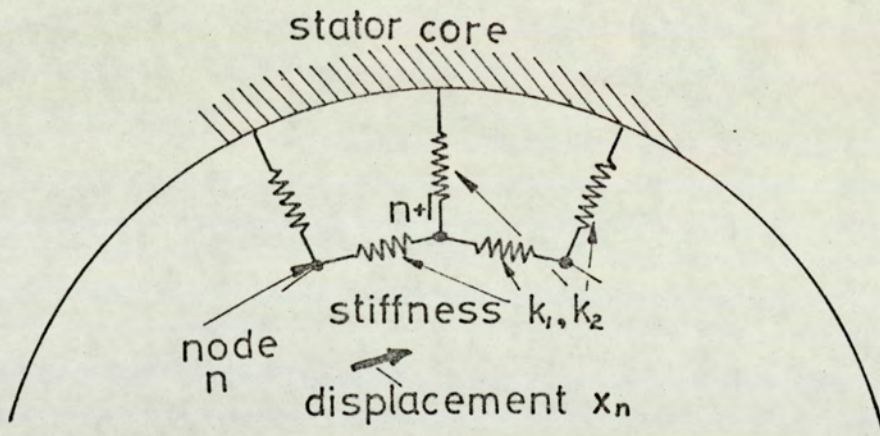


FIG.37. MODEL FOR ANALYSIS OF STRESS

If conductor number m is acted upon by an electromagnetic force F_m and is displaced tangentially a distance x_m , the force balance equation (inertial forces can be shown to be negligible) is:

$$F_m = k_2 x_m + k_1 (x_m - x_{m+1}) + k_1 (x_m - x_{m-1})$$

where k_1 and k_2 are the equivalent stiffnesses of the interturn and main insulation. Treating the insulation as a set of discrete blocks leads to:

$$k_1 = E l d / t_1$$

$$k_2 = K l y / t_2$$

where E = Youngs modulus

K = Bulk modulus

d = Conductor depth

y = Width of main insulation per conductor

t₁ = Thickness of interturn insulation

t₂ = Thickness of main insulation

The interturn stress σ_i is given by

$$\sigma_{im} = E (x_m - x_{m+1}) / t_1$$

and the stress between the conductor and the core σ₂ is given by

$$\sigma_{2m} = K x_m / t_2$$

The force balance equation may be written in terms of σ₂

and the E.M.S. σ₂ in matrix form:

$$\begin{bmatrix} 1+2\delta & -\delta & 0 & 0 \\ -\delta & 1+2\delta & -\delta & 0 \\ 0 & -\delta & 1+2\delta & \dots \\ 0 & & \dots & \dots \\ 0 & & & \dots \\ 0 & & & \dots \\ 0 & & & \dots \end{bmatrix} \begin{bmatrix} \sigma_{2,1} \\ \sigma_{2,2} \\ \vdots \\ \sigma_{2,n} \end{bmatrix} = \begin{bmatrix} \sigma_{e,1} \\ \vdots \\ \sigma_{e,n} \end{bmatrix} \times (w/y)$$

where the factor w/y allows for the main insulation width, y, being less than the conductor width, w. This would be the case with the trough and lid system. The term δ is given by E d t₂ / K y t₁

It can be shown that the matrix has an inverse of the form

$$\begin{bmatrix} a_1 & a_2 & a_3 & \dots & a_n \\ a_n & a_1 & a_2 & & \\ a_{n-1} & a_n & a_1 & & \\ a_2 & & & & \end{bmatrix}$$

where a_m = α_m a₁ + β_m

$$\alpha_{m+1} = (1+2\delta) \alpha_m / \delta - \alpha_{m-1}$$

$$\beta_{m+1} = (1+2\delta) \beta_m / \delta - \beta_{m-1}$$

$$\alpha_1 = 1, \quad \beta_1 = 0$$

$$\alpha_2 = \delta + 1/2, \quad \beta_2 = -1/2\delta$$

$$a_1 = \frac{\beta_n(1 + 2\delta) - \beta_{n-1}\delta}{\delta + \delta\alpha_{n-1} - (1 + 2\delta)\alpha_n}$$

The elements a_m of the inverse matrix represent the effect of a force applied to the conductor in producing a stress at another.

2.1.3 Twelve-Phase Winding.

Taking typical values for the following parameters:

$$\begin{array}{rcl}
 E & = & 10^{11} \text{ N/m}^2 \\
 K & = & 8.10^{10} \text{ N/m}^2 \\
 W & = & 0.42 \text{ m} \\
 y & = & 0.06 \text{ m} \\
 d & = & 0.05 \text{ m} \\
 t_2 & = & 0.03 \text{ m} \\
 t_1 & = & 0.06 \text{ m}
 \end{array}
 \left. \vphantom{\begin{array}{rcl} E \\ K \\ W \\ y \\ d \\ t_2 \\ t_1 \end{array}} \right\} \begin{array}{l} \text{Effective values assumed} \\ \text{for trough-lid structure} \end{array}$$

and assuming that each phase band occupies a separate trough-lid assembly and is represented by a single conductor

$$\begin{array}{rcl}
 \text{Then } \gamma & = & 0.5 \quad \text{and} \\
 a_1 & = & 0.5774 \\
 a_2, a_{12} & = & 0.1547 \\
 a_3, a_{11} & = & 0.0415 \\
 a_4, a_{10} & = & 0.0111 \\
 a_5, a_9 & = & 0.0030 \\
 a_6, a_8 & = & 0.0009 \\
 a_7 & = & 0.0004
 \end{array}$$

At the instant when the force on phase A (say) is at its maximum, the oscillatory component of the E.M.S. follows a sequence round the bore of $1, \frac{1}{2}, -\frac{1}{2}, -1, -\frac{1}{2}, \frac{1}{2}, 1, \frac{1}{2}, -\frac{1}{2}, -1, -\frac{1}{2}, \frac{1}{2}$ these forces multiplied by the appropriate a_m factors add together to produce a total force on phase A conductor of 0.67 times the applied force. Similarly, on the other phases the force is 0.67 times the applied force at that instant. Thus the oscillatory stress between the stator winding and core is 0.67 times the oscillatory part of the E.M.S. The steady component is unchanged.

Other types and thicknesses of insulation will produce different values of γ and the factor modifying the stress will be changed. Fig. 38 shows how this factor is affected by variations in γ .

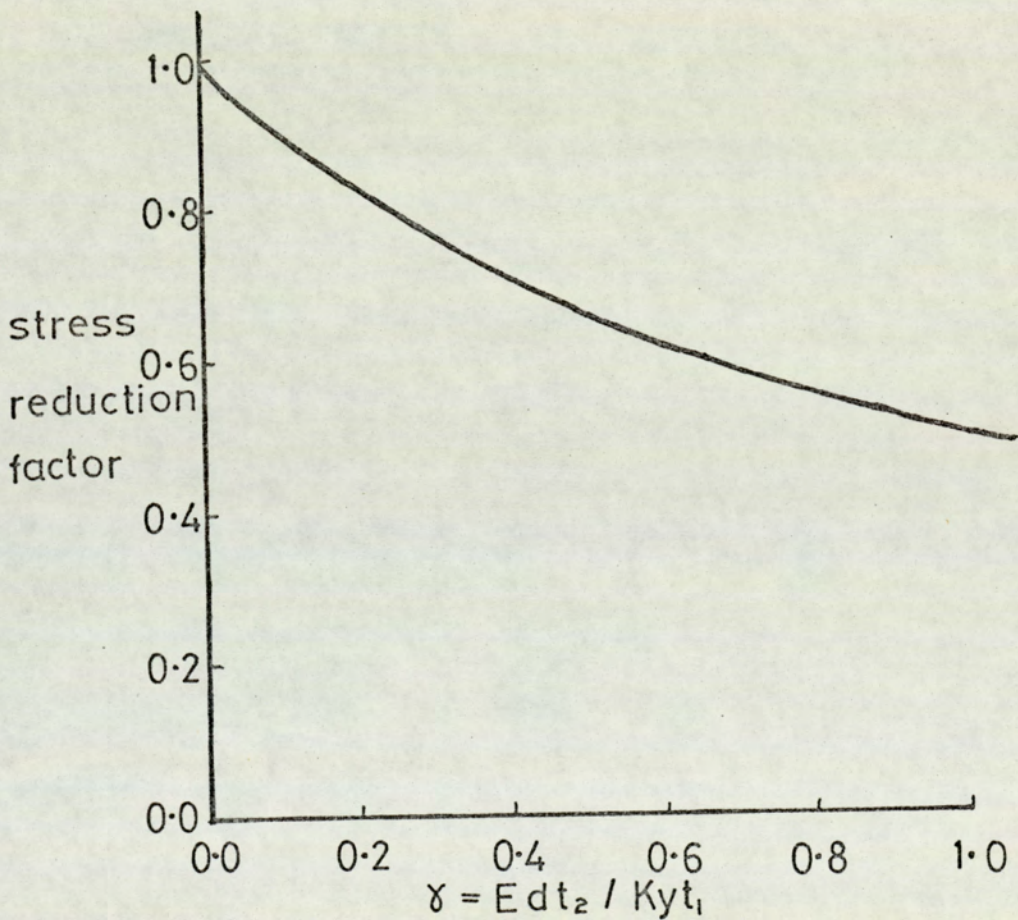


FIG.38 VARIATION OF STRESS REDUCTION FACTOR WITH RATIO OF STIFFNESSES γ

2.2 Fault Conditions.

2.2.1 Fault Current

At the start of a fault, the flux density at the rotor remains the same as before the fault because of eddy currents. The per-unit current which flows in the stator is, therefore, approximately the inverse of the per-unit leakage reactance of the machine. In addition, direct current of the same magnitude flows and decays during the transient period. The power factor during faults is low because the impedance limiting the current is mainly leakage reactance.

2.2.2 Electromagnetic Stress.

The total flux linking the stator winding is small if the fault is at the terminals because the stator resistance is small. Therefore, the leakage flux is nearly equal and opposite to the main flux emanating from the rotor. The leakage flux is distributed between the active and end regions of the machine in the same proportion as the leakage reactance. Thus, if the end region and active region leakage reactances are X_e and X_g , the per-unit leakage fluxes are $X_g/(X_g+X_e)$ in the active region and $X_e/(X_g+X_e)$ in the end region. Therefore, the total flux linking the stator winding in the active region is $X_e/(X_g+X_e)$. The radial flux density at the stator winding is therefore $X_e/(X_g+X_e)$ and the electromagnetic stress is $X_e/(X_g+X_e)^2$ times its steady state zero power factor value.

The direct current produces an additional electromagnetic stress of the same peak magnitude but oscillating at the fundamental frequency, this stress forms a stationary pulsating pattern whereas the component due to the alternating current forms a rotating stress wave. Therefore, at the point of the circumference where the direct current is highest the electromagnetic stress may be up to $2X_e/(X_g+X_e)^2$ times the steady state z.p.f. value.

If the fault is at some place other than the machine terminals, e.g. at the H.V. side of the transformer, additional reactance appears in the circuit. This may be regarded as extra end winding reactance and the same expressions can be used.

2.2.3 Mechanical Stress.

For the optimum 660 MW design, $B = 2.0$ T, $J_s = 300$ kA/m, $r_1 = 0.6$ m, $g = 0.171$ m, the z.p.f. E.M.S. is 182 kN/m². The stress reducing effect brings the mechanical stress to about 120 kN/m². If the conductors are supported over one seventh of their width the stress at the supports is 840 kN/m². This figure must be multiplied by $2X_e / (X_g + X_e)^2$ to obtain the maximum possible stress during a terminal fault. X_e and X_g are 3.252% and 1.565% respectively therefore the maximum average shear stress in the insulation is 23.6 MN/m².

In the twelve-phase winding, the maximum difference in shear stress between adjacent phase bands is equal to the peak value of the shear stress, therefore, the interturn tensile and compressive stress is 23.6 MN/m² $\times E t_2 / K t_1$ or 14.7 MN/m².

If the trough-lids are not to separate and damage the insulation it would be necessary to pre-compress the insulation to at least 14.7 MN/m² so that the total stress never becomes tensile.

For a transformer fault (15% leakage reactance assumed for the transformer) the shear and tensile stresses are 7.8 and 4.9 MN/m² respectively.

2.2.4 Methods of Reducing Stresses.

Stresses on short circuit may be modified by:

(a) Changing the basic design of the machine to alter the steady-state forces and the leakage reactances as discussed in chapter 3;

(b) Spreading the load over a greater area by supporting the conductors with thicker trough-lid structures.

(c) Altering the relative stiffnesses of the interturn and main insulation to change δ , but this will not produce large changes as can be seen from fig. 38.

Appendix III

Rotor Surface Eddy Current Loss.

3.1 Loss Mechanism.

The distributions of practical armature windings are never perfectly sinusoidal, therefore, even if balanced sinusoidal three-phase or twelve-phase currents are flowing there exist fields rotating at non-synchronous speed. The relative motion between these fields and the rotor surface causes eddy current loss which constitutes a large proportion of the stray load loss.

The loss depends mainly upon:

- (i) The stator harmonic winding factors.
- (ii) The spacing between stator iron, stator winding and rotor iron.
- (iii) The permeability and conductivity of the material at the rotor surface.

In the calculation of the loss the following assumptions are made:

- (i) The stator iron is infinitely permeable.
- (ii) The rotor surface material is magnetically linear.
- (iii) The rotor surface is a smooth continuous cylinder.
- (iv) End effects are negligible.

3.2 The Effect of Rotation.

The harmonics present are of order $6m \pm 1$ with a three-phase stator winding. Those of order $6m-1$ rotate backward and have a pole pitch $1/(6m-1)$ that of the fundamental. Therefore, to a point fixed to the rotor, the field appears to oscillate at $6m$ times fundamental frequency. Similarly the $6m+1$ harmonic fields rotate forward and so appear to oscillate at a frequency $6m$ times the fundamental.

The total harmonic field at the rotor surface is:

$$\sum_m \left\{ \hat{H}_{(6m-1)} \cos \left[\phi_{(6m-1)} + (6m-1)\theta - 6m\omega \right] + \hat{H}_{(6m+1)} \cos \left[\phi_{(6m+1)} + (6m+1)\theta - 6m\omega \right] \right\}$$

The loss due to this field is:

$$\sum_m \frac{1}{2\sigma\delta} \left\{ \hat{H}_{(6m-1)}^2 + \hat{H}_{(6m+1)}^2 + 2\hat{H}_{(6m-1)} \hat{H}_{(6m+1)} \cos \left[2\phi_{(6m+1)} - \phi_{(6m-1)} \right] \right\}$$

per unit surface area

where σ is the conductivity and δ the depth of penetration at the appropriate frequency.

The cosine variation round the rotor surface can be neglected in calculations of the total loss since it affects the distribution of loss but not the total. Therefore, the loss can be expressed as:

$$\sum_{\text{harmonics}} \hat{H}^2 / 2\sigma\delta$$

3.3 Calculation of Harmonic Fields.

The field in the airgap due to a harmonic current sheet, of radius R, is of the form:

$$A_n = \left\{ \frac{\mu_0 R J_n}{2n} \left(\frac{r}{R}\right)^{\pm n} + a_n r^n + b_n r^{-n} \right\} \cos n\theta$$

where J_n is the harmonic electric loading

The boundary condition at the infinitely permeable stator iron is $\partial A_n / \partial r = 0$

The rotor surface may be represented by the boundary condition. $A_n = k_n \partial A_n / \partial r$

where $k_n = (1 - j) \mu_r \delta_n / 2$ and μ_r is the relative permeability.

$$\text{Thus } a_n = J_n \frac{\mu_0 R}{2n} \frac{1}{R^n} \frac{D_n \frac{R^{2n}}{r_1^{2n}} - 1}{D_n \frac{r_4^{2n}}{r_1^{2n}} + 1}$$

$$b_n = J_n \frac{\mu_0 R}{2n} R^n \frac{\frac{r_4^{2n}}{R^{2n}} + 1}{D_n \frac{r_4^{2n}}{r_1^{2n}} + 1}$$

where r_4 is the inner radius of the stator iron

$$\text{and } D_n = (r_1 + nk_n) / (r_1 - nk_n)$$

The field due to a stator winding extending radially from r_2 to r_3 can be found by considering many elementary current sheets and integrating. The resulting field at r_1 , the rotor surface, is:

$$H_n = J_{sn} \frac{r_1}{2(n-2)} \left(\frac{r_4}{r_1}\right)^{2n} \left(\frac{D_n + 1}{D_n \frac{r_4^{2n}}{r_1^{2n}} + 1} \right) \left\{ \frac{r_1^{n-2}}{r_3^{n-2}} (1 - C_n r_3^{2n} / r_4^{2n}) - \frac{r_1^{n-2}}{r_2^{n-2}} (1 - C_n r_2^{2n} / r_4^{2n}) \right\} / (r_3 - r_2)$$

where $C_n = (n - 2) / (n + 2)$ and J is the harmonic current loading of the stator winding.

The total loss in the rotor surface is, therefore:

$$2\pi r_1 \int \frac{1}{2\sigma \delta_n} \left\{ \frac{J_{sn} r_1}{2(n-2)} \right\}^2 |E_n|^2 \left\{ F(r) - F(r) \right\} / (r_3 - r_2)^2$$

$$\text{where } E_n = (D_n + 1) / (D_n + r_1^{2n} / r_4^{2n})$$

$$F_n(r) = (r_1 / r)^{2n} (1 - C_n r^{2n} / r_4^{2n})$$

3.4 Example.

For the optimum 660 MW design $r_1 = 0.6$, $r_2 = 0.734$, $r_3 = 0.763$, $r_4 = 0.771$. Assuming $\sigma = 5 \cdot 10^6$ S/m and $\mu_r = 100$, the harmonic losses would be 23.7 MW for the 5th, 3.63 for the 7th, 0.41 for the 11th and 0.12 for the 13th if the harmonic current loadings were all equal to the fundamental loading of 300 kA/m. The actual current loadings J_{sn} are given by $J_s \cdot K_n/K_1$, where K_n is the nth harmonic winding factor. Therefore, the total loss in MW is:

$$\{23.7 \cdot K_5^2 + 3.63 \cdot K_7^2 + 0.41 \cdot K_{11}^2 + 0.12 \cdot K_{13}^2\} / K_1^2 \quad \text{etc.}$$

For the 1-4-1 interspersed 3-phase winding: $K_5/K_1 = 0.0594$, $K_7/K_1 = 0.0465$, $K_{11}/K_1 = 0.158$ and $K_{13}/K_1 = 0.182$; therefore, the total surface loss is approximately 105 kW. If a twelve-phase winding were used, $K_5 = K_7 = 0$, $K_{11}/K_1 = 0.955$ and $K_{13}/K_1 = 0.802$ making the total loss about 4.5 kW.

The above figures are based on the assumption that the rotor consists solely of a smooth steel cylinder. However, the rotor conductors will carry harmonic eddy currents making the real situation somewhat different from the ideal model. Nevertheless, the above figures indicate the probable size of this loss, and demonstrate the significant reduction to be gained by using a twelve-phase winding.

It is seen that this type of loss is small in slotless machines (typically 100 kW with a 3-phase winding) whereas in an equivalent conventional machine it may be as high as 500kW.

Appendix IV.

Calculation of Reactances.

4.1 Magnetising Reactance.

If no field current flows and a voltage is applied to the armature terminals such that the field in the airgap corresponds to the rated open-circuit armature voltage, V_T , the voltage across the magnetising part of the reactance, x_m in fig. 38, is equal to the rated open circuit voltage, and the current flowing is given by V_T/x_m .

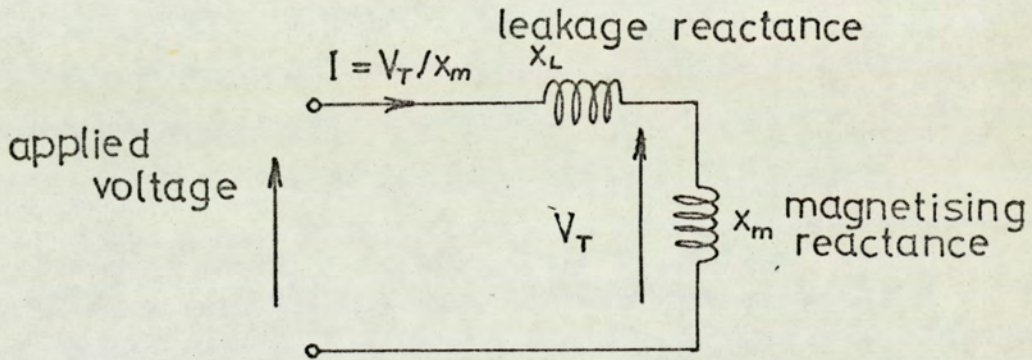


FIG.39. EQUIVALENT CIRCUIT OF A SYNCHRONOUS MACHINE WITHOUT EXCITATION

The per-unit value of the current would be $1/X_m$, where X_m is the per-unit magnetising reactance, and the stator current loading would be J_s/X_m , where J_s is the rated current loading.

The field pattern due to this current is shown in fig. 40. The flux which links the rotor winding is the magnetising component and the remainder is leakage flux.

The axial component of the vector potential (A_z) obeys Laplace's equation and is two-dimensional over most of the airgap length.

$$\text{Thus } \frac{\partial^2 Az}{\partial r^2} + \frac{1}{r} \frac{\partial Az}{\partial r} + \frac{1}{r^2} \frac{\partial^2 Az}{\partial \theta^2} = 0$$

If the rotor and stator iron surfaces are assumed to be infinitely permeable and the two windings are represented by thin sheets of radius R_s and R_R , the vector potential for $r < R_s$ is:

$$Az = \left\{ \frac{\mu_0 J_s}{2 X_m} \frac{r_1}{R_s} \cdot r + ar + b/r \right\} \cos \theta$$

$$\text{where } a = \frac{\mu_0 J_s}{2 X_m} \frac{r_1}{R_s} \frac{r_1^2 + R_s^2}{r_s^2 - r_1^2}$$

$$b = \frac{\mu_0 J_s}{2 X_m} \frac{r_1}{R_s} \frac{r_s^2 + R_s^2}{r_s^2 - r_1^2}$$

where J_s is the rated current loading referred to the rotor radius, r_1 , and r_s is the stator iron inner radius.

The vector potential at R_R is

$$\frac{\mu_0 J_s}{2 X_m} \frac{r_1}{R_s} \frac{(r_1^2 + R_R^2)(r_s^2 + R_s^2)}{R_R (r_s^2 - r_1^2)}$$

Therefore the total flux linking the rotor winding is:

$$\frac{\mu_0 J_s}{2 X_m} \frac{r_1}{R_s} \frac{(r_1^2 + R_R^2)(r_s^2 + R_s^2)}{R_R (r_s^2 - r_1^2)} \cdot 2 \cdot \ell.$$

which is equal to the rated flux which is very nearly $2B_r \ell$.

Therefore:

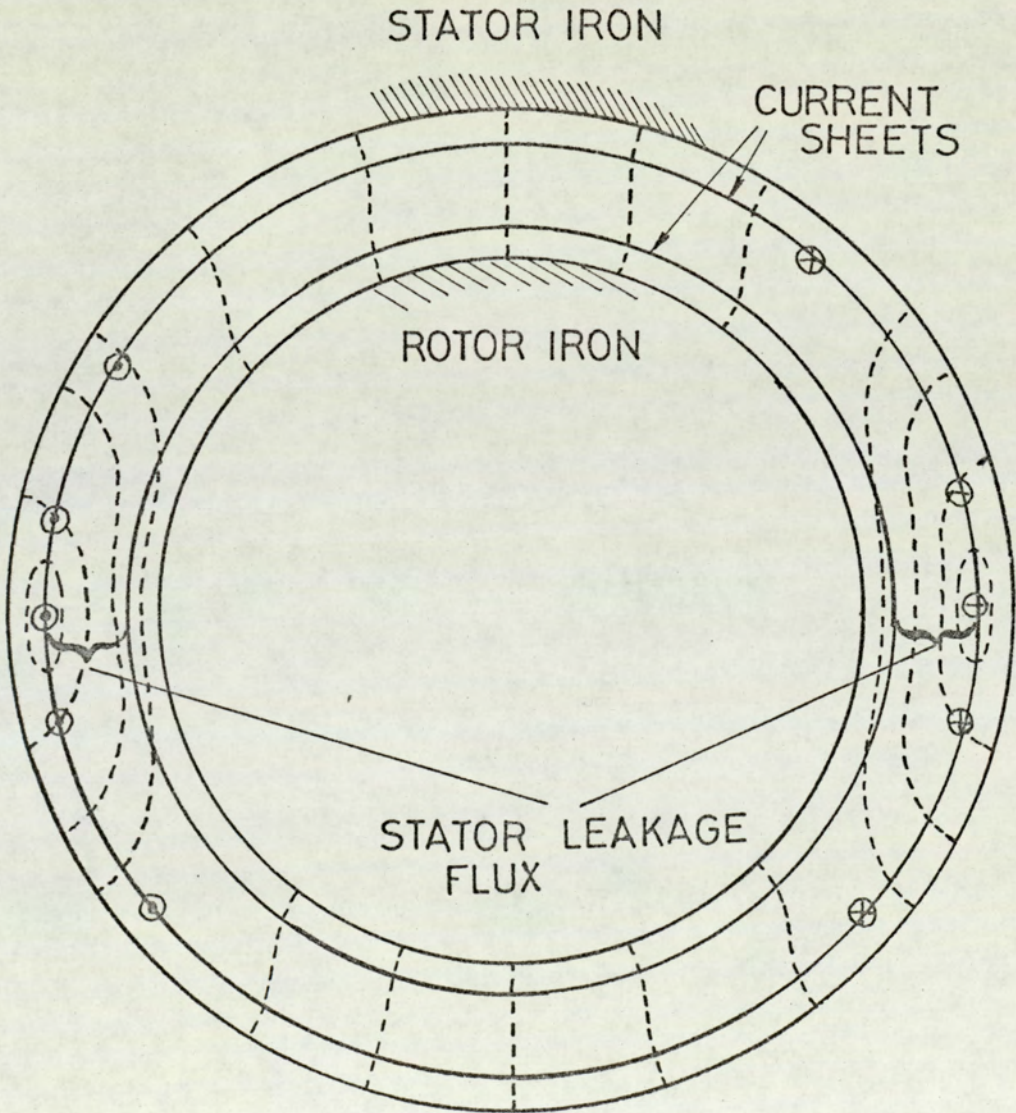
$$X_m = \frac{\mu_0 J_s (r_1^2 + R_R^2)(r_s^2 + R_s^2)}{2B R_s R_R (r_s^2 - r_1^2)}$$

4.2 Stator Leakage Reactance.

The stator leakage reactance can be considered as two separate parts, one due to the stray flux in the end region linking the end winding, and another due to airgap flux which does not link the rotor winding; X_e and X_g respectively.

FIG 40

STATOR LEAKAGE FLUX PATHS



4.2.1 Airgap Leakage Reactance.

The ratio between the leakage and magnetising reactances is equal to the ratio between the leakage and magnetising fluxes. The field analysis used above to find the magnetising reactance gives the ratio between the vector potential difference between the two windings and the vector potential at the rotor winding and hence the ratio X_g / X_m . Thus:

$$X_g = X_m \left\{ R_R / R_S - (r_1^2 + R_R^2) / (r_1^2 + R_S^2) \right\}$$

4.2.2 End Winding Leakage Reactance.

End winding shapes and end region boundaries are extremely complicated. However, Lawrenson (1970) describes a simple approximate formula for the inductance of end windings. The inductance of a single end turn is approximately proportional to its length, which, in turn, is approximately proportional to the radius. The rotor radius is taken for convenience as the radius determining the length.

If there are n conductors then the end winding inductance is:

$$L_e \approx k r_1 n^2$$

The peak conductor current is:

$$\hat{I} \propto J_s r_1 / n$$

Therefore, the peak flux linking the end turns is:

$$\Phi_e \propto r_1^2 n J_s$$

The main flux linking the winding is:

$$\Phi_m \propto 2 r_1 B l n$$

The per-unit leakage reactance is the ratio Φ_e / Φ_m

$$\therefore X_e \propto r_1 J_s / B l$$

Substituting for l

$$X_e \propto r_1^3 J_s^2 / S$$

Lawrenson's formula gives a value of $\sim 4\%$ for a 555 MVA machine with a current loading of 300 kA/m and a rotor radius of 570 mm.

Therefore:

$$X_e \approx 1.3 \times 10^{-3} J_s^2 r_1^3 / S$$

4.3 Rotor Leakage Reactance

A similar analysis to that above for the stator leakage reactance gives the leakage reactance of the rotor as:

$$X_R = X_m \left\{ \frac{R_S}{R_R} \left(\frac{R_R^2 + r_S^2}{R_S^2 + r_S^2} \right) - 1 \right\}$$

The machine transient reactance is given in turn by:

$$X_e + X_D + X_m X_R / (X_m + X_R)$$

See Adkins (1964) pp. 123

4.4 Approximate Formula for Magnetising Reactance.

The expression given above (section 4.1) for the magnetising reactance, X_m , cannot easily be used to derive the airgap, g , needed to produce a specified X_m .

A more convenient formula results from the assumption that the flux in the airgap is all radial. The magnetic stored energy is then given by:

$$E = \frac{L}{2\mu_0} \int_0^{2\pi} \int_{r_1}^{r_1+g} \left(B \frac{r_1}{r} \right)^2 \cos^2 \theta r dr d\theta$$

$$= \pi r_1^2 \frac{L}{2\mu_0} B^2 \ln (1 + g/r_1) / 2\mu_0$$

providing the steel parts of the magnetic circuit are infinitely permeable.

If the machine has N phases and a peak terminal voltage of V , the total energy stored in the magnetising reactance is:

$$E = \frac{1}{2} N \frac{V^2}{\omega X_m}$$

which gives

$$X_m = \frac{N V^2}{2 E \omega}$$

in per-unit

$$X_m = \frac{N V^2}{2 E \omega} \times \frac{(S/N)}{V^2}$$

where S is the MVA base and the voltage base is taken as V

$$\therefore X_m = S/2E\omega$$

substituting for S and E

$$X_m = \mu_0 J_s / B \ln (1+g/r_1)$$

Bibliography.

Airgap-wound machines.

1. DAVIES E.J. "Airgap windings for large turbogenerators", Proc. I.E.E., 118 3/4 Mar/Apr. 71.
2. DAVIES E.J. "A Slotless Turbogenerator", Electronics and Power 1968 14 p.209.
3. AICHHOLZER. "New ways of building turbogenerators up to 2 GVA, 60 kV "Elektrotechnische und Maschinenbau. Jan 1972.
4. British patent 837,546 W.D. Horsley.
5. British patent 881,468 J.W.H. Morgan & J.T. Wilkins.
6. British patent 1,096,177 A.S.E.A.
7. British patent 1,196,924 P. Richardson
8. British patent application 52449/65 A.S.E.A.
9. British patent application 55,329/67 E.J. Davies
10. Technical disclosure bulletin no. 171. National Reference Library for Science and Invention (Holborn Division) E. Spooner.
11. REECE A.B.J., PRESTON T. (1972) Private Communication.

Machines in general.

12. LAITHWAITE E.R. "The goodness of a machine", Proc. I.E.E. 112 No. 3 Mar 65.
13. ADKINS B. "The general theory of electrical machines", Chapman and Hall Ltd. 1964.
14. SAY M.G. "The performance and design of alternating current machines", 3rd Ed. Pitman 1958.
15. CARTER G.W. "The electromagnetic field in its engineering aspects", Longmans 1954.
16. KRICK N. and HIEBLER H. "Generators for Nuclear Power Stations", Brown Boveri Review May 1970.
17. "Evolution of Large Generators", Electrical review 2 April 71.
18. "Water Cooled Rotors". Energy International Feb. 71.

19. ALLEN P.H.G. Private communication 1971.
20. NOSER R.R. and POHL H. "Cooling large turbogenerators without hydrogen", Trans I.E.E.E. paper no. 71 TP 186 - PWR.
21. NEIDHOFER G. "Roebel Bar Windings for large Synchronous Machines", Brown Boveri Review Jan. 70.
22. ROBERT P., DISPAUX J. and DACIER J. "Improvement of Turbo-alternator efficiency", C.I.G.R.E. 1966.
23. British patent 1,104,844 P. Richardson & N. Young.
24. British patent 1,107,704 E.R. Hartill
25. CHALMERS B.J. "A.C. machine windings with reduced harmonic content", Proc I.E.E. 111. 11 Nov. 64.
26. LAWRENSON P.J. "Calculation of machine end winding inductances with special reference to turbogenerators", Proc I.E.E. 117 6 June 1970.
27. A.E.I. Turbine-Generators Ltd. 1968 "Turbine-Generator Engineering".
28. SOPER J.A. and FAGG A.R., "Divided-Winding-Rotor Synchronous Generators", Proc I.E.E. 1969 116(1) pp. 113-126.

Superconducting machines.

29. MULHALL B.E. "Superconducting Electrical Machines", Physics Bulletin Dec. 71.
30. MOLE C.J., HALLER H.E. III, LITZ D.C. "Superconducting Synchronous Generators", 1972 Applied Superconductivity conference.
31. WOODSON H.H., SMITH J.L., THULLEN P., KIRTLEY J.L., "The application of Superconductors in the field windings of large synchronous machines", I.E.E.E. trans. PAS-90 Mar/Apr 71.
32. LORCH H.O. I.E.E. discussion on superconducting machines. International cryogenics exhibition and meetings. Brighton April 71.

33. BAKER D.W.C. and BAYLLIS J.A. "Superconductivity and the electrical engineer" I.E.E. Students quarterly journal June 72.
34. HARROWELL R.V. "Preliminary studies of superconducting alternators" Cryogenics April 72.
35. APFLETON A.D., ANDERSON A.E., "A review of the critical aspects of superconducting A.C. generators" 1972 Applied superconductivity conference.
36. THULLEN, P., SMITH, J.L. Jr., and WOODSON, H.H., "Economic and operational aspects of the application of superconductors in steam turbine generator field windings Paper no. 70 CP 211-PWR 1970 I.E.E.E. Winter Power meeting.

General.

37. HAM A.C. "Carbon fibre composites for Aerospace Structures" Physics Bulletin 20 474-478.
38. MORLEY A., 1940, "Strength of Materials" 9th Ed. Longmans Green & Co. London.
39. SALISBURY J.K., Editor Kent's Mechanical Engineers Handbook 12th Ed. Power Vol J. Wiley & Sons Inc London 1950.